Langley Research Center

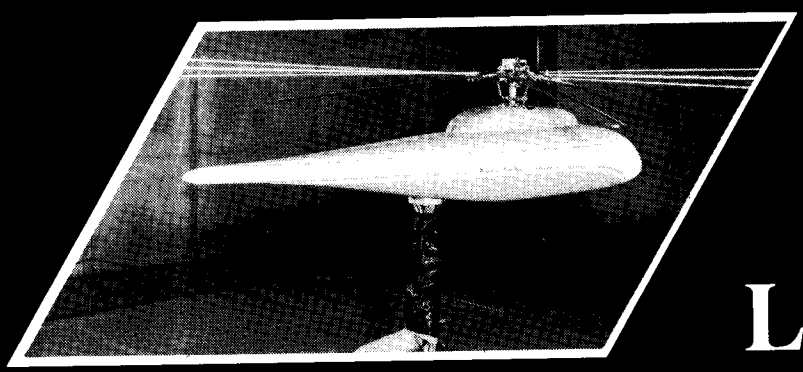

Langley AEROSPACE Test Highlights 1987

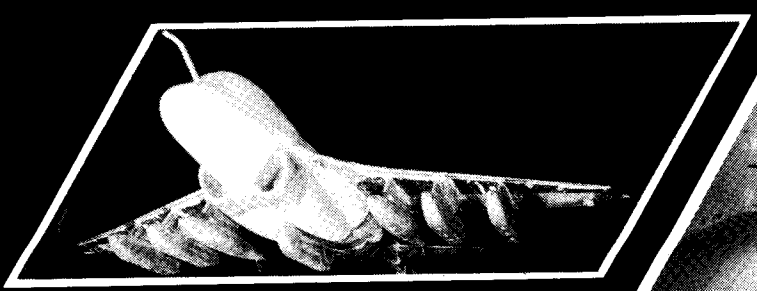

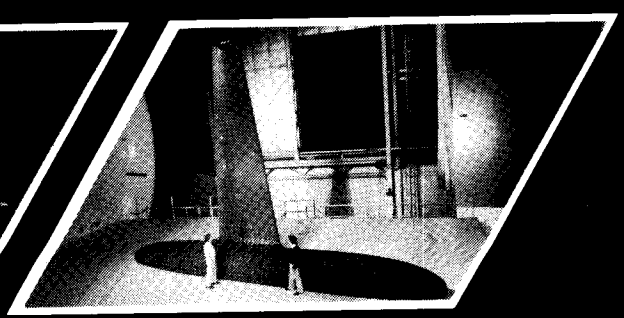

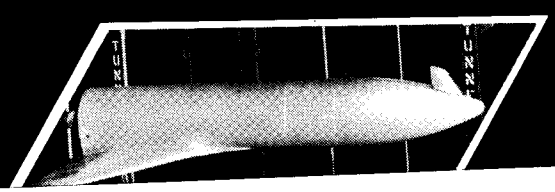

1917 Shaping Tomorrow 1987
NASA Langley Research Center

NASA Technical Memorandum 100595

Langley Research Center

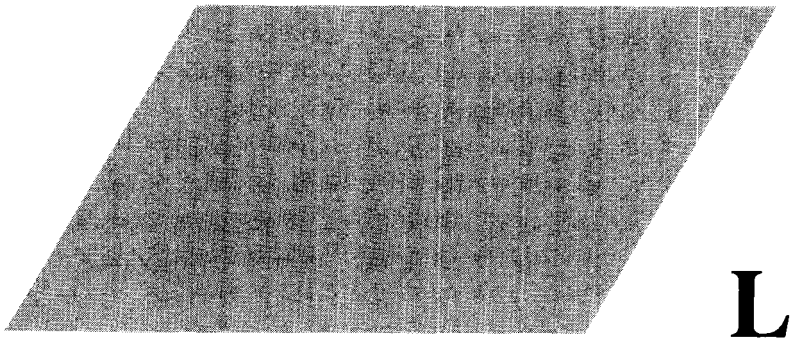

Langley AEROSPACE Test Highlights 1987

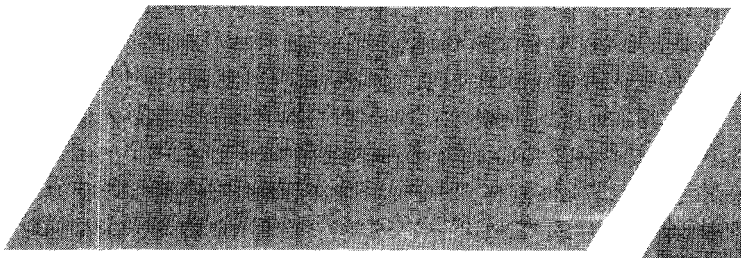

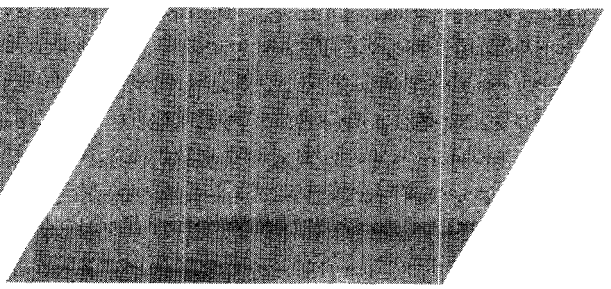

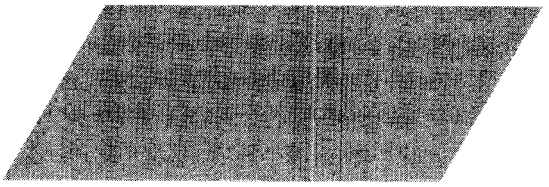

NASA
National Aeronautics and Space Administration

Langley Research Center
Hampton, Virginia 23665-5225

NASA Technical Memorandum 100595

Foreword

The role of the Langley Research Center is to perform basic and applied research necessary for the advancement of aeronautics and space flight, to generate new and advanced concepts for the accomplishment of related national goals, and to provide research advice, technological support, and assistance to other NASA installations, other government agencies, and industry. This report highlights some of the significant tests that were performed during calendar year 1987 in Langley Research Center test facilities, a number of which are unique in the world. The report illustrates both the broad range of the research and technology activities at the Langley Research Center and the contributions of this work toward maintaining United States leadership in aeronautics and space research. Other highlights of Langley research and technology for 1987 are described in *Research and Technology 1987 Annual Report of the Langley Research Center.* Further information about both reports is available from the Office of the Chief Scientist, Mail Stop 105-A, Langley Research Center, Hampton, Virginia 23665 (804-865-3316).

Richard H. Petersen
Director

Availability Information

For additional information on any highlight, contact one of the individuals identified with the highlight. This individual is either a member or a leader of the research group. Commercial telephone users may dial the listed extension preceded by (804) 865. Telephone users with access to the Federal Telecommunications System (FTS) may dial the extension preceded by 928.

Contents

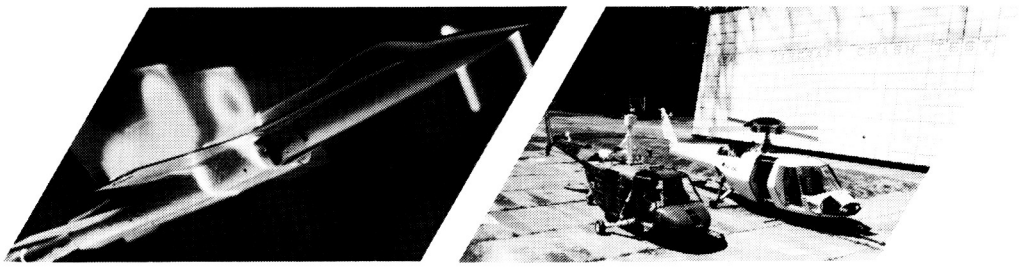

30- by 60-Foot Tunnel

The Langley 30- by 60-Foot Tunnel is a continuous-flow open-throat double-return tunnel powered by two 4000-horsepower electric motors, each driving a four-blade 35.5-ft-diameter fan. The tunnel test section is 30 ft high and 60 ft wide and is capable of speeds up to 100 mph. The tunnel was first put into operation in 1931 and has been used continuously since then to study the low-speed aerodynamics of commercial and military aircraft. The large open-throat test section lends itself readily to tests of large-scale models and to unique test methods with small-scale models.

Large-scale and full-scale aircraft tests are conducted with the strut mounting system. This test method can handle airplanes up to the size of present-day light twin-engine airplanes. Such tests provide static aerodynamic performance and stability and control data, including the measurement of power effects, wing pressure distributions, and flow visualization.

Small-scale models can be tested to determine both static and dynamic aerodynamics. For all captive tests, the models are sting mounted with internal strain-gauge balances. The captive test methods include conventional static tests for performance and stability and control, forced-oscillation tests for aerodynamic damping, and rotary tests for spin aerodynamics. Dynamically scaled subscale models, properly instrumented, are also freely flown in the large test section with a simple tether to study their dynamic stability characteristics at low speed and at high angles of attack. A small computer is used in this free-flight test technique to represent the important characteristics of the airplane flight control system.

The Langley 12-Foot Low-Speed Tunnel, which is used extensively for static tests prior to entry in the 30- by 60-Foot Tunnel, is an atmospheric wind tunnel with a 12-ft octagonal cross section for model testing. The tunnel serves as a diagnostic facility for exploratory research primarily in the area of high-angle-of-attack stability and control studies of various airplane and spacecraft configurations. Preliminary tests are conducted in the 12-Foot Low-Speed Tunnel on simple models prior to testing in higher speed facilities on more sophisticated models to obtain more efficient test planning and effective use of occupancy time in such facilities.

Advanced Turboprop

A research program is currently being conducted in the 30- by 60-Foot Tunnel to examine the basic aerodynamic characteristics of an advanced turboprop with pusher propellers. The tests utilize an 0.175-scale model, and the tunnel compressed air system provides power to drive two counterrotating air motors for scaled thrust effects including engine-out condition cases. The model, which has been tested with a canard to investigate three-surface configuration characteristics, has provisions for a forward-swept wing and tractor propellers.

Advanced turboprop in three-surface configuration. L-87-7056

Tests to date have been completed in the static and forced-oscillation modes, and these results will be applied to program control laws for free-flight tests in the 30- by 60-Foot Tunnel. The model has demonstrated stable aerodynamic characteristics and effective control power in the linear angle-of-attack regime. However, in the unpowered mode above the stall angle of attack, the model exhibits a nose-up tendency that cannot be corrected with only the use of the elevators. The application of power provides a nose-down pitching moment and appears to reduce flow separation on the horizontal tail, thus allowing improved elevator effectiveness.
(P. J. Davis, 2184)

Full-Scale Semispan Tests of Natural Laminar-Flow Airfoil

Tests of a full-scale semispan model were conducted in the 30- by 60-Foot Tunnel to study the low-speed high-lift characteristics of a three-dimensional wing using the HS-NLF-0213 airfoil section. The test setup is shown in the figure. The tests were conducted at a Reynolds number of 3.7×10^6 based on the wing mean aerodynamic chord and over an angle-of-attack range from $-10°$ to $30°$. A slotted 28-percent chord flap that extended from the wing root to a span location of $2y/b = 0.79$ was the high-lift device used for these tests.

A maximum lift coefficient $C_{L_{max}}$ of 1.4 was achieved with the flap undeflected, and a $C_{L_{max}}$ of 2.6 was achieved with the flap deflected 40°. The net result of having a significant amount of laminar flow for drag reduction was illustrated by fixing the boundary-layer transition at a chord station near the leading edge of the wing. With transition fixed at $x/c = 0.05$ on both the upper and lower surfaces, an increase in drag coefficient C_D of 0.003 was obtained at a lift coefficient $C_L = 0.27$. Data from two-dimensional tests indicate an increase in

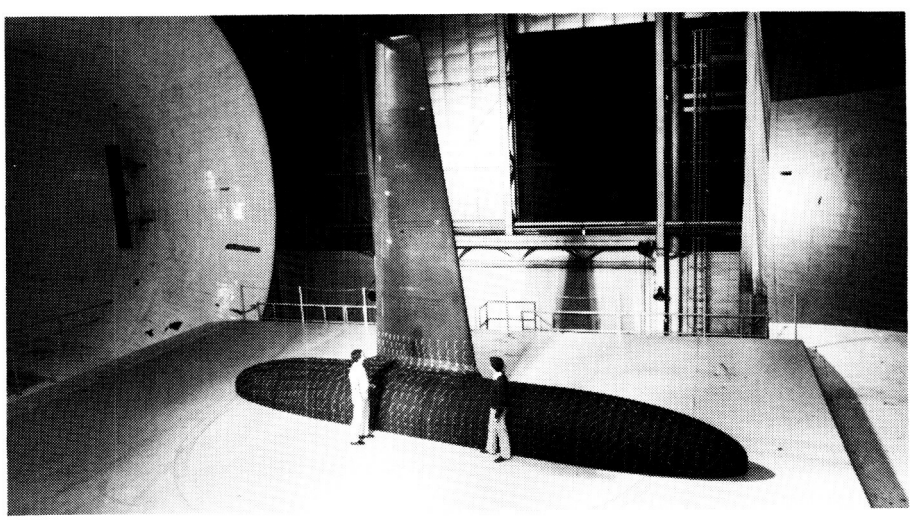

Large-scale semispan natural laminar-flow airfoil model. L-87-00300

C_D of 0.004 for similar conditions. Data concerning the effect of boundary-layer transition on the lift characteristics showed a slight loss in lift near $C_{L_{max}}$ for this airfoil. This reduction in C_L, however, is small, and its effect on performance is minimal. These results indicate that the high-lift characteristics of the HS-NLF-0213 airfoil are generally representative of those of more conventional airfoils, and this maximum-lift capability is adequate to satisfy the landing requirements of advanced transport and commuter designs.

(D. E. Hahne, F. L. Jordan, Jr., and P. J. Davis, 2184)

Wind Tunnel Free-Flight Tests of STOL and Maneuver Technology Demonstrator

A series of wind tunnel free-flight tests have been conducted in the 30- by 60-Foot Tunnel to investigate the low-speed flight dynamic behavior of the STOL (short takeoff and landing) and Maneuver Technology Demonstrator (S/MTD). The primary objective of the United States Air Force-sponsored S/MTD Program is to investigate, develop, and validate technology areas related to providing current and future fighter aircraft with STOL capability and enhanced maneuvering performance. The model used in these tests is a 13-percent scale model of the S/MTD configuration which is an F-15 aircraft modified to include canards and two-dimensional nozzles incorporating pitch vectoring and thrust reversing. Prior to free-flight tests, a comprehensive set of static and dynamic force data was obtained over a broad angle-of-attack range and was used in the design of the control laws for the airplane.

L-87-11121

13-percent scale F-15 S/MTD model during wind tunnel free-flight tests.

Free-flight tests were conducted on the model incorporating two control system configurations: conventional mode and combat mode. In the conventional mode, the pitch thrust vectoring was inactive so that only the aerodynamic controls were available. In this configuration, the model exhibited good flying characteristics up to 25° angle of attack α. At higher angles of attack, yaw control degraded rapidly due to loss of rudder effectiveness such that the model could not be flown above an angle of attack of approximately 40°. In the combat mode, pitch thrust vectoring was integrated with the aerodynamic controls through a complex blending scheme in the control laws. The free-flight results showed that the pitch control effectiveness was greatly enhanced with the addition of pitch vectoring. However, flight behavior in the stall region was still poor due to loss of rudder effectiveness. These results indicate that the S/MTD airplane will have good low-speed flight dynamic characteristics within its nominal test envelope ($\alpha < 30°$).

(D. G. Murri, 2184)

X-31 Dynamic Stability

The X-31 Program is a joint United States/German program aimed at flight demonstrating advanced maneuvering concepts for combat aircraft. A key goal is to explore the potential tactical benefits of poststall maneuvering involving intentional operation at extreme angles of attack. Achieving this goal will require that the X-31 test airplane perform highly dynamic maneuvers at low-speed, high-angle-of-attack flight conditions.

The current X-31 configuration evolved from a number of design studies conducted in the United States and Germany. The design is a small, single-place (one-person), single-engine config-

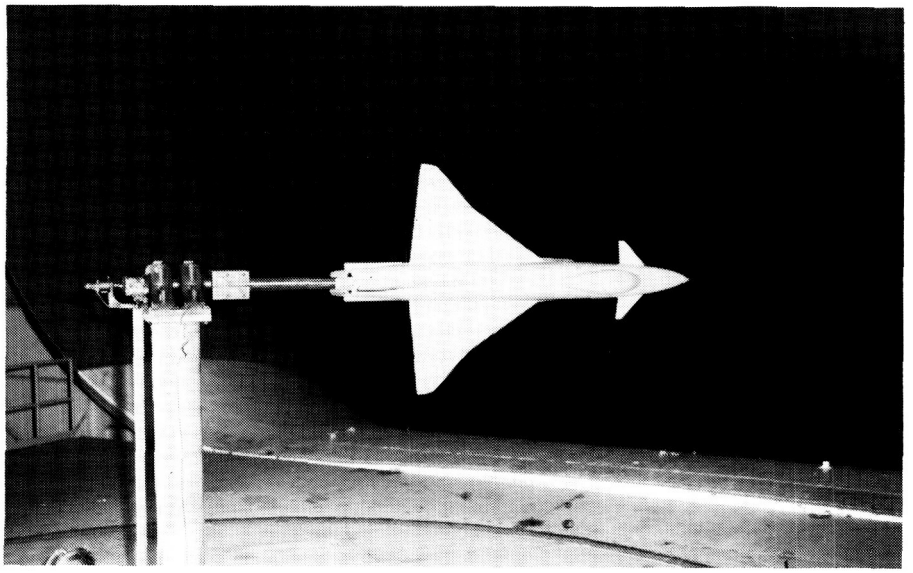

X-31 model on dynamic stability rig. L-87-7761

uration incorporating a delta wing, canards, and a multi-axes thrust-vectoring system. Because the airplane must be capable of performing highly dynamic maneuvers, a key characteristic that must be achieved in the design is good dynamic stability, particularly at critical high-angle-of-attack conditions. As a result, forced-oscillation tests were conducted in the 30- by 60-Foot Tunnel on an 0.19-scale model of the X-31 to investigate dynamic stability characteristics in the roll and yaw axes. The tests were conducted over an angle-of-attack range of 0° to 90° at two values of oscillation frequency. The tests revealed several areas of deficiencies such as severe unstable yaw damping near maximum lift and a tendency to wing rock because of a lack of roll damping. To address these problems, airframe modifications were developed in the form of strakes in different positions near the canard and on the forebody. The results are being used for configuration refinement prior to the initiation of full-scale hardware fabrication.
(M. A. Croom, 2184)

Low-Turbulence Pressure Tunnel

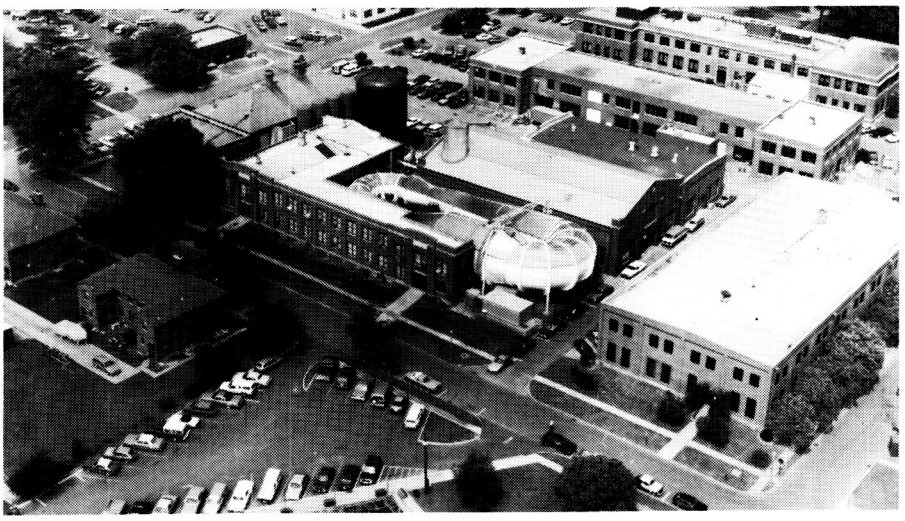

The Langley Low-Turbulence Pressure Tunnel (LTPT) is a single-return closed-circuit tunnel that can be operated at pressures from near vacuum to 10 atm. The test section is rectangular in shape (3 ft wide and 7.5 ft in height and length), and the contraction ratio is 17.6:1. The LTPT is capable of testing at Mach numbers from 0.05 to 0.50 and unit Reynolds numbers from 0.1 × 10^6 to 15 × 10^6 per foot. The tunnel has provisions for removal of the sidewall boundary layer by means of a closed-loop suction system mounted inside the pressure chamber. This system utilizes slotted vertical sidewalls just ahead of the model test section, and the removed air is reinjected through an annular slot downstream of the test section. A flow control system allows the flow and pressure requirements to be varied as dictated by tunnel operation. This system can be used to provide boundary-layer control (BLC) for low-drag airfoil research.

A BLC system for high-lift airfoil testing is also available. This system utilizes compressed dry air and involves tangential blowing from slots located on the sidewall mounting end plates. Flowmeters can be used to monitor the amount of air blown into the tunnel. An automatically controlled vent valve is utilized to remove the air injected into the tunnel by this system. A high-lift model support and force balance system is provided to handle both single-element and multiple-element airfoils. The LTPT is currently being modified to add a passive suction BLC system for high-lift testing and a three-component laser Doppler velocimeter (LDV).

The measured turbulence level of the LTPT is very low due to the large contraction ratio and the many fine-mesh anti-turbulence screens. The excellent flow quality of this facility makes it particularly suitable for testing low-drag airfoils. Recent flow quality measurements in the LTPT indicate that the velocity fluctuations in the test section range from 0.025 percent at Mach 0.05 to 0.30 percent at Mach 0.20 at the highest unit Reynolds number.

The drive system is a 2000-horsepower direct-current motor with power supplied from a motor-generator set. The tunnel stagnation temperature is controlled by a heat exchanger, which provides both heating and cooling via steam injectors and modulated valves that control the flow volume of water through a set of coils.

Performance Characteristics of Airfoils at Low Reynolds Numbers

Recent interest in low-Reynolds-number aerodynamics ($R \leq 500{,}000$) has increased for both military and civil applications with emphasis on providing improved vehicle performance. Applications are varied and include remotely piloted vehicles, wind turbines, and propellers. Wind tunnel results on the Eppler 387 airfoil in two European facilities have shown large differences in airfoil performance at low

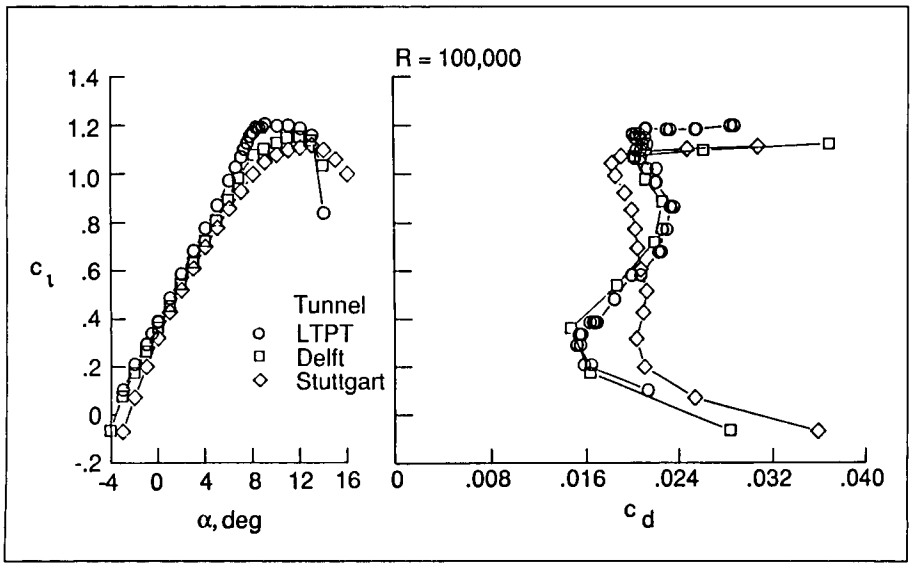

Comparison of section data on Eppler 387 airfoil from several facilities.

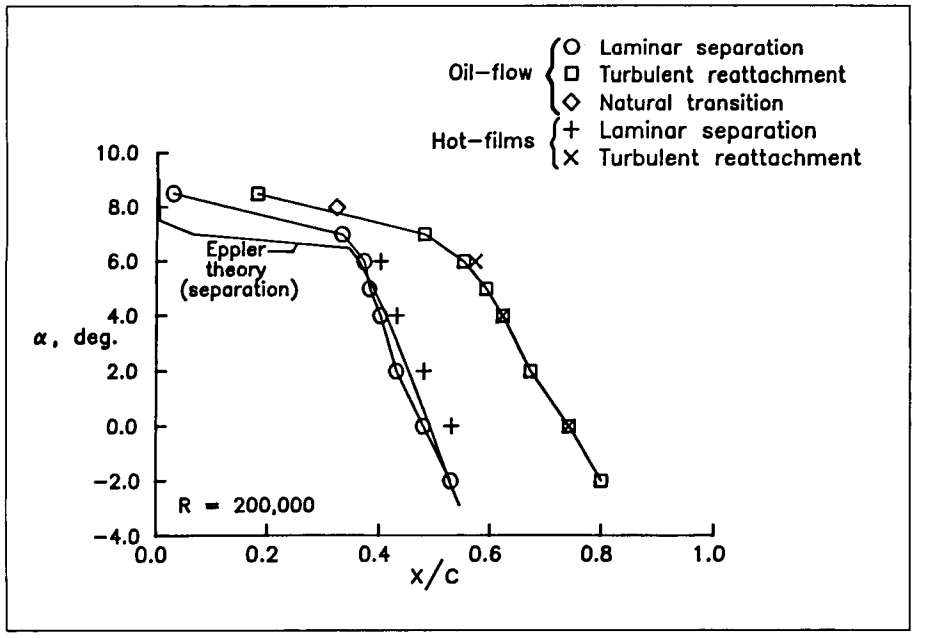

Separation and reattachment locations on Eppler 387 airfoil as measured in LTPT.

Reynolds numbers. The objective of this research was to obtain data on the Eppler 387 airfoil in the LTPT to compare with the European data and for code verification. The LTPT was selected because of its good flow quality, variable pressure capability, and precision pressure instrumentation.

A wind tunnel test was conducted on a pressure model of the Eppler 387 airfoil in the LTPT to determine the performance characteristics. Oil-flow visualization and hot-film sensors were used to determine laminar-separation and turbulent-reattachment locations.

The first figure shows the results of the present experiment compared with the European data at a Reynolds number of 100,000. Generally good agreement between the LTPT and Delft data is indicated. However, large differences are shown between the Stuttgart data and either the LTPT or Delft results. The second figure illustrates laminar-separation and turbulent-reattachment locations as measured in the LTPT from both oil-flow results and multielement hot-film sensors at a Reynolds number of 200,000. Generally good agreement between the measurement techniques and theory is shown.

Results illustrate the importance of tunnel flow quality, model contour accuracy, and instrumentation uncertainties in determining the aerodynamic behavior of airfoils for Reynolds numbers less than 500,000 where laminar separation bubbles are present. Also, a nonintrusive, cost-effective, multielement sensor for simultaneous measurement of laminar separation and turbulent reattachment was demonstrated in a low-turbulence environment. A force model of the Eppler 387 airfoil will be tested in the LTPT to further evaluate the measurement of drag at low Reynolds numbers.

(R. J. McGhee and J. P. Stack, 4516)

Airfoil Designed for High-Altitude, Long-Endurance, Remotely Piloted Vehicle

A current interest exists in the development of high-altitude, long-endurance, remotely piloted vehicles for a number of missions including communications relaying, weather monitoring, and providing targeting information for cruise missiles. The preliminary design of such aircraft is complicated, however, by the lack of data regarding suitable airfoils. This lack of data is due to the fact that such vehicles, unlike those for which the majority of airfoils have been developed in the past, operate at fairly high-lift coefficients and at relatively low Reynolds numbers. Thus, to provide realistic airfoil performance information for preliminary design efforts, a generic airfoil has been designed which is suited for aircraft with missions similar to those noted.

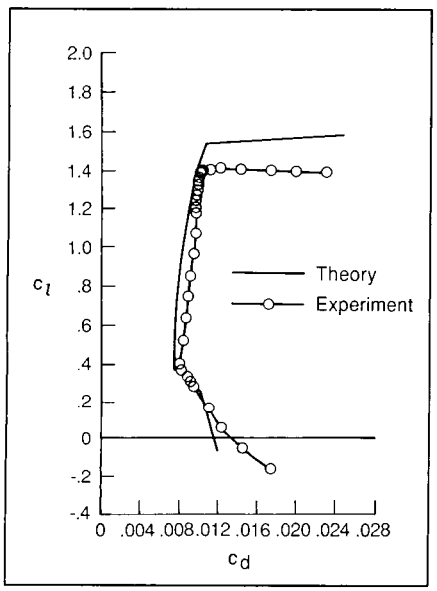

Comparison of theory and experiment of NLF(1)-1015 airfoil at $R = 0.7 \times 10^6$.

This airfoil, designated the NLF(1)-1015, is unflapped and has a thickness of 15-percent chord. The design Reynolds number range is 7×10^5 to 2×10^6. Low drag is predicted for lift coefficients ranging from 0.4 (the lift coefficient providing high-speed dash capability) to 1.6 (the maximum endurance design condition). Further, the airfoil is specifically designed such that the maximum-lift coefficient (approximately 1.8 at a Reynolds number of 2×10^6) is unaffected by surface contamination. Consequently, takeoff and landing in rain, or with insect residue on the wings, should present no special difficulties.

An experimental investigation has been conducted in the LTPT to obtain the basic, low-speed, two-dimensional aerodynamic characteristics of the airfoil. The results have been compared with predictions from the Eppler Airfoil Design and Analysis Program as shown in the figure.

(D. M. Somers and M. D. Maughmer, 4516)

Shuttle Crew Escape Tube Study

The National Aeronautics and Space Administration is investigating means of safe crew escape during the subsonic phase of the Space Shuttle flight. This situation could occur during an abort on the ascent where the orbiter has safely separated from the external tank and solid rocket boosters, has slowed to low subsonic speeds, and is in stable gliding flight but cannot reach a suitable landing site. It may also exist during entry if a guidance or other malfunction has made a safe landing impossible. A previous investigation conducted at the Langley Research Center indicated that unassisted crew bailout from the orbiter main side hatch would be extremely dangerous even at low speeds. Therefore, current work has concentrated on augmenting crew egress. Several schemes to aid crew bailout are under consideration. The study conducted at Langley considered a method that utilizes a deployable tube extending out of the main hatch and down the side of the vehicle. This method would allow the crew to slide down the tube and exit below the wing.

The investigation consisted of an engineering design feasibility study and wind tunnel tests. Two wind tunnel tests were conducted: one with an 0.03-scale orbiter model in the 12-Foot Low-Speed Tunnel to determine the length of the tube necessary to allow the crew figure models to exit safely, and a second with an 0.015-scale model in the Low-Turbulence Pressure Tunnel to determine the effect of the deployed tube on the stability and control characteristics of the orbiter.

In addition, measurements were made to determine the aerodynamic loads on the tube for design purposes.

The investigation revealed that the crew could exit safely if the escape tube extended 1 ft below the leading edge of the wing (approximately 42 in. below the bottom of the side hatch opening). The loads on the tube were found to be in the range that could be handled by current air-mat (an inflatable rubber/fabric material) technology, and the tube could be packaged and deployed from the orbiter.

(G. M. Ware, 3984)

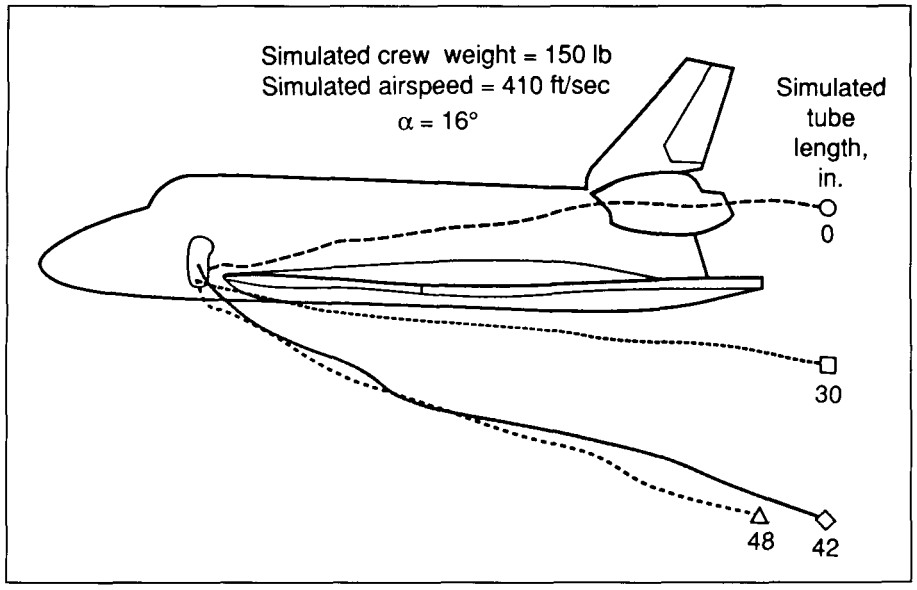

Effect of escape tube length on crew bailout trajectory.

20-Foot Vertical Spin Tunnel

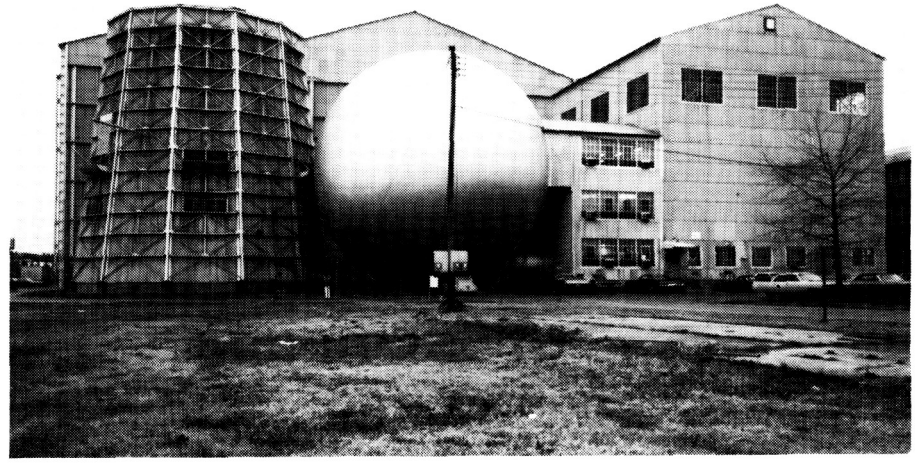

The Langley 20-Foot Vertical Spin Tunnel is the only operational spin tunnel in the United States and one of only two such tunnels in the free world. The tunnel, which is used to investigate spin characteristics of dynamically scaled aircraft models, is a vertical tunnel with a closed-circuit annular return passage. The vertical test section has 12 sides and is 20 ft wide and 25 ft high. The test medium is air. Tunnel speed can be varied from 0 ft/s to 90 ft/s with accelerations to 15 ft/s^2. This facility is powered by a 1300-horsepower main drive.

Spin recovery characteristics are studied by remote actuation of the aerodynamic controls of models to predetermined positions. Force and moment testing is performed with a gooseneck rotary-arm model support, which permits angles of attack from 0° to ±90° and sideslip angles from 0° to ±20°. Motion picture and video records are used to record the spinning and recovery characteristics in the spin tunnel tests. Force and moment data from the rotary balance tests are recorded in coefficient form and stored on magnetic tapes.

Pressure Measurement Tests on Wing of Spinning Model

The wing of an airplane configuration has always been known to exert a significant influence on spin entry and spin motion characteristics, but pressure distribution measurements over the surface of the wing during spinning conditions have not been made. In the present tests, pressure measurements were made for the first time on the upper and lower surface of the wing of an Australian Trainer model during spinning conditions. Pressure tests were previously made on the aft fuselage and empennage of the same

L-83-4450

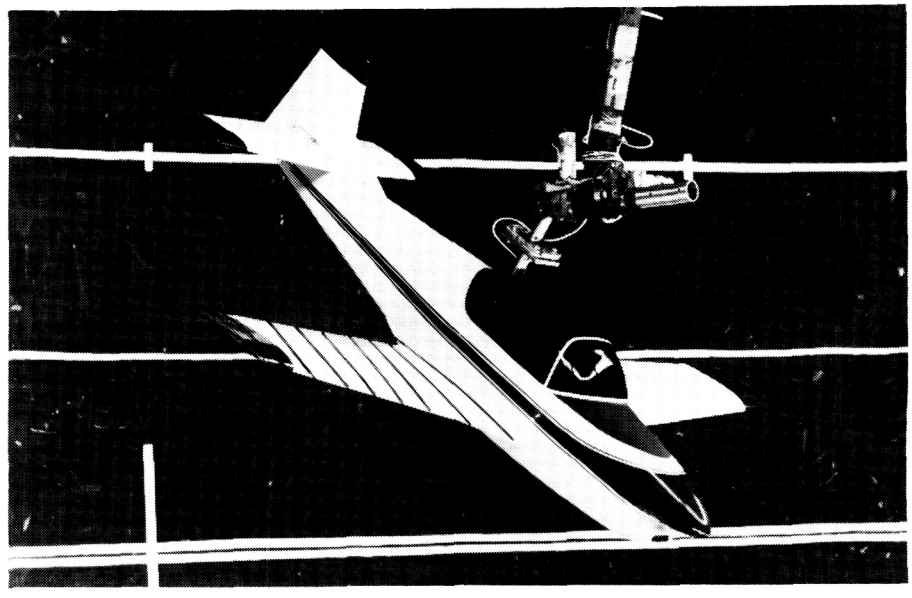

Australian trainer model mounted for wing pressure tests on rotary balance rig in 20-Foot Vertical Spin Tunnel.

model, and the results were reported last year.

The wing pressure test results showed that the wing provided a strong input to the spinning motion during low-to-medium angle-of-attack conditions, which represent spin entry and steep-spin attitudes. As the angle of attack was increased during rotation, the test results showed that the wing input to the spinning motion decreased, whereas the horizontal tail input to the spinning motion increased. This pressure measuring technique is a valuable research tool to provide information for analyzing spin aerodynamics and to determine the influences of airplane components (such as wing, fuselage, and tails) on spin characteristics. Such information gives the designer increased confidence to provide desired spin and recovery characteristics on new aircraft early in the development process.

(J. S. Bowman, Jr. and R. S. Hultberg, 2521)

Free-Spinning Landing Gear Study for F-4S

At the request of the United States Navy, an investigation was conducted in the 20-Foot Vertical Spin Tunnel to evaluate the effect of landing gear deployment during recovery from the flat spin of the F-4S. The investigation consisted of free-spinning tests of a 1/28 dynamically scaled model.

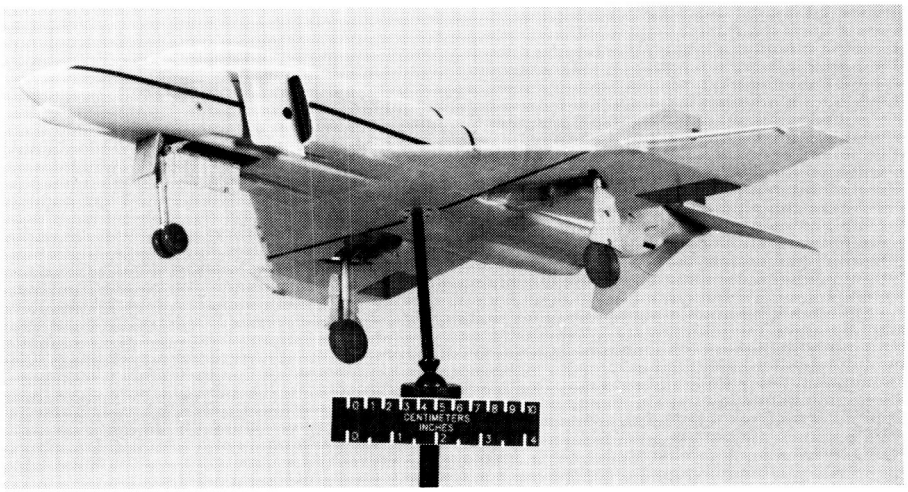

F-4S spin tunnel model with landing gear extended. L-87-1913

Previous spin tunnel and full-scale flight tests identified an unrecoverable flat-spin mode. Recently, at least two incidents of successful recoveries from apparent flat spins have been reported by F-4 aircrews. In both cases, recovery occurred after the landing gear was lowered, and it was conjectured that this action may have been a key factor in making the recoveries possible. Such landing gear effects were not previously evaluated.

Spin test data of the F-4S model showed a flat-spin mode with an angle of attack of 86° and a rotation rate of 2.0 s/turn for the following control setting: stabilator full trailing edge up, rudder full with the spin, and ailerons full against the spin. The landing gear deployment was initiated by radio control signals while pro-spin control settings were maintained. The results of gear deployment indicated no noticeable effect on angle of attack, although the turn rate increased to 1.67 s/turn. Additional tests assessing the effects of landing gear extension in conjunction with anti-spin control inputs showed that landing gear deployment actually delayed recovery.

(M. S. Hungness, 2244)

T-45A Free-Spin Tests

A spin tunnel test program, which was initiated at the request of the United States Navy, has been conducted on a 1/19 dynamically scaled model of the T-45A trainer. The tests were conducted to identify the spin modes, spin angle of attack, spin rate, and recovery characteristics, as well as the effects of speed brakes, wing fences, and stores. Also, the emergency spin-recovery parachute size was established.

The model exhibited both a no-spin mode and a steep spiral-like mode through the entire range of

control configurations and inertial loadings. The rate of descent for the spiral-like mode exceeded the maximum airspeed attainable in the tunnel and appeared to be constantly increasing. Speed brake deployment appeared to dampen the spiral, but not sufficiently to initiate a spin. Fences and stores, as well as asymmetric loading, had no effect on erect or inverted spins.

T-45A model being tested in 20-Foot Vertical Spin Tunnel. L-87-7328

Typical recovery configurations (rudder full against and aileron full with the spin), which were initiated during the spiral-like mode, resulted in extremely rapid recovery. A parachute size of 13.6-ft flat diameter and towline length of 73 ft was tested and found adequate for recovery from the spiral-like mode. **(D. Vairo, 2244)**

7- by 10-Foot High-Speed Tunnel

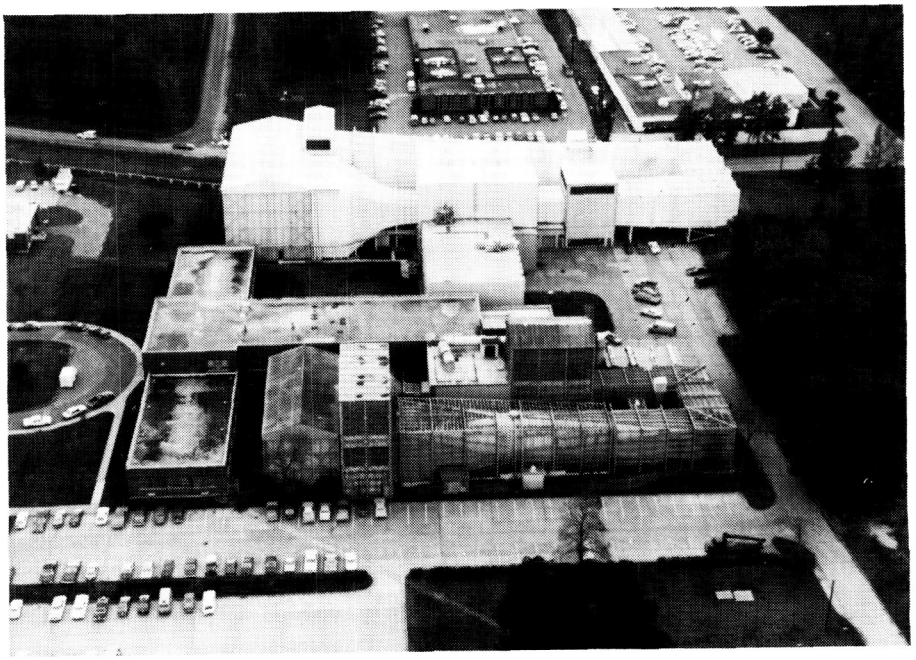

The Langley 7- by 10-Foot High-Speed Tunnel is a closed-circuit single-return continuous-flow atmospheric tunnel with a test section 6.6 ft high, 9.6 ft wide, and 10 ft long. The tunnel is fan driven and is powered by a 14,000-horsepower electric motor. It operates over a Mach number range from 0.2 to 0.9 to produce a maximum Reynolds number of 4 × 10^6 per foot. In addition to static testing of complete and semispan models, the facility is equipped for both steady-state roll and oscillatory stability testing.

The facility has an important role in a wide range of basic and applied aerodynamics research, including advanced vortex lift concepts, fuel-conservative aircraft design technology, highly maneuverable aircraft concepts, and the development of improved aerodynamic theories such as the difficult separated-flow and jet interaction effects needed for computer-aided design and analysis.

The 7- by 10-Foot High-Speed Tunnel is currently having new fan blades installed and has not been operational the past year. Work is scheduled to be completed in 1988.

14- by 22-Foot Subsonic Tunnel

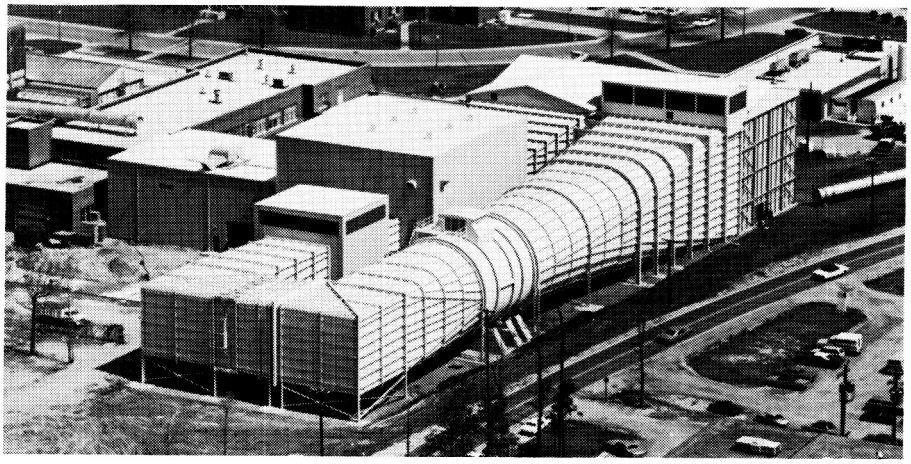

The Langley 14- by 22-Foot Subsonic Tunnel (formerly the 4- by 7-Meter Tunnel) is used for low-speed testing of powered and unpowered models of various fixed- and rotary-wing civil and military aircraft. The tunnel is powered by an 8000-horsepower electrical drive system, which can provide precise tunnel speed control from 0 to 318 ft/s with the Reynolds number per foot ranging from 0 to 2.1 × 10^6. The test section is 14.5 ft high, 21.8 ft wide, and approximately 50 ft long. The tunnel can be operated as a closed tunnel with slotted walls or as one or more open configurations when the side walls and ceiling are removed to allow extra testing capability, such as flow visualization and acoustic tests. The tunnel is equipped with a two-component laser velocimeter system. Furthermore, boundary-layer suction on the floor at the entrance to the test section and a moving-belt ground board for operation at test section flow velocities up to 111 ft/s can be installed for ground effect tests.

Langley has completed significant modifications to the 14- by 22-Foot Subsonic Tunnel to improve and expand its aerodynamic and acoustic test capability. One of the more significant aerodynamic improvements was achieved through the use of flow deflectors installed downstream of the first corner of the tunnel circuit to improve the performance of the tunnel fan. The deflectors resulted in a more uniform velocity distribution into the tunnel drive system and eliminated regions of large-scale flow separation in the return leg of the tunnel circuit.

A turbulence reduction system consisting of a grid, a honeycomb, and four fine-mesh screens dramatically reduced the level of longitudinal turbulence intensity in the tun-

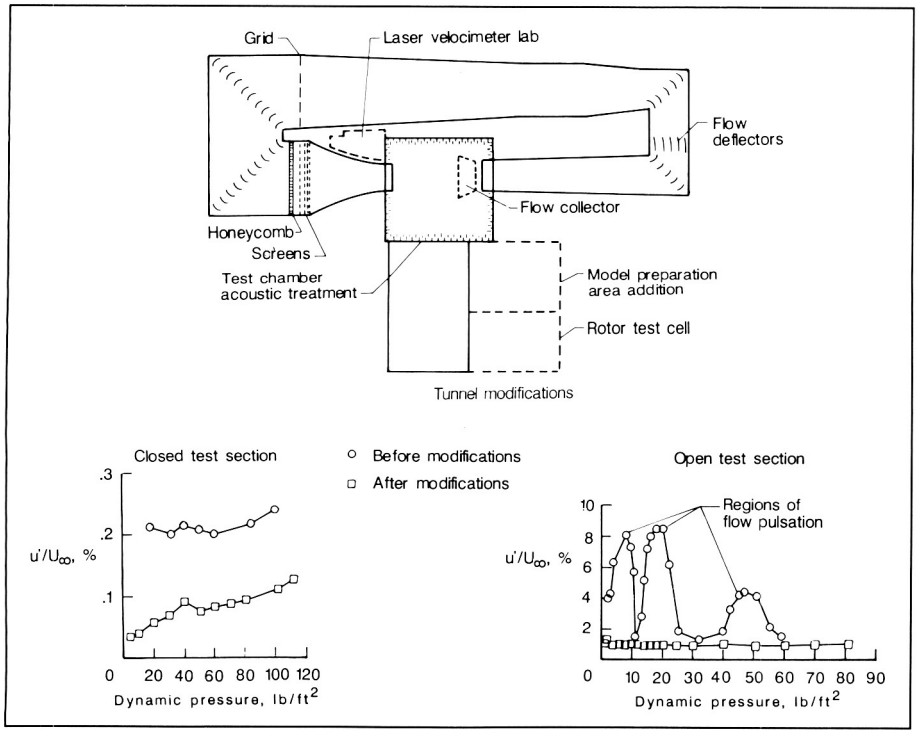

Effect of flow improvement modifications on longitudinal turbulence intensity ($u'/U\infty$).

nel test section. This system provided a reduction in turbulence of 50 percent or more for the closed test section configuration. Periodic flow pulsations that occurred at several speeds in the unmodified configuration of the open test section were eliminated by installation of a new flow collector.

Acoustic reverberations in the open test section were reduced through the use of sound-absorbing panels on the test chamber walls. A major operational improvement was achieved through the construction of a specially designed laser velocimeter laboratory for setup and maintenance of the two-component laser velocimetry system. Finally, an addition to the model preparation area which includes a support system and rotor test cell provides the capability to assemble and test rotor models in hovering conditions prior to actual entry into the tunnel.

F-18 High-Angle-of-Attack Aerodynamics

Aerodynamic phenomena, such as highly separated flows and vortex flows associated with high-angle-of-attack flight, and their influence on vehicle stability and control are not fully understood, and the complex nature of such flows can lead to confusing test results. For example, early flight tests of an F-18 displayed an unstable rolling moment that had not been observed in high Reynolds number wind tunnel tests; paradoxically, low Reynolds number testing in the 30- by 60-Foot Tunnel did exhibit the unstable rolling moment experienced by the airplane. It is not known whether this discrepancy is due in whole or in part to Reynolds number effects, or to other factors such as surface geometry, roughness, free-stream turbulence, or model support system interference.

L-86-6486

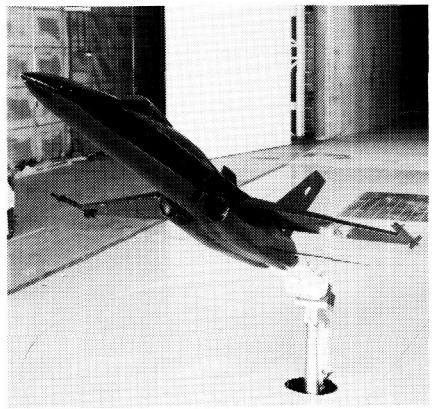

16-percent F-18 model installed in 14- by 22-Foot Subsonic Tunnel in high-angle-of-attack testing.

A series of wind tunnel and flight tests was initiated to attempt to identify and characterize this phenomenon as well as to understand better the complex nature of separated flows. A 16-percent F-18 model was tested in the 14- by 22-Foot Subsonic Tunnel to obtain pressure and surface flow visualization data on the forebody region and force and moment data at angles of attack up to 52°. Comparisons of the low Reynolds number data with the data from prior tests confirmed the lateral instability identified both in flight and in the 30- by 60-Foot Tunnel. By testing the same model in both the 30- by 60-Foot Tunnel and the 14- by 22-Foot Subsonic Tunnel, the possibility that tunnel conditions or support system interference may have been the cause of the anomaly was eliminated. A detailed analysis of the pressure measurements and surface flow visualization, combined with the force and moment data, is helping to provide understanding into the characteristics of high-angle-of-attack aerodynamic phenomena and valid wind tunnel testing procedures. **(D. W. Banks, 2877)**

X-31 High-Angle-of-Attack Demonstrator

A 19-percent scale model of the Defense Advanced Research Projects Agency X-31A research airplane was tested in the 14- by 22-Foot Subsonic Tunnel. The X-31 is a demonstrator aircraft designed to utilize extremely high angles of attack in an evaluation of enhanced agility and maneuverability. The wind tunnel investigation was performed to determine the static low-speed aerodynamic characteristics of the configuration at high angles of attack. The model was tested at angles of attack up to 68° and at sideslip angles from −16° to 16° for speeds up to 190 kn. In addition to studies of the

stability and control characteristics of the basic design, the effects of speed brake deployment, nose strakes, nose boom attachments, and inlet conditions were also investigated for these extreme pitch attitudes.

Preliminary results indicate that the basic configuration should be controllable throughout the pitch and yaw range tested. Nose geometry, including nose strakes and nose boom location, was found to have a very powerful influence on the overall aerodynamic characteristics. In addition, these data were very sensitive to minor variations in nose geometry. The data from the test will be used to refine the geometry for the final full-scale configuration. **(D. W. Banks and G. M. Gatlin, 2877)**

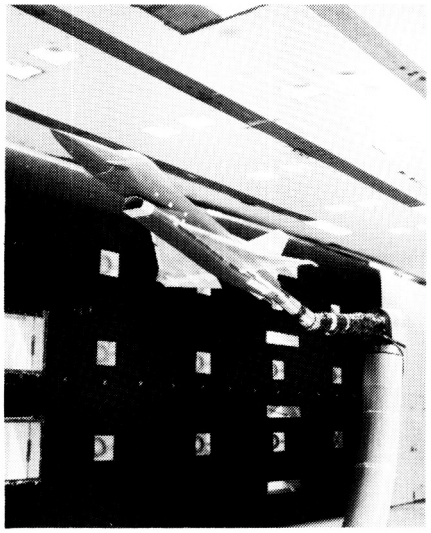

X-31 high-angle-of-attack demonstrator in 14- by 22-Foot Subsonic Tunnel.

Rotor Inflow Research Progress

Three experimental programs to study rotor inflow have been conducted during the past 2 years in the 14- by 22-Foot Subsonic Tunnel. With the completion of the most recent experiments, the inflow at the rotor disk has now been defined for a thrust coefficient of 0.0064 at advance ratios (free-steam velocity over hover tip speed) of 0.15, 0.23, and 0.30 for a rectangular blade planform, and at advance ratios of 0.15 and 0.23 for a 3-to-1 tapered blade planform. These measurements were obtained for the complete rotor disk in a plane parallel to, and one chord above, the rotor tip-path-plane. The data acquired at each measurement location included both time-averaged two-component velocity measurements and conditionally sampled blade-azimuth-position velocity measurements. The goal is to provide all of these data in data report format (included on a floppy disk) by early 1988.

Efforts are continuing in the correlation of the data with various analytic descriptions of rotor inflow. The computational methods being exercised include the United Technologies Research Center (UTRC) freewake, UTRC generalized wake, Computational Analytical Methods of Rotorcraft Aerodynamics and Dynamics (CAMRAD), T. S. Beddoes (an employee of Westland Helicopter, Ltd.) method, and some developing in-house methods. Each of these methods provides some degree of acceptability in its application to inflow predictions; however, preliminary results indicate there are some disparities between prediction and experimental data, particularly in the time-varying predictions. Further analysis of the data will be performed. **(D. Hoad, J. Elliott, S. Althoff, and R. Sailey, 3611)**

L-87-8863

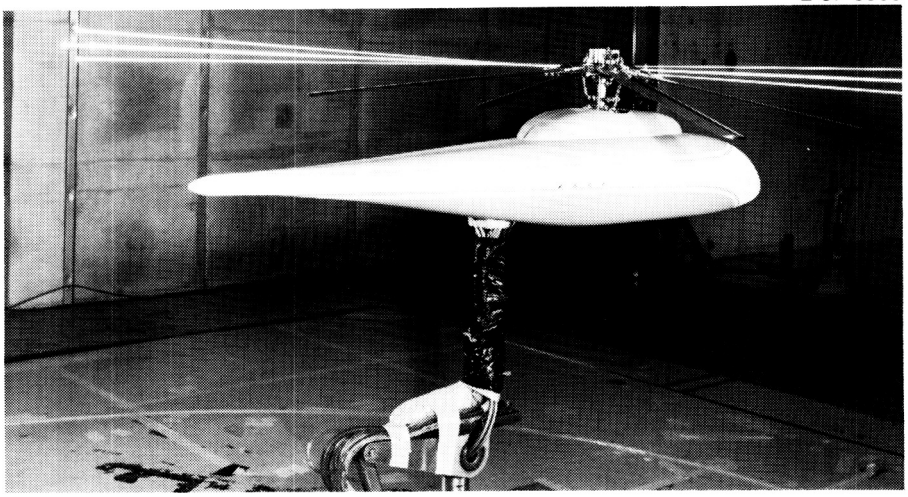

2-m rotor model with laser velocimeter in 14- by 22-Foot Subsonic Tunnel.

8-Foot Transonic Pressure Tunnel

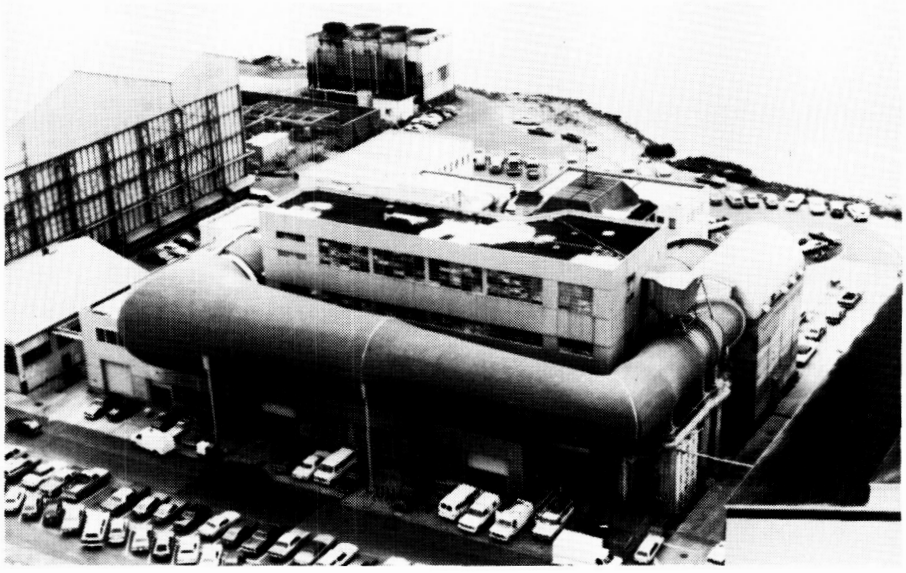

The Langley 8-Foot Transonic Pressure Tunnel is a closed-circuit single-return variable-density continuous-flow wind tunnel. The test section walls are slotted (5-percent porosity) at the top and bottom, with solid sidewalls fitted with windows for schlieren flow visualization. In 1982, the facility was modified for flow-quality improvements and reconfigured for low-drag testing of a large-chord swept laminar-flow control airfoil at transonic speeds. A honeycomb and screens were permanently installed in the settling chamber to suppress the turbulence level in the test section. A contoured liner was installed on all four walls of the test section to simulate interference-free flow about an infinite yawed wing. This contoured liner produces a contraction ratio of 25 to 1 and covers existing floor and ceiling slots. An adjustable sonic throat is also located at the end of the test section to block upstream propagation of diffuser noise.

The combination of honeycomb, screens, and choke provides a very low disturbance level in the test region at transonic speeds. Except for the honeycomb and screens, the changes are reversible. In the current configuration, the stagnation pressure can be varied from about 0.25 to 1.25 atm up to a Mach number of less than 0.85 with the transonic slots closed by the liner. The stagnation temperature is controlled by water-cooled fins upstream of the settling chamber. Tunnel air can be dried by a dryer that uses silica gel desiccant to prevent fogging due to expansion in the high-speed nozzle. Current plans call for this facility to be restored to the transonic three-dimensional test mode, following completion of the flow control experiment in 1988.

The Basic Aerodynamic Research Facility is an integral part of the 8-Foot Transonic Pressure Tunnel (8-Foot TPT) research complex. Utilizing two of the 8-Foot TPT 100,000 ft^3/min compressors, this facility can achieve continuous-flow Mach numbers up to 1.25 in its 18-in. by 18-in. test section. Historically, this facility has been used as a test bed for research to be performed in the larger and more costly wind tunnels. To expand the capability of this facility, the test section has been configured to accommodate an orthogonal, three-dimensional laser velocimeter system. This small wind tunnel is ideal for direct comparisons of different transonic flow diagnostic techniques.

Laminar-Flow Control Tests

Langley Research Center researchers have defined an experiment designed to investigate the physical phenomena associated with laminar-flow control (LFC) and low-profile drag on advanced swept supercritical airfoils. Tests will allow the evaluation and documentation of the combination of boundary-layer control through surface suction and supercritical airfoil technol-

ogy at conditions typical of high-performance transports.

The LFC experiment, installed in the 8-Foot Transonic Pressure Tunnel, has been ongoing since September 1982. Two suction concepts have been evaluated for their ability to maintain laminar flow over the same airfoil geometry. One concept involved removal of the slow moving air near the surface through discretely spaced slots along the airfoil span. The other concept accomplishes this by suction through perforated spanwise strips.

Results on the swept airfoil with discrete slots or perforated skin indicated that full-chord suction laminarization could be achieved with very low drag at the high-subsonic speeds typical of high-performance transports. This drag was considerably below that for an equivalent supercritical turbulent airfoil.

A third configuration involving boundary-layer control through a combination of geometric shaping and surface suction is now being installed. This "hybrid" design replaces the two aft upper-surface panels (26-percent to 90-percent chord) with new nonsuction panels so that the upper surface of the airfoil will have suction only over the first 26-percent chord. The new panels are of slightly different contour so as to have a pressure distribution designed to enhance the continuation of laminar flow from the end of suction at 26-percent chord to about 60-percent chord. If successful, this design would achieve drag levels approaching those of the full-chord suction wing with reduced suction requirements and considerably less suction ducting structure.

(C. W. Brooks, Jr. and J. C. Ferris, 2631)

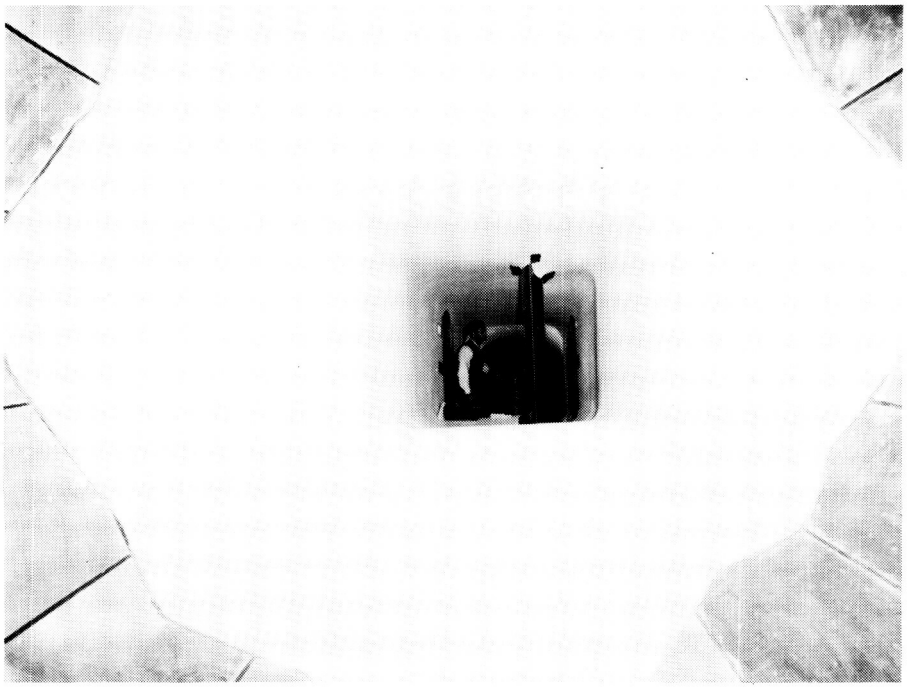

Laminar-flow control wing and liner looking downstream. L-82-3618

Transonic Dynamics Tunnel

Conversion of the original Langley 19-Foot Pressure Tunnel into the Transonic Dynamics Tunnel (TDT) was begun in the late 1950's to satisfy the need for a large transonic wind tunnel dedicated specifically to work on the dynamics and aeroelastic problems associated with the development of high-speed aircraft. Since the facility became operational in 1960, it has been used almost exclusively to clear new designs for safety from flutter and buffet, to evaluate solutions to aeroelastic problems, and to research aeroelastic phenomena at transonic speeds.

The tunnel is a slotted-throat single-return closed-circuit wind tunnel with a 16-ft^2 test section. The stagnation pressure can be varied from slightly above atmospheric to near vacuum, and the Mach number can be varied from 0 to 1.2. Both test section Mach number and density are continuously controllable. The facility can use either air or Freon 12 as the test medium. Freon is usually used because it has several advantages over air as a test medium for dynamically scaled aeroelastic model testing. The tunnel has a Freon reclamation system so that the gas can be purified and reused.

The facility is equipped with many features uniquely suited to dynamic and aeroelasticity testing. These include a new computerized data acquisition system especially designed to rapidly process large quantities of dynamic data, a means of rapidly reducing test section Mach number and dynamic pressure to protect models from damage when aeroelastic instabilities occur, a system of oscillating vanes to generate sinusoidal variations in tunnel flow angle for use in gust response studies, and special mount systems that enable simulation of airplane free-flight dynamic motions.

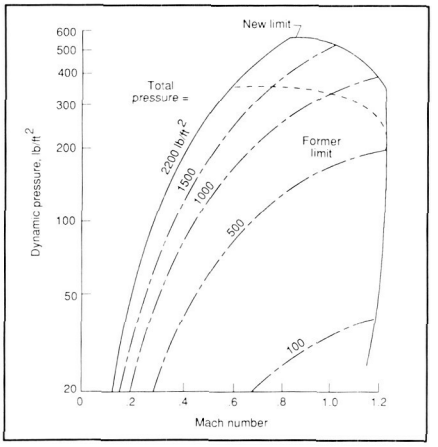

Former and present operational boundaries of TDT.

During much of 1985, the tunnel complex was modified to provide 50-percent higher test dynamic pressures in the transonic speed range. The test medium density capability was increased by 50 percent in that speed range, which allows models to be built 50 percent heavier and still meet the mass density scaling ratios required for proper modeling of full-size aircraft. For strength considerations, this becomes very significant as full-size aircraft become more structurally efficient. To provide this increased density capability, the existing fan motor was rewound to increase the power rating from 20,000 to 30,000 hp. Additional tunnel cooling capacity was provided to accommodate the increased tunnel power limit. Other major modifications included changes to the electrical power distribution system and installation of a new speed control system.

Evaluation of Improved Adaptive Suppression System

Modern fighter aircraft carry a large variety of external wing-mounted stores. In some instances it is necessary to placard the operational envelope because of flutter. One approach to avoid this restriction is to use an active control system to suppress flutter. Such a system operates by sensing wing motion and feeding back these signals through appropriate control laws to drive control surfaces to produce forces and moments to suppress flutter. Adaptive control systems are particularly attractive for this application because no knowledge of the store configuration being flown is required. Adaptive control systems continually measure system response due to control inputs and update control laws based on these measurements.

A 1/4-scale, cable-mounted, full-span F-16 aeroelastic model (shown in the figure), which was equipped with an Adaptive Flutter Suppression System (AFSS), was tested in the TDT in a joint United States Air Force/NASA/General Dynamics test. Accelerometers were used to measure wing motion. The AFSS digital computer was located in the control room. Computer-generated signals were sent to the flaperons to provide a continuous low-amplitude random excitation to the model. The resultant wing motion was measured, and a mathematical representation of the model was determined by using an analysis implemented on the digital computer. Using this derived mathematical model, a control law was then developed to suppress flutter.

Flutter data, with the AFSS off and on, were obtained for three flutter critical store configurations. Basic systems-on testing began below the flutter boundary and proceeded above the system-off flutter boundary. The improved adaptive control law updated itself significantly faster than on a previous test (up to 2500 times during a test pass) without failing to suppress the flutter. For two of the store configurations (one with mild flutter onset, the other with moderate flutter onset) a 30-percent increase in flutter speed was demonstrated; for the third configuration (violent flutter onset) approximately a 20-percent increase in flutter speed was obtained. The results of the system for two store configurations are given in the figure. In addition to the basic testing, the system was evaluated using computer-simulated store drops in addition to actual store drops where wing tip missiles were ejected during testing causing the model to rapidly change from a stable flutter free configuration to an unstable flutter configuration. In these instances the AFSS quickly recognized that the dynamics of the model had changed and updated itself to suppress the flutter. Adaptive flutter suppression with no predetermined control laws or knowledge of store configuration has been successfully demonstrated on a full-span, "free-flying" model. Data obtained during this study provide an invaluable foundation upon which to build future studies and flight applications. **(F. W. Cazier, Jr., M. H. Durham, and M. G. Farmer, 2661)**

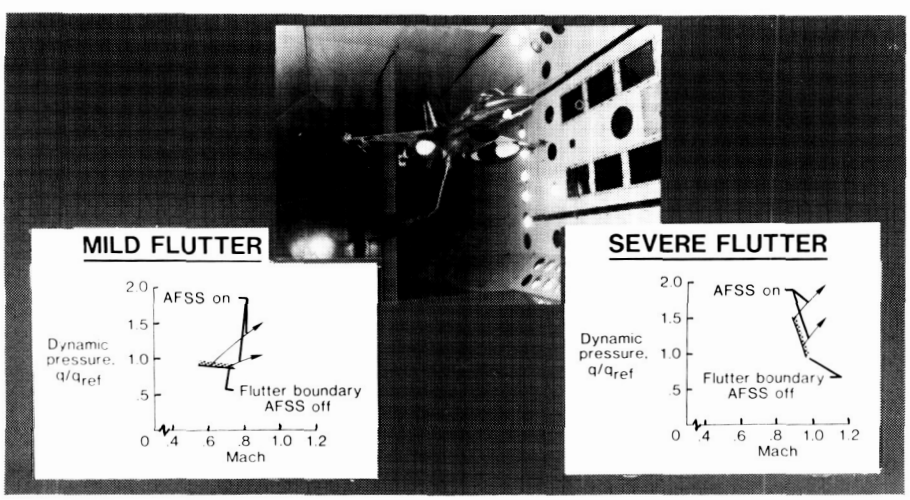

Improved adaptive flutter suppression system evaluated in TDT tests. L-87-8915

Effects of Speed Brakes on Wing Flutter

Speed brakes, spoilers, and other devices that are extended from the surface of a wing have been used effectively in many stability and control applications in aeronautics. One use that has not been studied, however, is as a flutter suppressor. The purpose of this study was to obtain some parametric results of the effects of speed brake size and deployment angle on wing flutter.

A relatively simple, paddle-type flutter model was equipped with a speed brake that could be deployed over a range of angles by adjusting a mechanical mechanism. The model was tested at a Mach number M of 0.80 in the Transonic Dynamics Tunnel with provisions for using speed brakes of varying sizes. That portion of the paddle model exposed to the flow was "rigid." Model stiffness was determined by the dimensions of the "paddle handle" that was behind the splitter plate which was used to get the wing root outside the wind tunnel wall boundary layer. The bending and twisting of the handle provided the wing with flapping and pitching degrees of freedom. The paddle handle was shielded from the flow by a fairing. The model was ballasted so that the mass and inertia did not change as speed brake

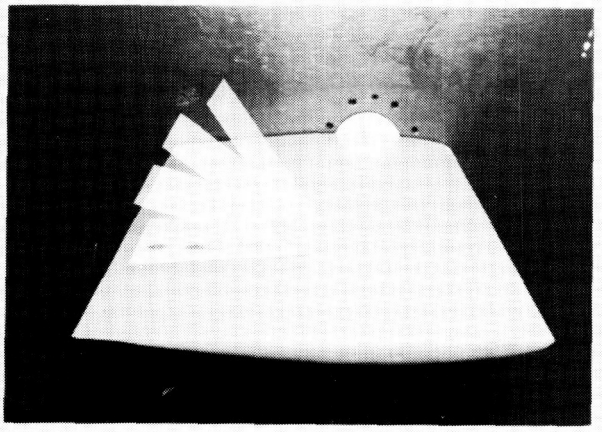

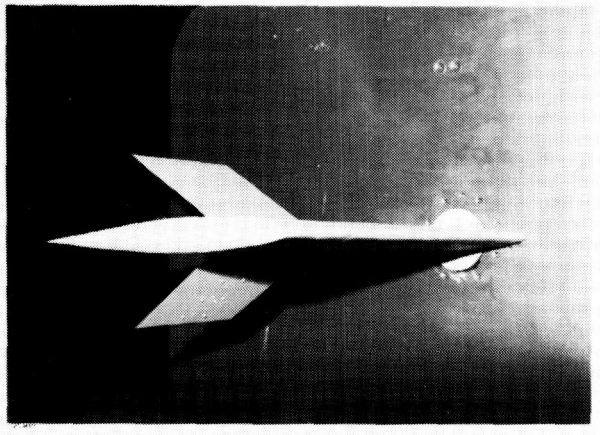

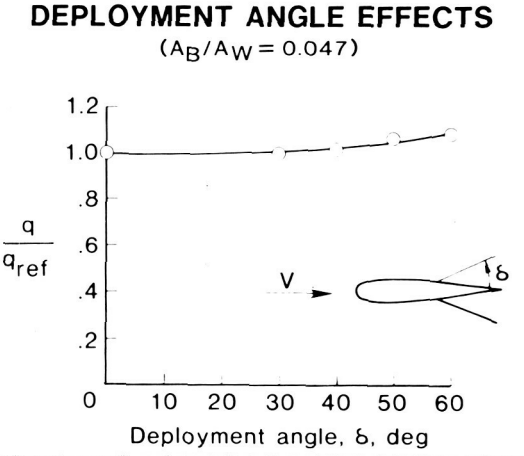

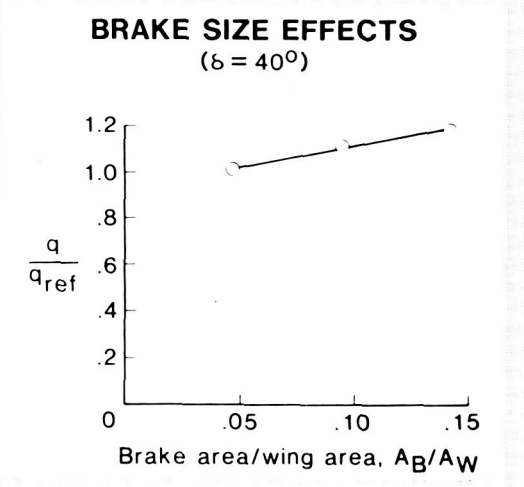

Speed brake effects on wing flutter.

L-87-8945

parameters were varied; thus, the natural frequencies remained the same such that flutter characteristics could be directly attributed to aerodynamic effects of the speed brakes.

Experimental flutter results were obtained at $M = 0.80$ for variations in speed brake deployment angle for a constant speed brake size and for variations in speed brake size for a given deployment angle. These results are shown in the figure as the relative variation of flutter dynamic pressure with the respective parameter. These results show that by increasing either deployment angle or size the flutter dynamic pressure is increased, and that a significant deployment angle is required before the flutter speed is affected. Further, the data show that speed brake size has a stronger effect on flutter than does deployment angle over the range of variables studied. **(R. V. Doggett, Jr., 2661)**

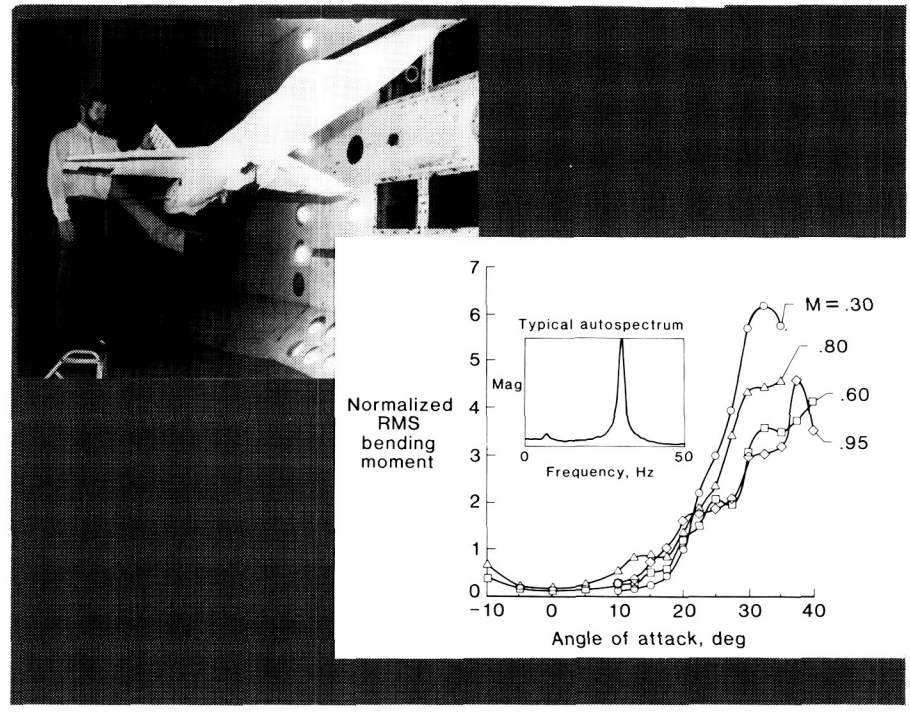

Mach number effects on twin-vertical-tail buffet (dynamic pressure q equals 50 lb/ft^2).

Effects of Mach Number on Buffet Response of Twin-Vertical-Tail Airplane

Recent experiences from the operational use of high-performance, twin-vertical-tail airplane configurations have shown that relatively large dynamic response of the tail structure occurs at certain often-encountered flight conditions. These buffet-like responses are larger than those anticipated in the structural design and can have a significant adverse effect on service life. The objective of this study has been to obtain data that can be used to better understand the characteristics of these undesirable responses.

A full-span, "rigid," sting-mounted model of a high-performance twin-vertical-tail airplane was equipped with elastic vertical tail and buffet tested over a range of angles of attack and Mach numbers in the TDT. Although the elastic tails did not scale the dynamic characteristics of a specific full-scale design, their stiffness and mass were chosen so that the dynamics characteristics were representative.

Experimental buffet response data are shown in the figure as the variation of a normalized root-mean-square bending-moment response parameter with angle of attack for several different Mach numbers M. The commonly used response parameter is derived from generalized harmonic analysis considerations. It is assumed that the aerodynamic damping is very small compared to the structural damping, a responsible assumption because the tails were at near-zero lift during the test. The response was primarily in one structural mode as shown by the spectra. The data for all Mach numbers are similar in that the bending moment is small and relatively constant up to an angle of attack

of about 15°, where a relatively sharp increase in bending moment begins to occur. Although the details of the data are different for different Mach numbers, it does appear that a peak response occurs at an angle of attack of approximately 30° to 35°. The magnitude of the maximum value appears to be a function of Mach number. These data provide a basis for assessing the Mach number effects on the buffet characteristics to twin-vertical-tail airplane configurations.

(S. L. Moss and S. R. Cole, 2661)

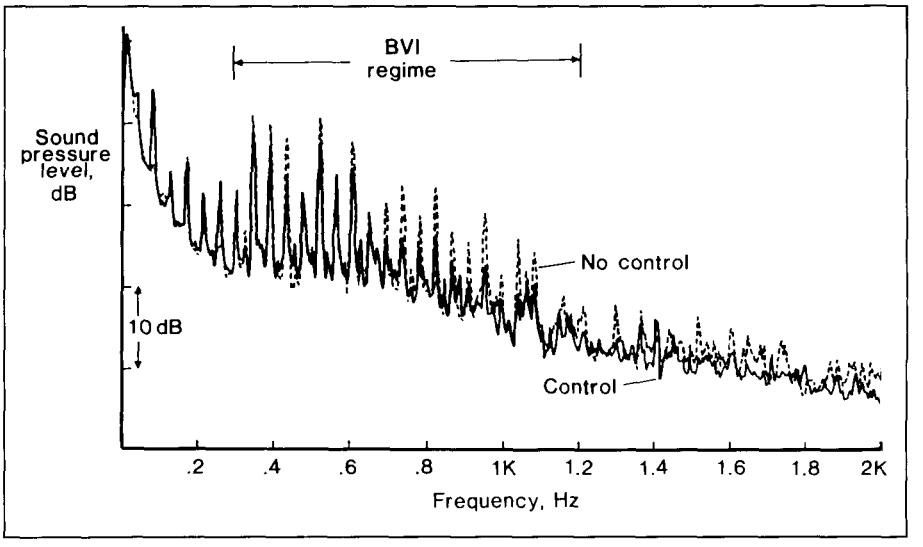

Sound spectra with and without acoustic loads control. L-87-6661

Demonstration of BVI Noise Reduction Concept

Blade/vortex interaction (BVI) is an intense source of helicopter noise. The present research demonstrates a concept for reduction of this noise source which grew out of earlier in-house analytical studies in which the sound pressure level produced by BVI was shown to depend upon several parameters, including the lift on the blade at the time of interaction. Since this noise source primarily occurs during descent (when maintaining lift is not of crucial importance), it appears feasible to reduce the BVI noise level by a lift reduction at the time of interaction. In addition, the position of such interactions is highly localized, occurring on the advancing side of the rotor disk at an azimuth angle of approximately 50° (where zero is directly behind the helicopter). Thus, an active control (AC) capability can be utilized to effect the necessary lift reduction.

A preliminary feasibility study of this concept was conducted in the TDT utilizing the Aeroelastic Rotor Experimental System (ARES). The model used four untwisted NACA 0012 blades of 4.5-ft radius and 4.24-in. chord which rotated at a tip Mach number of 0.628. A microphone was mounted in the ceiling of the tunnel above the expected location of the BVI. This test, over a range of tunnel speeds and tip-path-plane (TPP) angles, was the first acoustic test conducted in the Freon environment of the TDT. The figure displays measured acoustic pressure spectra at a tunnel speed of 52 ft/s (with a Mach number of 0.106 and an advance ratio of 0.17). The figure presents a comparison of the noise spectra at a TPP angle of 4°, where BVI is intense, with and without AC control of the blades. The BVI phenomenon is responsible for the high-pressure levels observed at multiples of the blade passage frequency (BPF) in the range 0.3 to 1.2 kHz. The lower spectrum is for the case in which AC was employed in an attempt to reduce the lift at the time of interaction. As each blade passed through the region where BVI is expected, its blade pitch angle θ was reduced by only 1°. As can be seen in the figure, this small local reduction in θ, which had little effect on the average thrust of the rotor, appears to reduce the noise level at the BPF harmonics in the range of interest by 3 to 4 dB. Theoretically, greater levels of control would produce even more noise reduction.

(E. R. Booth, Jr., 2645, J. C. Hardin, W. T. Yeager, Jr., M. L. Wilbur, C. W. Langston, and J. D. Singleton)

16-Foot Transonic Tunnel

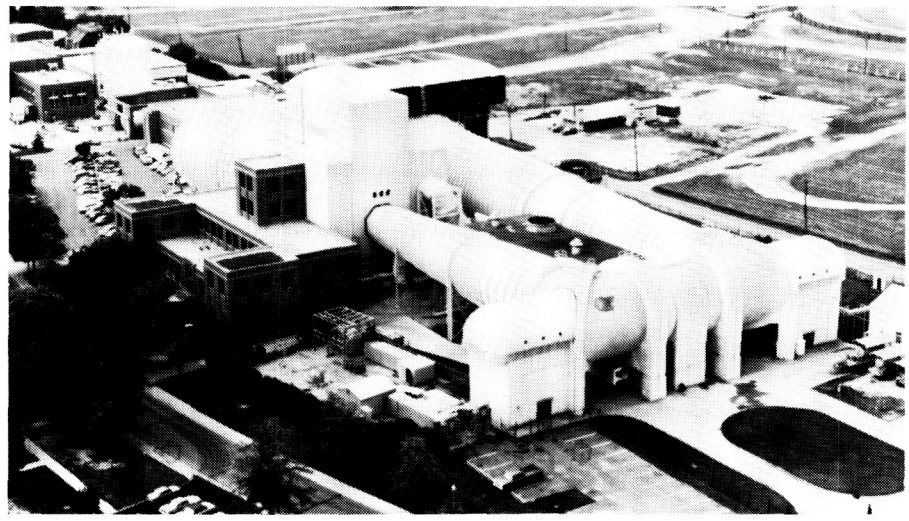

The Langley 16-Foot Transonic Tunnel is a closed-circuit single-return continuous-flow atmospheric tunnel. Speeds up to Mach 1.05 are obtained with the tunnel main-drive fans, and speeds from Mach 1.05 up to Mach 1.30 are obtained with a combination of main-drive and test section plenum suction. The slotted octagonal test section measures 15.5 ft across the flats. The tunnel is equipped with an air exchanger with adjustable intake and exit vanes to provide some temperature control. This facility has a main drive power of 60,000 horsepower, and a 36,000-horsepower compressor provides test section plenum suction.

The tunnel is used for force, moment, pressure, flow visualization, and propulsion-airframe integration studies. Model mounting consists of sting, sting-strut, and fixed-strut arrangements; propulsion simulation studies are made with dry, cold, high-pressure air.

The 16-Foot Transonic Tunnel is currently undergoing major modifications. In these modifications, the current strut support system will be replaced with a support system of higher strength and greater capability. A floor-mount system will be added to facilitate semispan model testing, and a model preparation area for model buildup and calibration is also included.

Force and Pressure Test of Maneuver Improvement Modifications for EA-6B Configuration

A wind tunnel investigation was conducted as part of a Navy/Grumman/NASA program to determine the effects of modifications of the leading-edge slats and trailing-edge flaps on the maneuver capability and stall margins of the EA-6B electronic countermeasures aircraft. Up to seven stores could be mounted under the wing and fuselage, and an electronics pod was mounted on the vertical tail on the 1/8.5-scale model. The test was conducted in the 16-Foot Transonic Tunnel at Mach numbers from 0.3 to 0.9, angles of attack up to 21°, and angles of sideslip from −4° to +12°. Force data were obtained from a main balance and two wing balances. Pressure distributions were obtained at five wing-span stations as well as on one of the seven stores and on the tail pod. The test was completed in October 1987.

Previous tests on the EA-6B configuration were conducted in the 7- × 10-Foot High-Speed Tunnel and the National Transonic Facility on a 1/16-scale model without wing pressure instrumentation. The effects of reduced wing base area, outboard droop, and a split aileron were also investigated. Clean wing-body configurations (with no stores and no tail) were included to provide data useful in the validation of transonic wing-body computational codes.

Results from this test verified the improved lift characteristics and minimal cruise drag penalties shown in

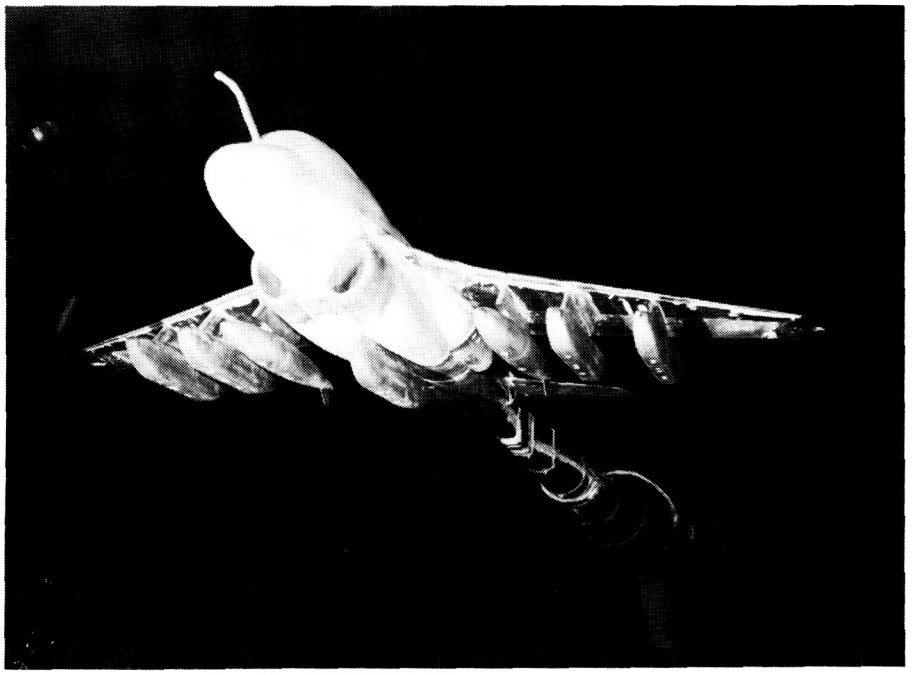

EA-6B model stores in 16-Foot Transonic Tunnel. L-87-09401

the earlier tests. The present test also showed that reducing wing base area produced no drag reduction but increased lift slightly. No measurable drag penalty was found for the outboard droop, which is known to be beneficial to longitudinal stability.
(D. O. Allison, 2601 and W. G. Sewall)

National Transonic Facility

The National Transonic Facility (NTF) is a cryogenic fan-drive transonic wind tunnel designed to provide full-scale Reynolds number simulation in the critical flight regions of most current and planned aircraft. It can operate at Mach numbers from 0.2 to 1.2, stagnation pressures from 1 to 9 atm, and stagnation temperatures from 340 K to 80 K. The maximum Reynolds number capability is 120 × 10⁶ at a Mach number of 1.0, based on a reference length of 0.25 m.

Construction of the NTF was completed in September 1982. The tunnel was declared operational in August 1984, and aerodynamic calibration and research and development testing were begun in 1984. The unique transonic capabilities of the NTF have been used primarily for highly important military programs during the past year.

Investigation Using Scale Model of Boeing 767

This test program was conducted as the first part of a Memorandum of Agreement (MOA) between NASA Langley Research Center (LaRC), NASA Ames Research Center (ARC), and the Boeing Commerical Airplane Company. The objectives of the MOA were first to obtain a comparable set of data between the ARC 11-Foot Transonic Tunnel, the Boeing Transonic Wind Tunnel (BTWT), and the LaRC National Transonic Facility (NTF) as a reference point among the three tunnels and then to conduct tests in the NTF to full-scale Reynolds numbers. An 0.03-scale model of the Boeing 767-200 airplane, specifically designed and fabricated for testing at cryogenic conditions, was used.

The first series of tests was conducted in air at a Reynolds number of 4×10^6/ft and 7.5×10^6/ft. Subsequent tests will be conducted at cryogenic temperatures. Ad-

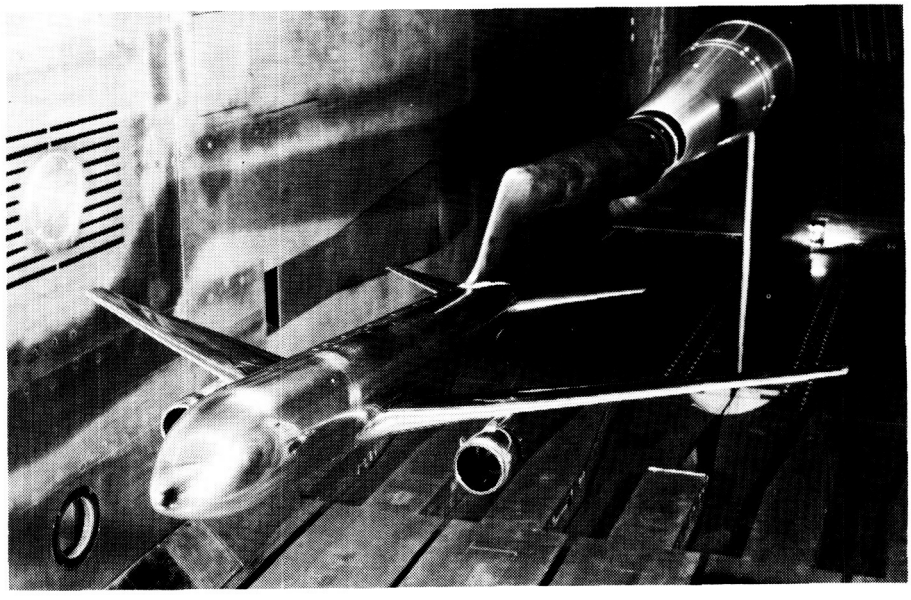

Boeing 767 in NTF. L-87-4167

ditionally, a flow angularity probe that traversed across the test section at approximately the same location as the Boeing 767 wing was tested in all three tunnels. Flow angularity in the NTF at these low Reynolds numbers was shown to be approximately 0.02°. Data from all these tests are currently being analyzed.
(S. G. Flechner, 2701)

Lockheed-Georgia 0.03-Scale Advanced Technology Wing

A cooperative research program between the Lockheed Aeronautical Systems Company–Georgia Division and NASA Langley Research Center has been conducted in the NTF to provide data for validating computational codes used by Lockheed in designing transport aircraft for the transonic speed regime. The model used for this study was the Lockheed-Georgia 0.03-Scale Advanced Technology Wing attached to the NTF *Pathfinder I* fuselage.

Pressure measurements were obtained on the wing, and force balance data were obtained for the complete configuration. The model was tested at Mach numbers from 0.2 to 0.85, at angles of attack from −4° to 6°, and at Reynolds numbers up to 40×10^6/ft over the temperature range of 120°F to −250°F. This range of Reynolds numbers will extend the current data base for defining the Reynolds number scaling effects.
(E. B. Plentovich, 2701)

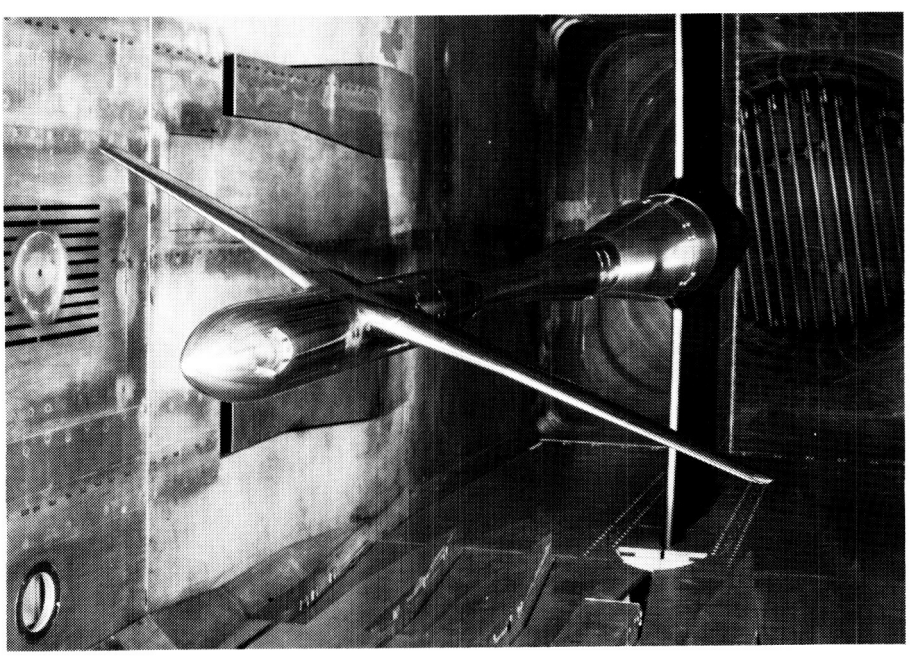

Lockheed-Georgia 0.03-Scale Advanced Technology Wing in NTF. L-87-12,187

0.3-Meter Transonic Cryogenic Tunnel

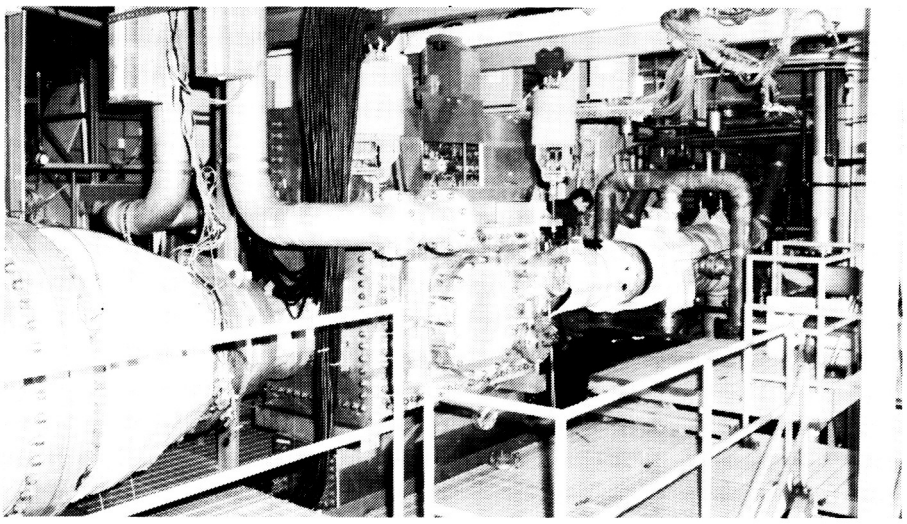

The Langley 0.3-Meter Transonic Cryogenic Tunnel (TCT) is a continuous-flow fan-driven transonic tunnel that uses nitrogen gas as a test medium. It is capable of Mach numbers up to approximately 1.0, stagnation pressures up to 6 atm, and stagnation temperatures from 340 K to approximately 80 K. The tunnel has been designed to permit different test sections to be installed in the circuit.

The facility was placed in operation in 1973 as a three-dimensional pilot tunnel to demonstrate the cryogenic wind tunnel concept at transonic speeds. The original test section was octagonal and was designed with a manually driven sting-type model support system. The successful demonstration of the cryogenic concept in the 0.3-Meter TCT played a major role in the decision to build the National Transonic Facility. In 1975, the three-dimensional test section was replaced with an 8- by 24-in. two-dimensional test section with slotted top and bottom walls. The two-dimensional test section has motorized model support turntables and a traversing wake survey probe, both of which are computer controlled. At the maximum test condition with a 6-in. model, a chord Reynolds number of 50 × 10^6 is possible. In 1985, the 8- by 24-in. test section was replaced with a 13- by 13-in. adaptive wall test section.

Adaptive wall test section.

In two-dimensional testing, adaptive walls reduce or eliminate top and bottom wall interference. A residual interference associated with the sidewalls can remain in the data. The change in the growth of the test section sidewall boundary layer with the model present causes the sidewall interference. The 9.0-in. CAST 10-2/DOA 2 model with sidewall boundary-layer removal upstream of the model was tested. These initial tests studied the problems of integrating the removal and injection of the test gas with the tunnel control system. Limited data were obtained with different removal rates to study the sidewall interference.

Two separate tests were made using a 180 mm (7.08 in.) chord CAST 10-2/DOA 2 airfoil in the adaptive wall test section. This model has been tested in the ONERA (Office National d'Etudes et de Recherches Aerospatiales) T2 adaptive wall wind tunnel and a DFVLR (Deutsche Forschung- und Versuchsanstalt fuer Luft und Raumfahrt) conventional wall wind tunnel. The original wall adaptation software was used to find the top and bottom wall shape for the first test. During the second test, a version of the ONERA T2 software was used to find the wall shape. These four tests offer a unique opportunity to study the effects of the adaptive wall test section hardware configuration and of the wall adaptation software algorithm on the airfoil data. The results of these tests are being studied.

(R. E. Mineck, 4385)

Unitary Plan Wind Tunnel

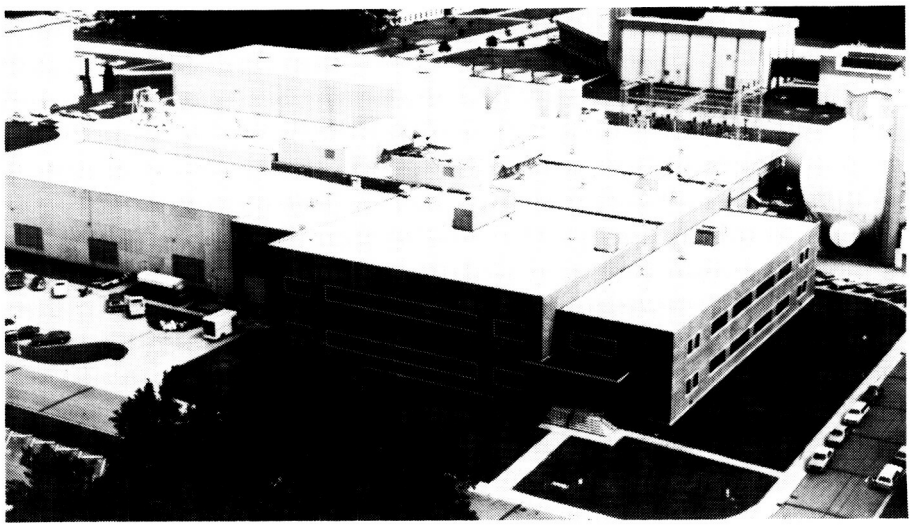

Immediately following World War II, the need for wind tunnel equipment to develop advanced airplanes and missiles was recognized. The military and the National Advisory Committee for Aeronautics (NACA) developed a plan for a series of facilities which was approved by the U.S. Congress in the Unitary Wind Tunnel Plan Act of 1949. This plan included five wind tunnel facilities, three at NACA laboratories and two at the Arnold Engineering Development Center. The Langley Unitary Plan Wind Tunnel (UPWT) was among the three built by NACA. The UPWT is a closed-circuit continuous-flow variable-density tunnel with two 4-ft by 4-ft by 7-ft test sections. The low-range test section has a design Mach number range of 1.5 to 2.9, and the high-range section Mach number varies from 2.3 to 4.6. The tunnel has sliding-block-type nozzles that allow continuous variation in Mach number while on-line. The maximum Reynolds number per foot varies from 6×10^6 to 11×10^6 depending on Mach number. The tunnel is used for force and moment, pressure distribution, jet effects, dynamic stability, and heat transfer studies. Flow visualization data, which are available in both test sections, include schlieren, oil flow, and vapor screen.

Off-Axis Wing/Body Tests

Recent advances in computational fluid dynamics (CFD) have resulted in computer codes tailored for application to supersonic missile aerodynamics. The Zonal Euler Solver (ZEUS) code, in particular, has relaxed some of the fin geometry restrictions that existed in earlier codes. For the first time, engineering CFD solutions are possible on missiles on which fins do not extend radially from the body centerline.

In order to assess the computational accuracy of these codes, experimental verification was needed. Thus, a wind tunnel study was initiated to provide a high-quality, systematic set of pressure and flow visualization data for use in assessing these codes. The model was designed such that its data would be compatible with the computational output from space-marching CFD codes. The body was a simple, slender ogive cylinder on which four sets of interchangeable fins could be mounted. These fins could be located in either a high-, mid-, or low-monoplanar wing arrangement as well as a "v" arrangement. In several of these positions, the relaxed fin geometry requirements of the ZEUS code could be experimentally tested.

The tests were performed in the low Mach number test section of the Unitary Plan Wind Tunnel at Mach numbers from 1.70 to 2.86, angles of attack from –4° to 24°, and various roll angles. Pressure sensors were mounted inside the model to eliminate lag-time problems in the data acquisition process. Vapor-screen photographs were taken to evaluate the vortex structures of the various wing-body combinations. The model contained a total

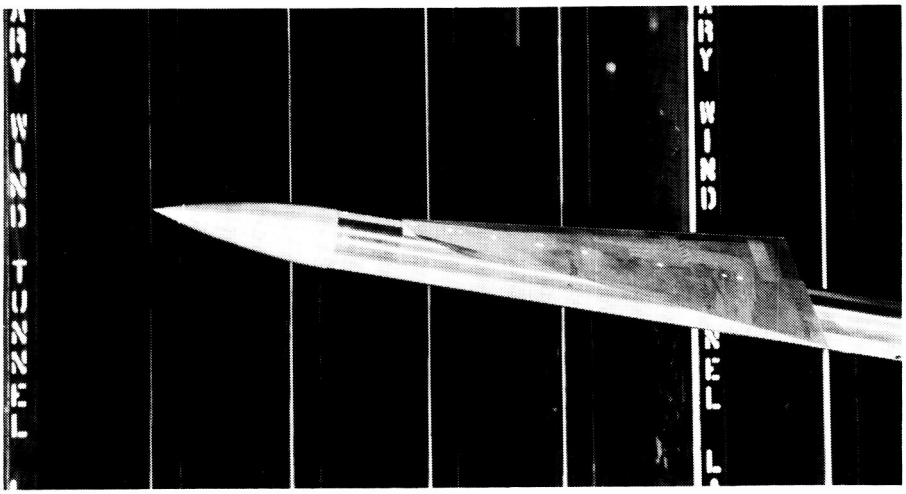

Off-axis wing/body model. L-87-8151

of 114 pressure orifices that were located across the entire configuration at constant longitudinal stations. At these stations, orifices were located around the body and on both the upper and lower surfaces of the fins. Reduction of the wind tunnel data has been completed, and comparison with the computational codes has begun. Preliminary experimental results show that the fin location has a large effect on both the fin and body pressures.
(P. S. Fulton, 4014 and J. M. Allen)

Passive Venting System for Reducing Cavity Drag

Existing data available in the literature have shown that at supersonic speeds the drag of rectangular cavities having length-to-height ratios approximately ≥ 12 is substantially greater than for smaller length-to-height ratios. This increase in drag is associated with a change in the cavity flow field resulting in an increase in pressure ahead of the cavity rear face and a decrease in pressure downstream of the forward face. An experimental investigation has been conducted in the Unitary Plan Wind Tunnel to determine the effectiveness of a passive venting system for reducing this cavity drag increase. The passive venting system consisted of a cavity that had a porous floor with a vent chamber beneath the floor which would permit the high-pressure air at the rear of the cavity to vent to the low-pressure region at the front of the cavity. It was expected that the venting process would modify the cavity flow field and reduce the cavity drag.

The wind tunnel model consisted of a flat plate, cavity pallet, and balance. The cavity pallet was mounted on a one-component (axial force) balance such that only the drag of the cavity was measured. The length of the cavity could be varied by using rectangular block inserts. Both solid and porous floor configurations were tested at Mach numbers of 1.6, 1.9, 2.16, and 2.86.

The solid-floor-cavity results showed the typical

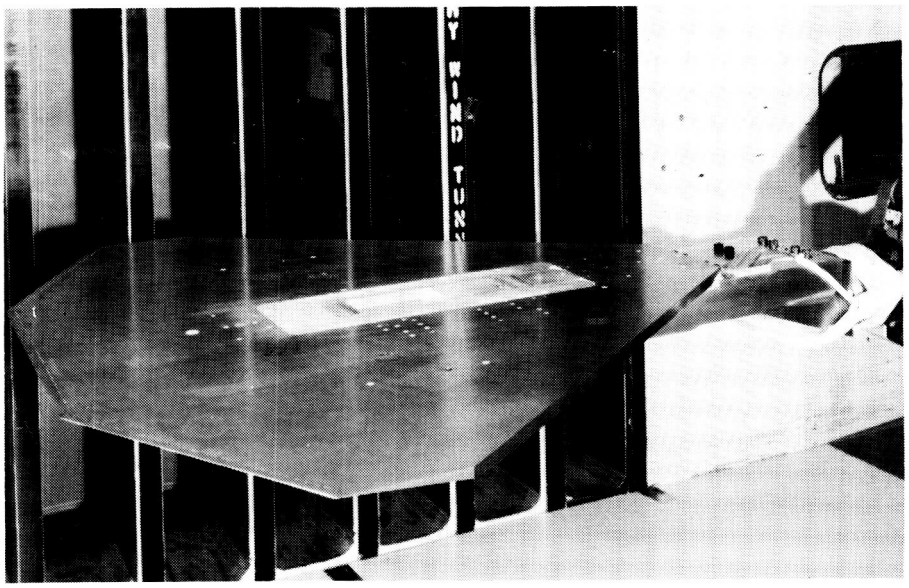

Cavity mounted in flat plate. L-87-3157

large drag increase as the cavity length-to-height ratio was increased; the porous-floor-cavity data eliminated this drag increase. Also, varying the vent chamber height had little effect on the porous floor cavity drag.
(F. J. Wilcox, 4010)

Investigation of Porous Cavity on Conical Wing in Supersonic Flow

In the subsonic/transonic flow regime, localized wing-surface porosity above an isolated cavity has been found to reduce drag by controlling the boundary-layer shock interaction on two-dimensional wings. Crossflow-shock/boundary-layer interaction on three-dimensional wings in supersonic flow has been shown to reduce aerodynamic performance; therefore, a means of reducing the crossflow-shock strength over a wide range of Mach numbers and angles of attack is appealing. To explore the application of wing-surface porosity at supersonic speeds, a wind tunnel investigation was conducted in the Unitary Plan Wind Tunnel to determine the effects on a conical wing in a supersonic flow. A porous cavity was installed in a 57° swept conical wing at a location that had been previously determined to have a crossflow shock. Porosities of 11.2 and 22.4 percent, porosity hole diameters of 0.025 in. and 0.050 in., and cavity depths of 0.067 and 0.255 in. were investigated.

The tests were conducted at a Reynolds number of 2×10^6/ft at Mach numbers of 1.62, 1.70, 1.86, and 2.0. The angle of attack varied between −2° and 10°. Upper-surface pressures and vapor-screen flow-visualization results were obtained to evaluate the flow characteristics about the wing.

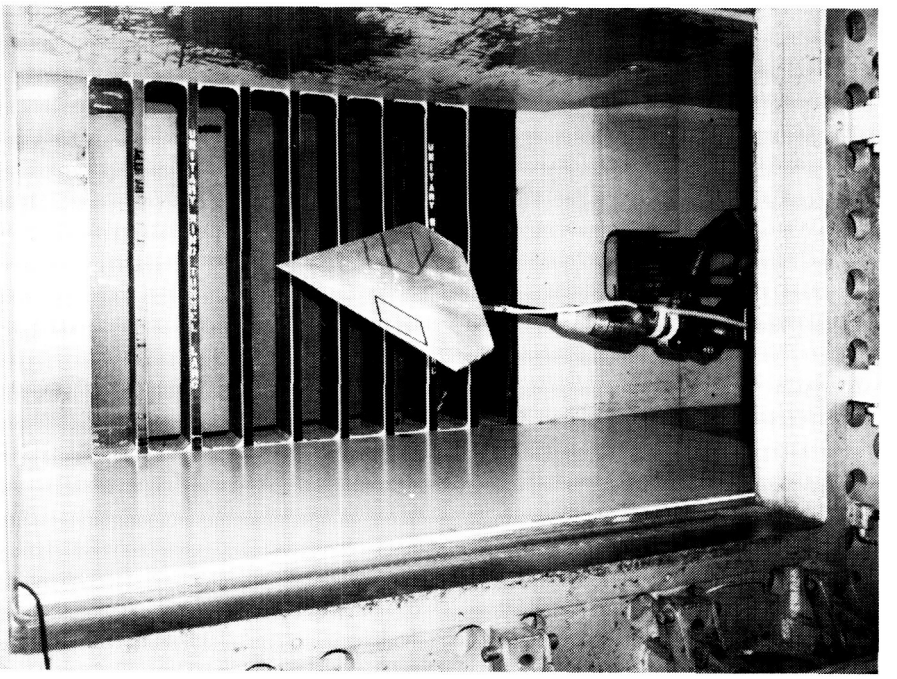

Wing with porous cavity in Unitary Plan Wind Tunnel. L-86-8785

Test results with the porous cavity were compared with those obtained from a solid-surface wing. From pressure coefficient plots and vapor-screen photographs, it was found that the boundary-layer separation was delayed over the porous surface to higher lift conditions due to a reduction in the shock strength. These characteristics were observed at all test Mach numbers. In addition, the experimental data indicated that only hole size and surface porosity had a strong impact on the effectiveness of the porous cavity.
(S. X. S. Bauer, 3181)

Hypersonic Facilities Complex

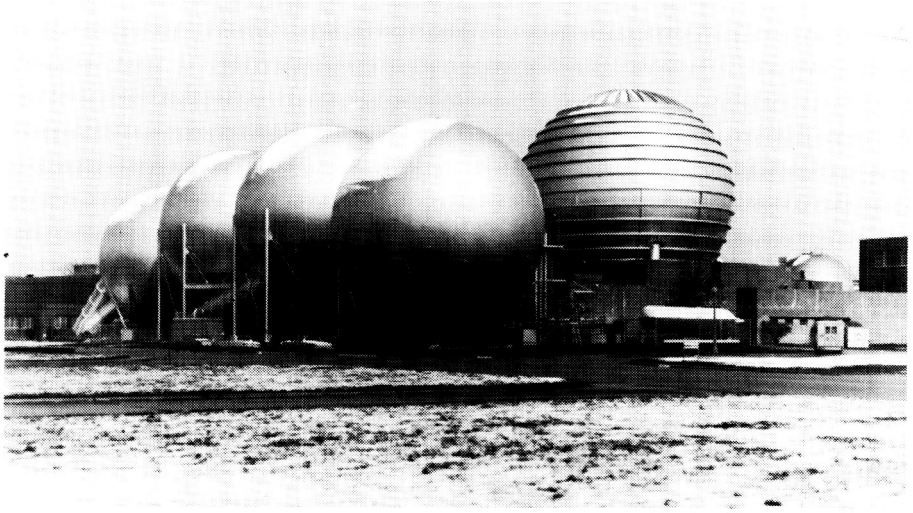

The Hypersonic Facilities Complex consists of several hypersonic wind tunnels located at four Langley Research Center sites. They are considered as a complex because these facilities represent a major unique national resource for wind tunnel testing. The complex currently includes the Hypersonic CF_4 (tetrafluoromethane) Tunnel (M = 6), the Mach 6 High Reynolds Number Tunnel, the 20-Inch Mach 6 Tunnel, the Mach 8 Variable-Density Tunnel, the 31-Inch Mach 10 Tunnel, the Hypersonic Nitrogen Tunnel (M = 17), and the Hypersonic Helium Tunnel and its open jet leg (M = 20). These facilities are used to study the aerodynamic and aerothermodynamic phenomena associated with the development of advanced space transportation systems, including future orbital-transfer and launch vehicles; to support the development of Aero-Space Plane technology; to support the development of future planetary entry probes; to support the development of hypersonic missiles and transports; to perform basic fluid mechanics studies, to establish data bases for verification of computer codes, and to develop measurement and testing techniques. A significant amount of the current testing in these facilities is classified, thus restricting the amount and content of test results that can be reported in the open literature.

CF_4 TUNNEL
$M_\infty = 6$ CF_4 $R_\infty = 0.25\text{-}0.55 \times 10^6$

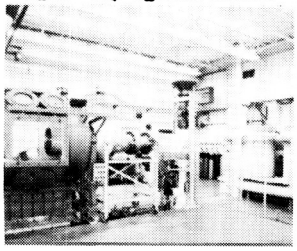

HIGH R_∞ M-6 TUNNEL
$M_\infty = 6$ AIR $R_\infty = 0.8\text{-}42.0 \times 10^6$

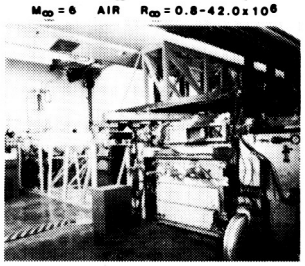

20-INCH M-6 TUNNEL
$M_\infty = 6$ AIR $R_\infty = 0.7\text{-}9.0 \times 10^6$

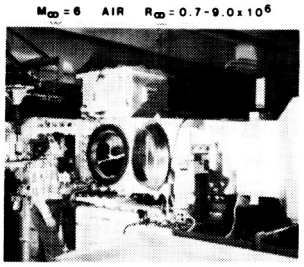

M-8 VAR.-DENS. TUNNEL
$M_\infty = 8$ AIR $R_\infty = 0.1\text{-}10.7 \times 10^6$

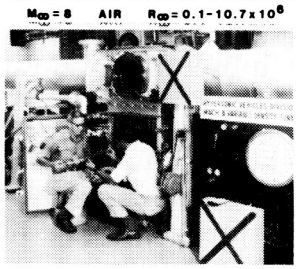

31-INCH M-10 TUNNEL
$M_\infty = 10$ AIR $R_\infty = 0.4\text{-}2.4 \times 10^6$

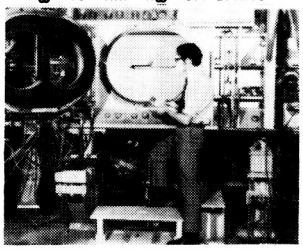

NITROGEN TUNNEL
$M_\infty = 17$ N_2 $R_\infty = 0.35 \times 10^6$

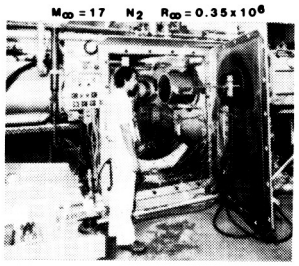

HELIUM TUNNEL
$M_\infty = 19\text{-}21.6$ He $R_\infty = 3.5\text{-}12.5 \times 10^6$

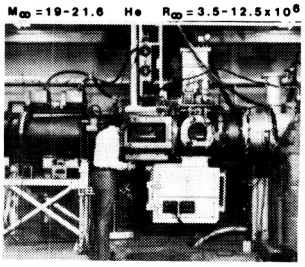

OPEN JET LEG-HE TUNNEL
$M_\infty = 20$ He $R_\infty = 6.0 \times 10^6$

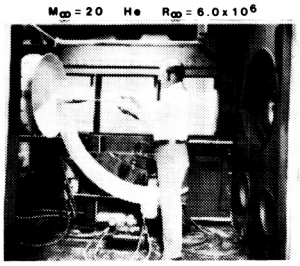

This complex of facilities provides an unparalleled capability at a single installation to study the effects of Mach number, Reynolds number, test gas, and viscous interactions on the hypersonic characteristics of aerospace vehicles. Several modifications have been made to the facilities to improve their capabilities.

Demonstration of two-color phosphor thermography system in hypersonic wind tunnel.

A study was initiated to develop a method for obtaining simultaneous heat-transfer measurements and aerodynamic force and moment measurements on hypersonic wind tunnel models. The study approach was to develop a thermal imaging system using an appropriate optical measurement technique providing quantitative surface temperature data. A technique for quantitative thermal imaging was developed using two-color thermographic phosphors.

The thermal imaging technique is based on the ratio of measured blue to green (450, 520 nm) emission from a phosphor coating excited by an ultraviolet (365 nm) source. Separately filtered images are recorded from a three-tube color camera, utilizing off-the-shelf front-end video optics to discriminate wavelengths. Digital processing is used to calculate surface temperature profiles from video image data.

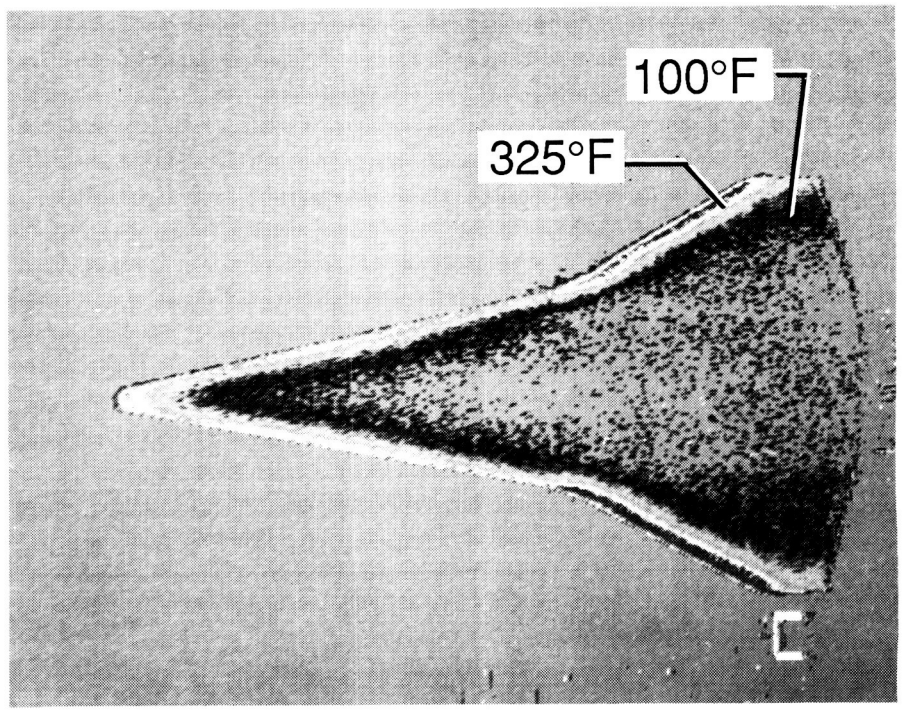

Windward surface temperature mapping on a transatmospheric model in 31-Inch Mach 10 Tunnel.

The technique provides ideal surface temperature-time data necessary in calculating heat-transfer coefficients.

Tests demonstrating the Thermal Imaging System (TIS) (also discussed on page 100 describing the Image Processing Laboratory) were performed in the 31-Inch Mach 10 Tunnel using phosphor-coated cast ceramic models (as shown in the figure). Models tested included a 12.84°/7° straight biconic with a 3-in. base, an 11-in. strake/wing transatmospheric vehicle, and a 9.5-in. slender blunted cone. Cone models were cast around stainless-steel balance insertion sleeves, although force and moment measurements were not conducted for this TIS demonstration test. Image data were recorded on 3/4-in. videotape and processed at Langley Research Center's Image Processing Laboratory. Work is currently under way to develop a dedicated digital acquisition/image processing system. **(G. M. Buck, 3984)**

Low-density flow in hypersonic CF_4 Tunnel.

Some of the aerodynamic effects of air dissociation (real-gas effects) between the shock and body of an entry vehicle during flight can be simulated by reproducing the density ratio across the normal shock in a wind tunnel. The Hypersonic CF_4 Tunnel uses tetrafluoromethane (CF_4)

as a test gas, which allows a partial simulation of real-gas effects by producing a normal shock density ratio of approximately 12. This ratio is closer to the flight value (approximately 17) than the ratio obtainable in an air or nitrogen tunnel (approximately 6). Some vehicles not only fly at very high velocities (thus resulting in shock-induced dissociation) but also at very high altitudes. This high-altitude flight occurs in a low-density flow field that is not generally available as a test condition in this nation's hypersonic facilities. These low-density effects can change vehicle aerodynamic characteristics dramatically,

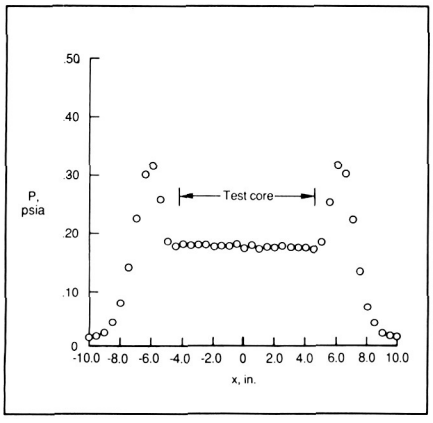

Test stream pitot pressure profile in Hypersonic CF_4 Tunnel at reservoir pressure of 133 lb/in^2.

particularly for blunt-body configurations. (An example of a class of high-velocity, high-altitude flight vehicles with blunt configurations is the Aeroassisted Orbital Transfer Vehicle, AOTV.)

Recently, in an attempt to better simulate high-altitude, low-density flight conditions, the Hypersonic CF_4 Tunnel has been successfully operated at a reservoir pressure as low as 100 lb/in^2. The normal reservoir operating pressure is in the range from 1500 lb/in^2 to 2000 lb/in^2. Measurement with a pitot rake at the low-pressure condition indicated a nearly constant pitot pressure distribution over an 8-in.-diameter core, which is comparable to the high-pressure test core size.

Much work will be required to assure that flow conditions are correctly calculated and that all types of wind tunnel testing can be carried out in this low-density environment. However, results obtained so far suggest that the effects of a high value of normal shock density ratio and low test stream density may be obtained in the same test environment.

(R. E. Midden and W. L. Wells, 3984)

Pitot-pressure probe for flow field surveys.

A relatively fast response (less than 0.3 s), miniaturized pitot-pressure probe has been designed, fabricated, and successfully demonstrated in the flow field about a 2 to 1 elliptical cone in the 20-Inch Mach 6 Tunnel. The probe, which has an 0.013-in. outside diameter, has the pressure transducer located within the probe body approximately 2.5 in. from the probe tip and is surrounded by a water jacket. The water cooling reduced the temperature at the transducer during the tunnel tests from 325°F to 103°F, which is normally low enough to avoid thermal effects on the accuracy of the transducer. During the tunnel tests, the probe was also shown to be small enough to eliminate the intrusive interference that occurred between a

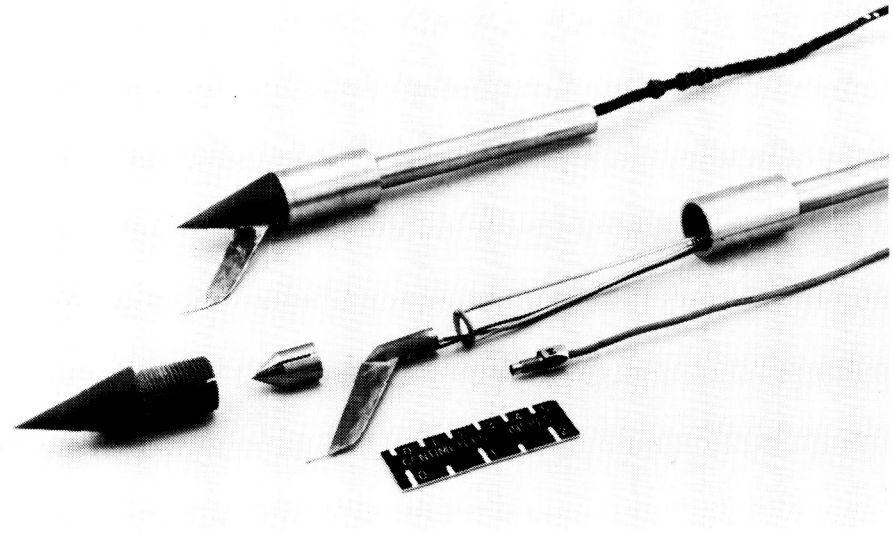

Assembled probe and disassembled probe components. L-87-8455

larger probe and the laminar boundary layer on the cone model.
(G. C. Ashby, Jr., 3984)

Supersonic Characteristics of Modified Circular Body Vehicles

One concept now under study as an advanced space transportation system is based on the requirement of full reusability. This requirement results in a single-stage-to-orbit vehicle that carries the propellant internally, is launched vertically, and lands horizontally. The basic configuration consists of a fuselage having a circular cross section, a cropped delta wing, and a large vertical tail. The circular body vehicle is 197 ft long, which is about twice the size of the Space Shuttle orbiter. This study has been expanded to ascertain the effects of two alternate versions on the aerodynamic characteristics. One version employed wing tip fins instead of the vertical tail, whereas the second version used a small nose-mounted dorsal fin with fuselage side brakes. Force and moment tests were conducted in the Unitary Plan Wind Tunnel at Mach numbers of 2.3, 2.96, 3.9, and 4.6. Data on the basic vehicle and the two alternate versions were obtained over an angle-of-attack range of 0° to 22° at a Reynolds number of 4.3×10^6 based on fuselage length.

For all three models, stable trim conditions were obtained at $M = 3.9$ and 4.6 by using elevon controls. The vertical-tail model yielded stable trim at the two lower Mach numbers. The tip fin and dorsal versions generally had only neutral stability for $M = 2.96$. At $M = 2.3$, the dorsal model indicated stable conditions at the operational angle of attack of 10°, whereas the tip fin model was unstable. With the center of gravity located at 72 percent of the fuselage length, the tip fin and dorsal versions were directionally unstable. Directional stability existed for the vertical-tail model, but only at angles of attack below approximately 10°. A positive effective dihedral was obtained over the angle-of-attack range of 0° to 22° for the vertical-tail model. For the other two versions, a positive dihedral was indicated at angles of attack above approximately 10°. In general, it appears that the basic model with the large vertical tail yielded better longitudinal and directional stability characteristics when compared with the alternate versions.
(P. T. Bernot, 3984)

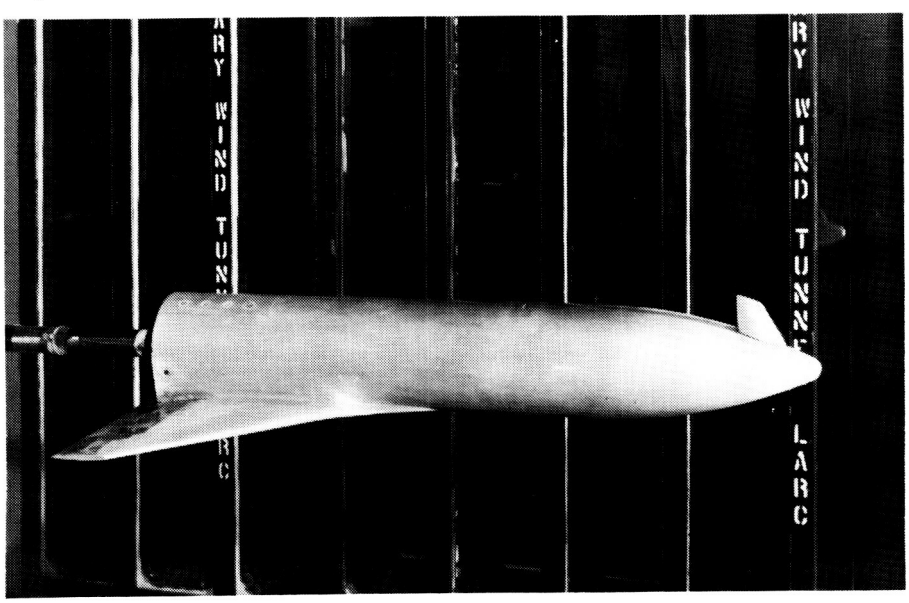

Dorsal fin alternate model mounted in Unitary Plan Wind Tunnel. L-87-4420

Exploratory Hypersonic Helium Tests on Inlet

The emphasis on the National Aero-Space Plane (NASP) has generated the need to extend simple inlet testing to high Mach numbers. A variety of simple inlet models existed which were tested in air at $M = 4$, and one model was adapted for installation in the Hypersonic Helium Tunnel with modifications to provide for additional parametric variations. Contraction ratio, cowl position and sweep, and Reynolds number were among the test variables considered. Mea-

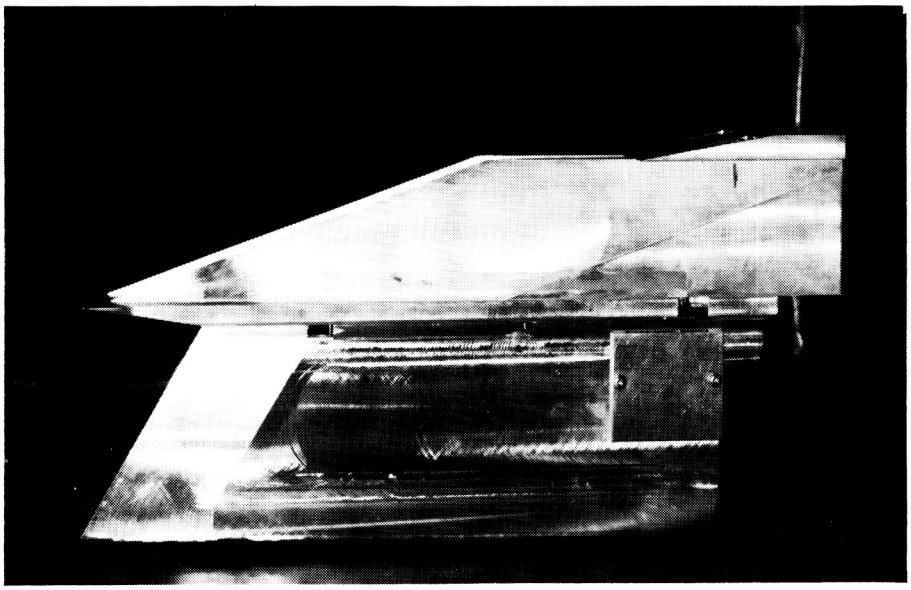

70° swept simple hypersonic inlet installed in Hypersonic Helium Tunnel (22-in. leg). L-87-7809

sured data included pressures on the centerline and at two locations on the side walls. Flow visualization was provided by the electron beam technique. Concerns included the possibility of an unstarted tunnel or inlet because there was no previous test experience either in this facility or others at these high Mach numbers (M = 20). Test objectives included determining the ability to test reasonably sized inlets at M = 20 in helium and to generate sufficient data for computational fluid dynamics (CFD) calibration.

Tunnel flow conditions were fully established for the extremes of tunnel operation (M = 18 to 22, and Reynolds number = 2×10^6 to 12×10^6/ft). Measured pressures and flow visualization data were obtained for both started and unstarted inlets, depending on inlet configuration and test conditions. Both 30° and 70° swept inlets appeared to start at contraction ratios of 4 and 5 with the cowl at the throat. Moving the cowl forward produced an unstarted flow for the 30° inlet, but the 70° inlet remained started at the lower contraction ratio. All configurations exhibited possible corner flow effects and flow separation. Results confirmed the ability to determine internal pressure, shock structure, surface flow structure, and mass flow of a variety of inlet configurations at M = 20 for CFD calibration.

(W. C. Woods, 3984)

Simulation of Real-Gas Effects on Pressure Distributions for Proposed Aeroassist Flight Experiment Vehicle

An extensive hypersonic aerodynamic/aerothermodynamic data base for the

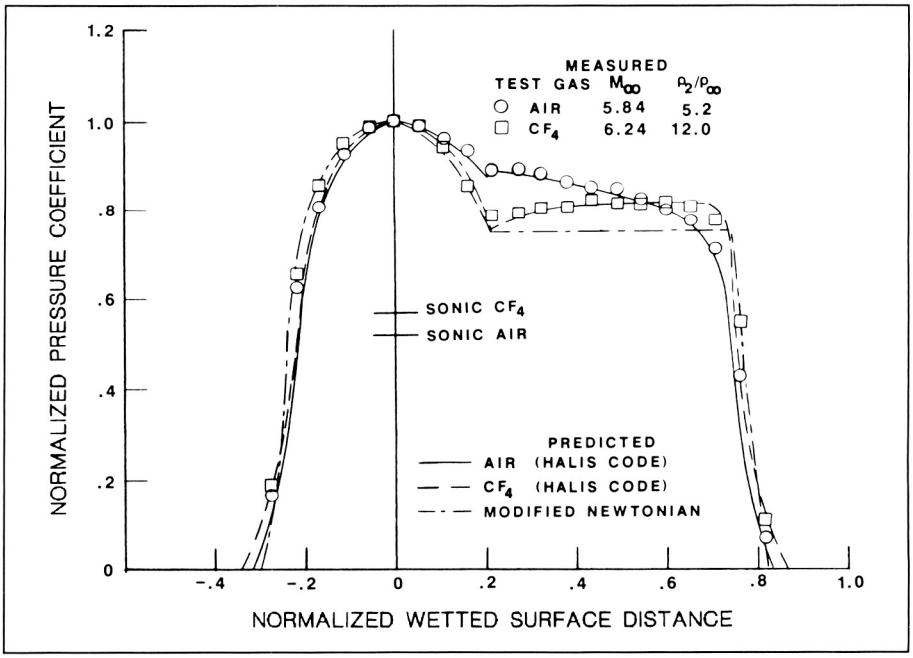

Effect of normal shock density ratio (ρ_2/ρ_∞) on pressure distributions for AFE vehicle at α = 0° and Mach = 6.

Aeroassist Flight Experiment (AFE) vehicle has been initiated at the Langley Research Center. The experimental data base, when completed, will include forces and moments, pressures, and heat transfer rates measured over the forebody and in the wake-flow regions of the AFE. These data will be used to validate computational fluid dynamics codes over a wide range of hypersonic continuum-flow conditions.

Tests were recently performed in the Hypersonic Facilities Complex to examine the effects of angle of attack, Reynolds number, and normal shock density ratio on detailed pressure distributions over the forebody of the AFE. The high-density ratio aspect of a real gas in thermochemical equilibrium was investigated at Mach 6 by testing in ideal air (density ratio equal to 5.25) and in CF_4 (density ratio equal to 12.0). Reynolds number was varied from 0.60×10^6/ft to 2.2×10^6/ft in air and from 0.25×10^6/ft to 0.58×10^6/ft in CF_4. Pressure distributions predicted with modified Newtonian theory and an inviscid flow field computer code known as HALIS (High Alpha Inviscid Solution) were compared to measurements for angles of attack of 0°, −10°, and 10°.

Results indicate a significant density ratio effect in the nose/cone expansion region of the configuration; however, the magnitude of this effect decreased with increasing angle of attack. A negligible effect of Reynolds number was observed over the range of angle of attack for the present test conditions. Pressure distributions predicted with the HALIS code were in good agreement with measurement (as shown in the figure). Predictions with the modified Newtonian theory were in poor agreement with measurements over the cone section for air, but in reasonable agreement with the CF_4 data.

(J. R. Micol, 3984)

Scramjet Test Complex

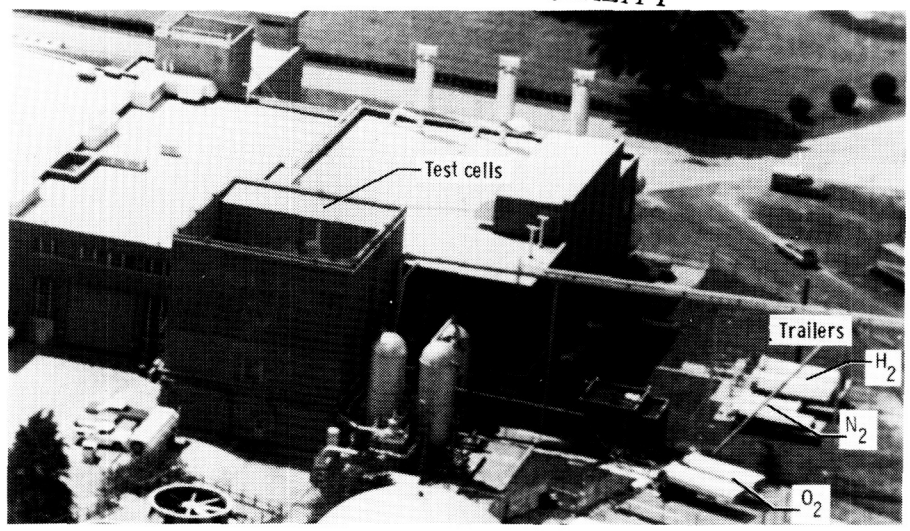

After an almost 15-year lull in interest for hypersonic flight, there is again a strong emphasis on the potential for a number of applications. These applications include an Aero-Space Plane or transatmospheric vehicle, which would be able to take off from a conventional runway and fly to orbit, as well as a variety of hypersonic airplane concepts for military reconnaissance, strike, or semiglobal transports. Langley Research Center has maintained a research team that has been working on basic hypersonics continuously throughout the last several decades. Facilities that played a key role at Langley in developing the present Space Shuttle configuration have been applied to a wide variety of other aerospace vehicles. Langley, the lead Center in defining Shuttle II, has been the only research organization in the nation to continuously maintain a viable effort in hydrogen-fueled supersonic combustion ramjet propulsion since the 1960's. Ground tests of subscale engines conducted in the Scramjet Test Complex have demonstrated levels of net thrust sufficient to accelerate at Mach 4 and to cruise an airplane at speeds up to Mach 8 and beyond. These results are entirely consistent with the projection of attractive performance up to much higher speeds, even approaching orbital velocity.

A research program to develop technology for a hydrogen-burning airframe-integrated supersonic combustion ramjet (scramjet) propulsion system has been under way for several years at Langley. The experimental portion of this research consists of tests of engine components (inlets, combustors, and nozzles) and complete, component integration engine models.

Small-scale inlet tests for "screening" potential inlet designs are performed in a 9- by 9-in. Mach 4 blowdown tunnel. Larger scale inlet tests are performed in various other Langley aerodynamic wind tunnels. Small-scale direct-connect combustor tests that simulate a portion of the engine combustor are conducted in Test Cell #2 to provide basic research data on supersonic mixing, ignition, and combustion processes. The hot test gas is supplied to the combustor models by a hydrogen-air-oxygen combustion heater, which maintains 21-percent free oxygen by volume to simulate air with enthalpy levels ranging up to Mach 8 flight speeds. Various facility nozzles produce the desired combustor entrance flow conditions.

Designs from the individual component tests are assembled to form component integration engines so that tests can be conducted to understand any interactions between the various engine components and to determine the overall engine performance. These component integration tests are conducted in engine test facilities. The feature that separates these propulsion facilities from aerodynamic wind tunnels is their capability to produce true-velocity, true-temperature, and true-pressure flow for flight simulation.

The Combustion-Heated Scramjet Test Facility (CHSTF, Test Cell #1) uses a hydrogen-air-oxygen com-

Small-Scale Inlet Tests

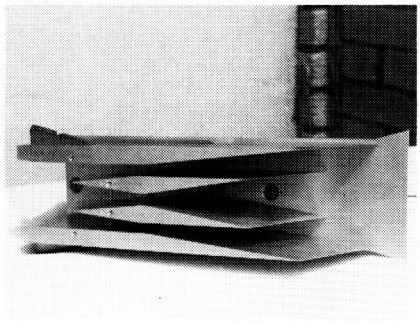

Inlet Model

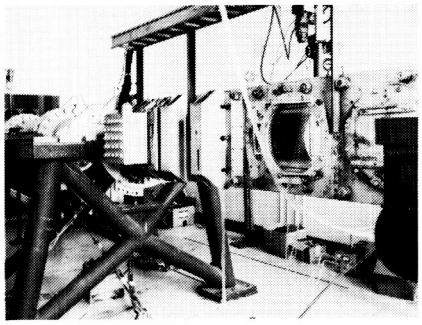

Mach 4 Blowdown Tunnel

Small-Scale Combustor Tests

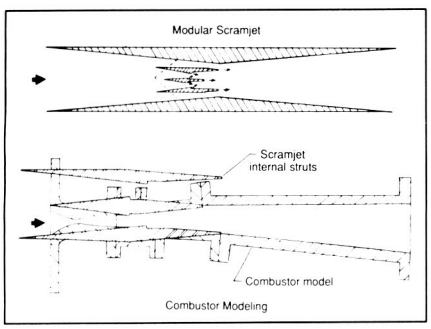

Combustor Modeling

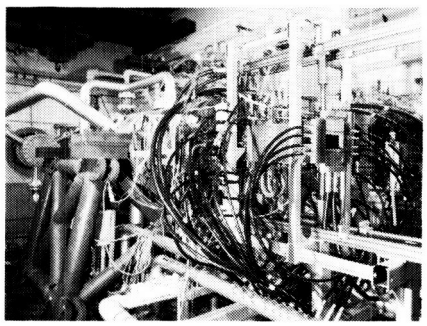

Test Cell #2

Engine Model Tests

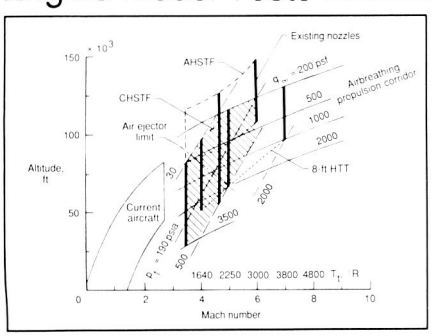

Potential Test Capability

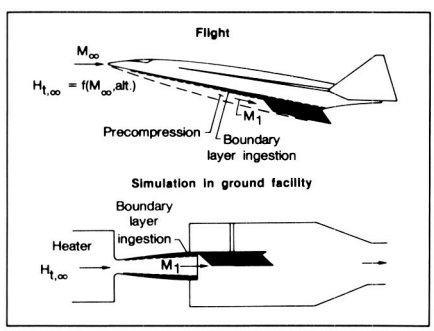

Flight Condition Simulation

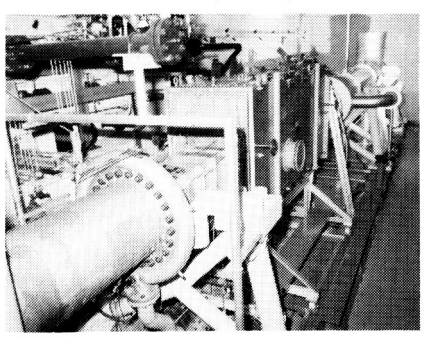

CHSTF; Test Cell #1

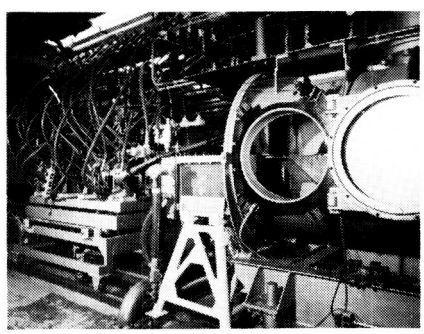

AHSTF

bustion heater to duplicate Mach 4 flight enthalpy. The test gas is exhausted to the atmosphere with the aid of an air ejector. A Mach 3.5 contoured nozzle with a 13-in.-square exit is presently attached to the heater to yield a free-jet tunnel flow (simulating Mach 4 flight conditions) for subscale engine tests. The Arc-Heated Scramjet Test Facility (AHSTF, Test Cell #2) uses an electric-arc heater to produce enthalpy levels corresponding to flight speeds up to Mach 8. The tunnel exhausts into a 100-ft-diameter vacuum sphere. Eleven-in.-square exit nozzles (Mach 4.7 and 6) are used to deliver a free-jet tunnel flow for scramjet engine tests. The same size models (frontal view approximately 6 by 8 in.) are tested in both these facilities.

By 1989, an oxygen replenishment system and new facility nozzles will be added to the Langley 8-Foot High-Temperature Tunnel (8-Foot HTT), which is presently part of the Aerothermal Loads Complex. This tunnel will then be capable of testing large-scale engines (about 20 by 28 in.), multiple engines, or engines that have full nozzle expansion surfaces at Mach numbers of 4, 5, and 7. In addition, the operational capability of the Combustion-Heated Scramjet Test Facility is being enhanced by a new test gas heater, a new Mach 4.7 nozzle, and a new vacuum sphere/steam ejector system. Upon completion of these modifications, the 8-Foot HTT, together with the smaller scale facilities described, will

comprise a Scramjet Test Complex at Langley unequaled in the western world. The potential operational envelope of this complex would extend over a flight Mach number range from 3.5 up to 7. Some of the current testing in these facilities is classified, thus restricting the amount and content of test results that can be reported in the open literature.

Parametric Scramjet Engine Tests

The many complex flow phenomena that occur in a scramjet can be most easily studied in an engine with a simple internal geometry; however, geometric versatility is also essential. The parametric scramjet shown in the first figure was designed at Langley Research Center to meet these needs. The internal geometry of the model is simply a converging/diverging channel with rectangular cross sections. Inlet compression and combustor/nozzle expansion are accomplished on the engine sidewalls, which are each composed of five segments. The engine top surface and bottom cowl are flat plates within the scramjet. Both plates contain slotted bolt holes so that the entire sidewalls, or any of the five individual segments, can be moved (or exchanged) between tests to change model internal width (or geometry). When the sidewalls are moved as units, the contraction ratio is changed. Movement of individual sidewall segments in the combustor can be used to create forward and/or rearward-facing steps to study flameholding, etc. Several fuel manifolds, located along the length of the combustor sidewalls, are used to tailor fuel injection distribution and, hence, fuel/air mixing and heat release.

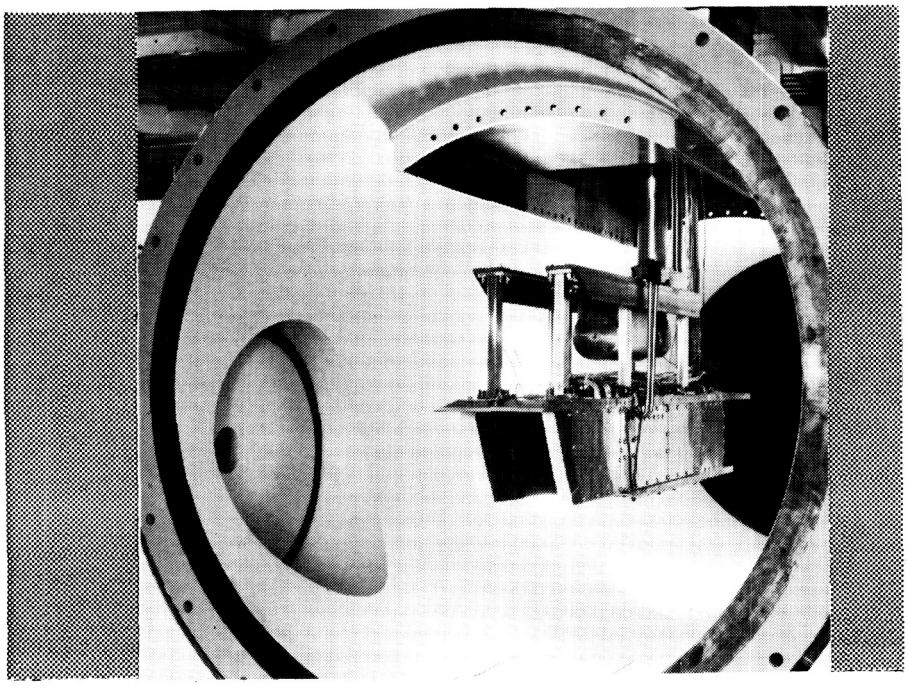

Parametric scramjet in Arc-Heated Scramjet Test Facility. L-86-3872

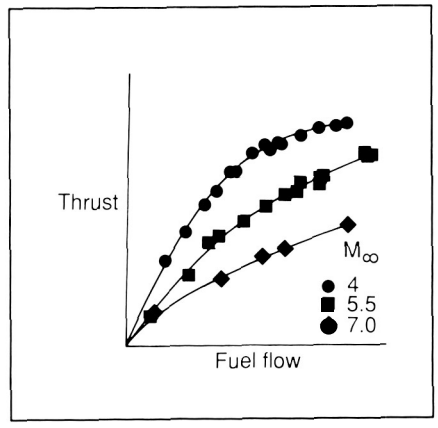

Parametric engine test results.

The parametric scramjet has been extensively tested in the Arc-Heated Scramjet Test Facility and in the Combustion-Heated Scramjet Test Facility over a simulated flight Mach number range from 3.5 to 8. Numerous geometric configurations of the engine have been tested, and experimental information is available on thrust performance (as indicated in the second figure), simulated aircraft forebody precompression, boundary-layer ingestion, flameholding, combustor-inlet interaction, and inlet unstart. Some of these data have been used to develop correlations that can be used to reduce the number of engine tests required and to define various scramjet limits. Results obtained from tests of the parametric scramjet

have provided a significant portion of the scramjet data base available for use in the National Aero-Space Plane (NASP) Technology Maturation Program.
(R. W. Guy, 3772)

Scramjet Exhaust Gas Simulation on Two-Dimensional Nozzle Model

A study performed during the 1970's by the Grumman Aerospace Corporation (under contract to the Langley Research Center) examined the requirements for adequate experimental wind tunnel simulation of scramjet exhaust flows. It was found that the combustor exit Mach number, ratio of specific heats, and transport properties are important simulation parameters and that any of several relatively cold substitute gas mixtures are applicable. A substitute gas-mixing apparatus for the Langley 20-Inch Mach 6 Tunnel was then designed and constructed. Testing on a two-dimensional (2-D) scramjet nozzle model with argon/Freon gas mixtures was initiated; however, the test matrix was not completed.

A recent effort has been begun in support of the National Aero-Space Plane Program to reactivate this dormant apparatus and to complete testing on the 2- D scramjet nozzle model. In the first phase, the apparatus was recertified and the model tested with only air; this phase has just been completed.

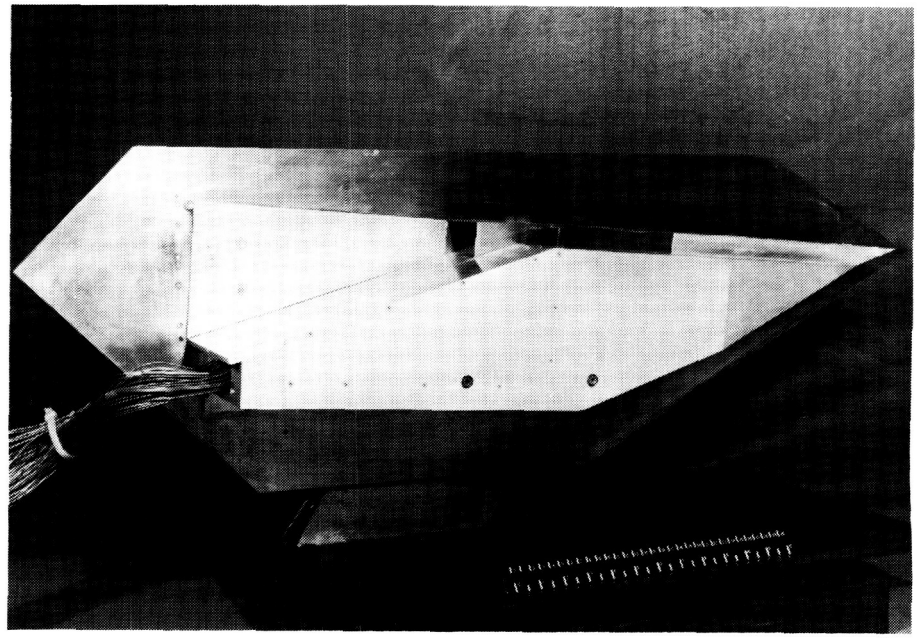

2-D scramjet nozzle wind tunnel model. L-87-2305

The wind tunnel model shown in the figure was designed to simulate the external nozzle created by a scramjet exhausting onto a vehicle afterbody. The flat inclined ramp illustrated was instrumented to measure surface pressures and could be configured with or without a flow fence. Tests were conducted over a range of angles of attack, ramp angles, and combustor exit pressure ratios at a free-stream Mach number of 6.

A comparison of preliminary results of the present air tests with the previous substitute gas tests indicates significant differences in the pressure levels on the ramp afterbody. The greatest differences were measured just aft of the nozzle exit and decreased to zero at approximately midlength of the ramp. The results of these tests, although preliminary, clearly indicate the necessity for properly simulating key exhaust flow parameters such as transport properties and the ratio of specific heats as well as combustor exit Mach number and nozzle pressure ratio to obtain meaningful powered configuration data, particularly at hypersonic speeds. Analysis of the current data is continuing, and plans for further simulating gas testing (the second phase) are being implemented.
(W. J. Monta, 4014)

Aerothermal Loads Complex

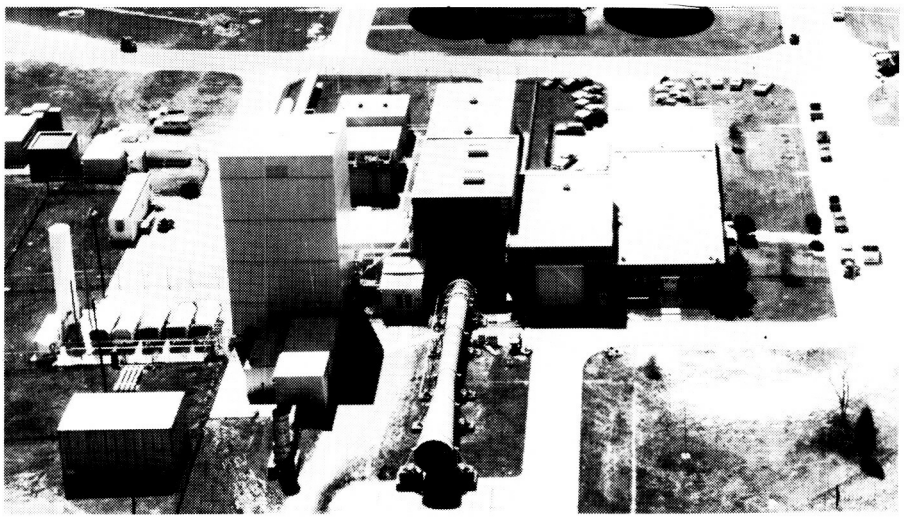

The Aerothermal Loads Complex consists of four facilities that are used to carry out research in aerothermal loads and high-temperature structures and thermal protection systems. The 8-Foot High-Temperature Tunnel (8-Foot HTT) is a Mach 7 blowdown-type facility in which methane is burned in air under pressure and the resulting combustion products are used as the test medium with a maximum stagnation temperature near 3800°R in order to reach the required energy level for flight simulation. The nozzle is an axisymmetrical contoured design with an exit diameter of 8 ft. Model mounting is semispan or sting with insertion after the tunnel is started. A single-stage air ejector is used as a downstream pump to permit low-pressure (high-altitude) simulation. The Reynolds number ranges from 0.3 to 2.2 × 10^6 per foot with a nominal Mach number of 7, and the run time ranges from 20 to 180 s. The tunnel is used for studying detailed thermal-loads flow phenomena as well as for evaluating the performance of high-speed and entry vehicle structural components. A major effort is under way to provide alternate Mach number capability as well as O_2 enrichment

8-FOOT HIGH-TEMPERATURE TUNNEL
M = 7 R_n = 0.3 - 2.2 × 10^6
H = 700 - 1000 BTU/lb

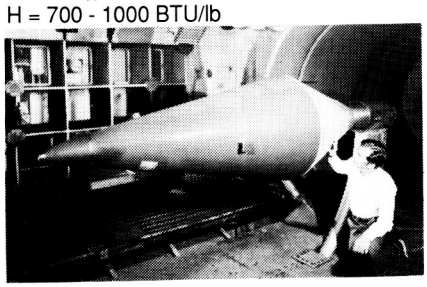

7-INCH HIGH-TEMPERATURE TUNNEL
M = 7 R_n = 0.3 - 2.2 × 10^6
H = 700 - 1000 BTU/lb

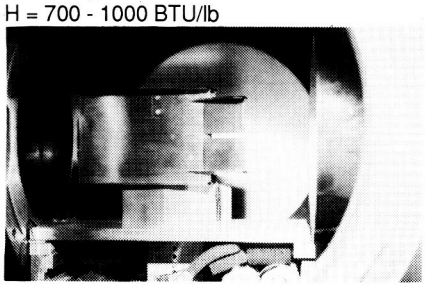

8-FOOT MODIFICATION PROJECT SCHEDULE

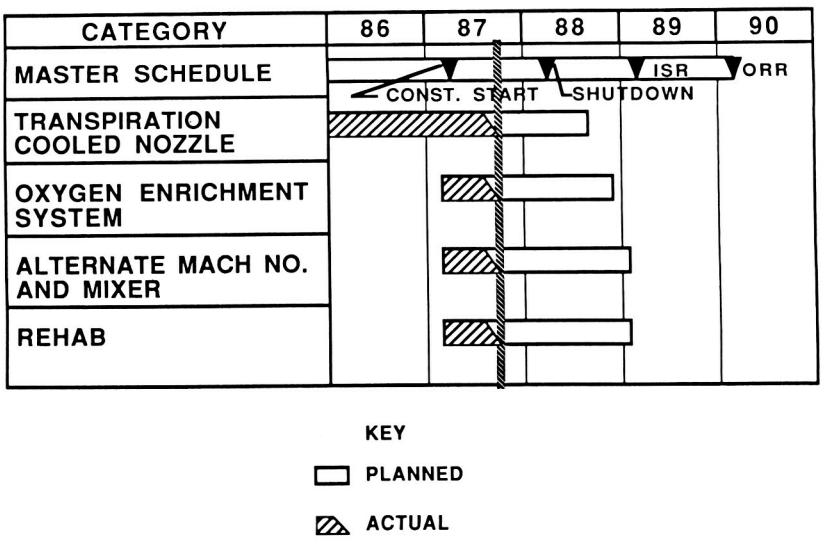

for the test medium. This is being done primarily to allow models that have hypersonic airbreathing propulsion applications to be tested.

The 7-Inch High-Temperature Tunnel (7-Inch HTT) is a 1/12-scale version of the 8-Foot HTT with basically the same capabilities as the larger tunnel. It is used primarily as an aid in the design of larger models for the 8-Foot HTT and for aerothermal loads tests on subscale models. The 7-Inch HTT is currently being used to evaluate various new systems for the planned modifications of the 8-Foot HTT.

The 20-MW and 5-MW Aerothermal Arc Tunnels are used to test models in an environment that simulates the flight reentry envelope for high-speed vehicles such as the Space Shuttle. The amount of energy available to the test medium in these facilities is 9 MW and 2 MW, respectively. The 5-MW is a three-phase AC arc heater and the 20-MW is a DC arc heater. Test conditions such as temperature, flow rate, and enthalpy vary greatly since a variety of nozzles and throats are available and model sizes can range from 3 in. in diameter to 1- by 2-ft panels. These facilities are currently on standby status.

Aerothermal Study of Simulated Space Shuttle Chine Tile Gaps

The objective of this study was to experimentally determine the pressures and heat transfer rates in the gaps between the reusable surface insulation tiles typical of the Space Shuttle chine area. Extensive studies on flat surfaces have shown gap width and length and flow

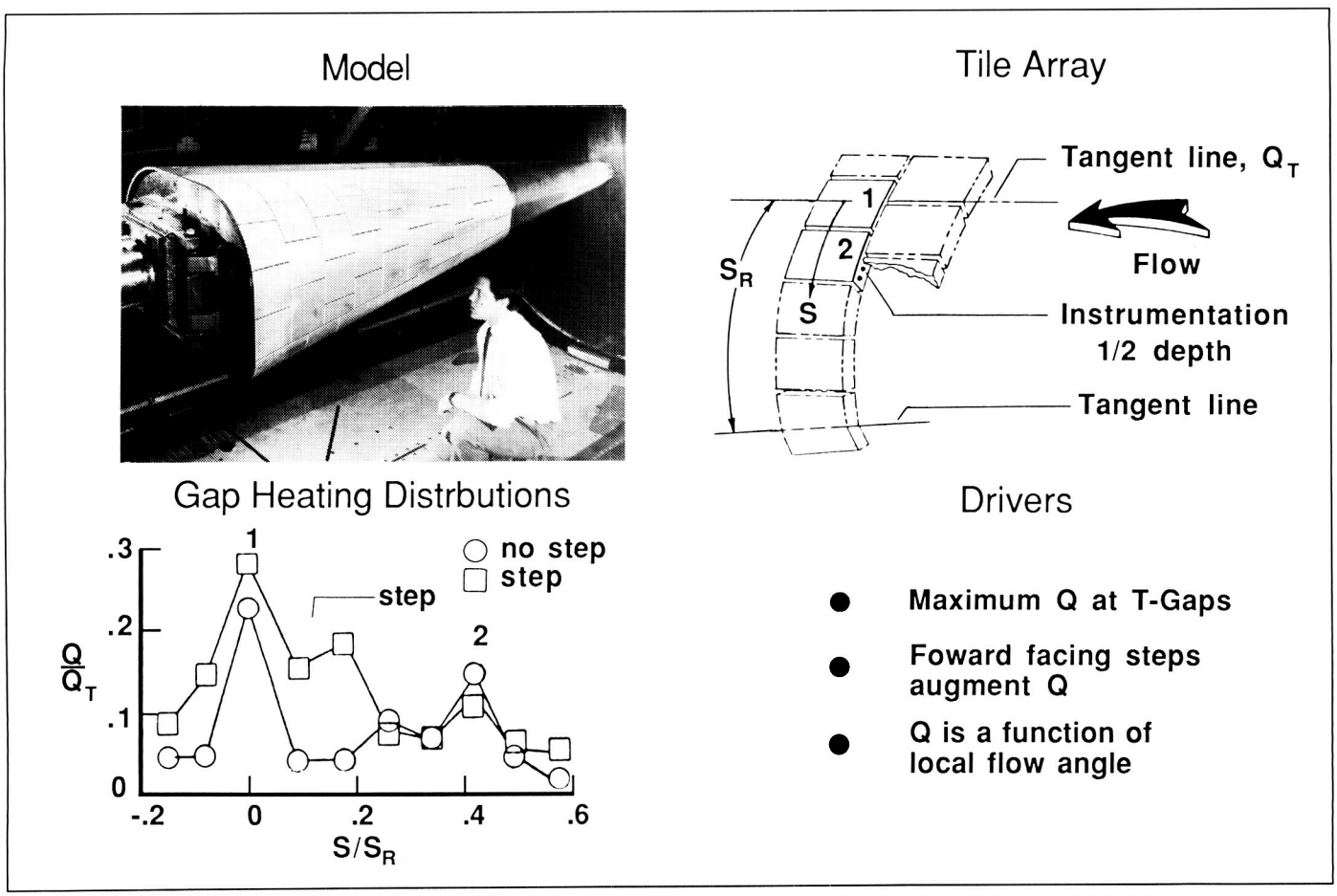

"Intertile" step and gap orientation that drives chine gap heating. Mach number is 6.8 and angle of attack is 10°.

angularity relative to the gap to be important. Chined or curved surfaces, unlike flat surfaces, result in pressure gradients that cause greater flow ingestion into the tile gaps and hence augment the aerothermal loads. Because of the limited data base, many of the Space Shuttle tile chine gaps are filled to reduce the aerothermal loads, at a sacrifice in weight and labor.

The Curved Surface Test Apparatus has been developed as a generalized test bed, which is representative of the forward portion of a lifting body, for the Langley 8-Foot High-Temperature Tunnel. Chine radii of 4 in. and 10 in. are used to vary the surface pressure gradient. The large, 10-in. chine configuration is shown in the figure. Thin-wall, metallic heat-transfer tiles were installed in selected locations adjacent to pressure instrumented solid tiles to determine the pressures and heat transfer rates in the tile gaps.

Preliminary results at Mach 6.8, a total temperature of 3400°R, Reynolds numbers of 0.4 to 1.5×10^6/ft, and angles of attack of 7°, 10°, and 13° indicate that the gap heating is driven by "intertile" steps (surface misalignments) and the gap orientation to the flow, just as was the case for flat surfaces. The gap heating Q, normalized to the external heating Q_T, at the windward tangent line of the chine, is plotted as a function of the surface distance S around the chine radius, normalized by the total distance S_T. The maximum heating occurs at the junction of the longitudinal gap terminating at a transverse gap (T-gap) as shown in the figure. From T-gap 1 to 2 the gap impingement heating decreased because of increased local flow angularity relative to the gap. Also, forward facing steps caused by a downstream tile being raised above the upstream tile augmented the local gap heating. For both configurations, selectively placed gap flow-stoppers were found to be effective in reducing the gap heat loads.

(L. R. Hunt, 3423, and K. K. Notestine)

Aircraft Noise Reduction Laboratory

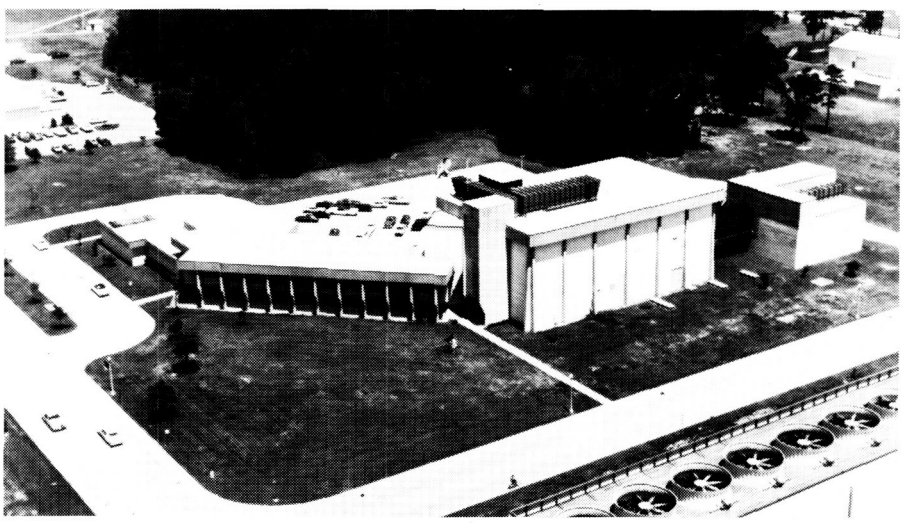

The Langley Aircraft Noise Reduction Laboratory (ANRL) provides the principal focus for acoustics research at Langley Research Center. The ANRL consists of the quiet flow facility, the reverberation chamber, the transmission loss apparatus, and the human-response-to-noise laboratories. The quiet flow facility has a test chamber treated with sound-absorbing wedges and is equipped with a low-turbulence, low-noise test flow to allow aeroacoustic studies of aircraft components and models. The test flow, which is provided by either horizontal high-pressure or vertical low-pressure air systems, varies in Mach number up to 0.5. The reverberation chamber is used to diffuse the sound generated by a noise source and provides a means of measuring the total acoustic power spectrum of the source. The transmission loss apparatus has a source and a receiving room, which are joined by a connecting wall. A test specimen such as an aircraft fuselage panel is mounted in the connecting wall for sound transmission loss studies. The human response laboratories consist of the exterior effects room, the anechoic listening room, and the Space Station/aircraft acoustic simulator.

Three laboratory companions of the ANRL are the Anechoic Noise Facility, the Jet Noise Laboratory, and the Thermal Acoustic Fatigue Apparatus (TAFA). The Anechoic Noise Facility is equipped with a very high-pressure air supply used primarily for simulating nozzle exhaust flow. The Jet Noise Laboratory has two coannular supersonic jets for studying turbulence evolution in the two interacting shear flows that are typical of high-speed aircraft engines. TAFA provides the capability to subject flat structural panels to high-level acoustic pressures and high-temperature radiant heating to 1000°F.

Thermal acoustic fatigue apparatus.

Future aerospace vehicles, such as the National Aero-Space Plane and the Advanced Launch System, will be subjected to intense noise and thermal environments during at least part of their normal flight regimes. To ensure the integrity of such systems under extreme environments, both analytical and experimental techniques will be used. One of the experimental techniques is to subject various components or panels of the vehicles to the expected environments of intense noise and heat in TAFA. TAFA (shown in the first figure) is a grazing incidence, high-intensity noise facility with capability of sound pressure levels from 120 db to 160 dB in the frequency range of 40 Hz to 500 Hz. The noise originates from a modulated pressurized air source and is expanded through a horn section to the test specimen. The temperature capability is a function of both the sound pressure level (SPL) and the air pressure (psig; gauge pressure) as well as the heat source. Utilizing 12 2000 W quartz lamps opposite the test specimen, 1000°F was obtained at 0 psig (no flow), and 820°F was obtained at 10 psig and 160 dB (as shown in the second

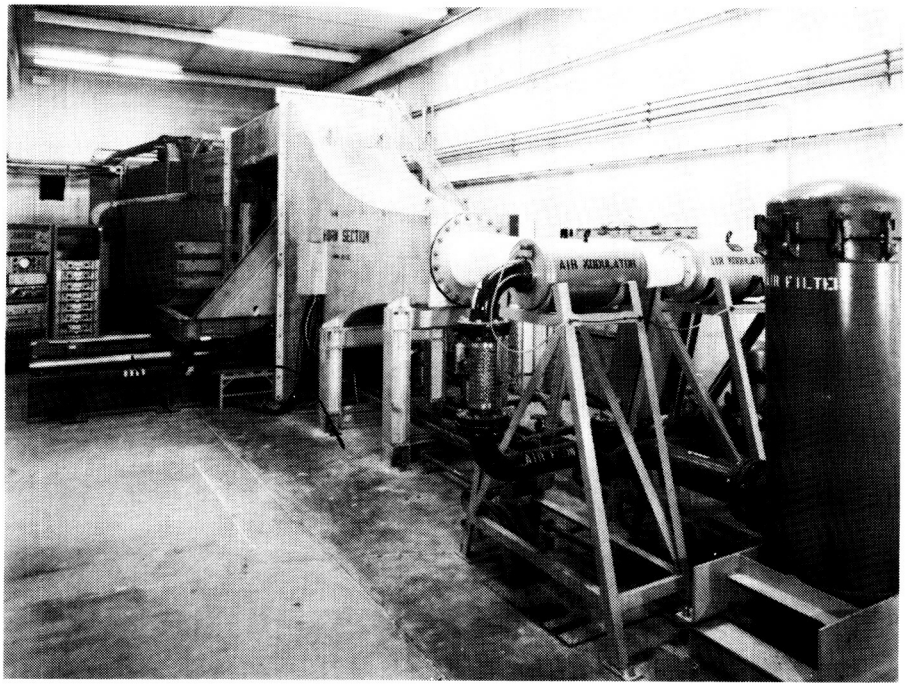

Thermal Acoustic Fatigue Apparatus. L-87-02004

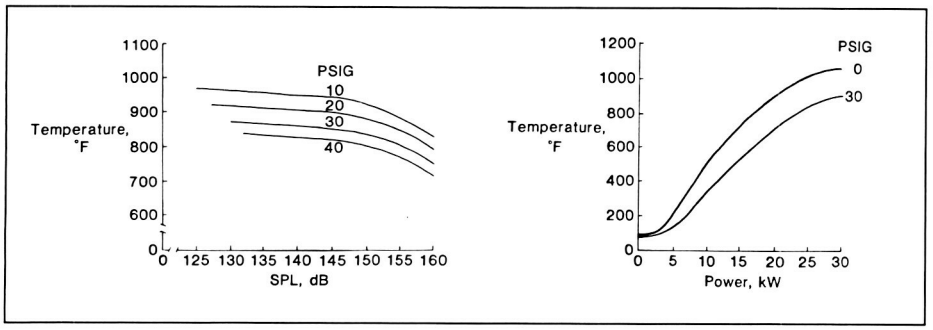

Temperature and noise capabilities of TAFA.

figure). Since several future aerospace vehicles will be exposed to noise and temperature levels in excess of this current capability, a number of studies are being conducted to measure the capabilities of both heat and noise in TAFA.
(S. A. Clevenson, 3561)

Acoustic Loads on ASTOVL Aircraft in Hover

Designers of advanced supersonic short takeoff and vertical landing (ASTOVL) aircraft are faced with increased thermal and acoustic loading due to engines operating at higher pressures and temperatures than their subsonic counterparts. Generic model experiments to define the dynamic loads generated by supersonic jet impingement that simulates ASTOVL hover conditions have been initiated in the ANRL.

A convergent rectangular nozzle of aspect ratio 4 provided the supersonic jet that impinged on a ground plane consisting of a circular plate. The plate was moved axially by digital traverse and was instrumented with dynamic pressure transducers to define the structures generated by the impingement process. A microphone near the nozzle exit recorded the noise that propagated back toward the aircraft fuselage. In addition to broadband noise, this propagated noise can consist of the screech tones present in the free jet as well as tones generated by the impingement process. The wavelength λ of the dominant tone measured at a typical hover condition (nozzle pressure ratio = 2.3) is shown in the figure as a function of the nozzle-to-ground distance h (both nondimensionalized by the nozzle width w). Also shown is the sound pressure level of the dominant tone. At nozzle-to-ground distances above 12 nozzle widths, a screech tone dominates the noise, its wavelength and amplitude corresponding to that measured in the free-jet condition. At smaller separations the noise spectra are dominated by the impingement process, with the dominant tone varying in both wavelength and amplitude. The sound pressure level of the dominant tone exceeds that in the free jet by as much as

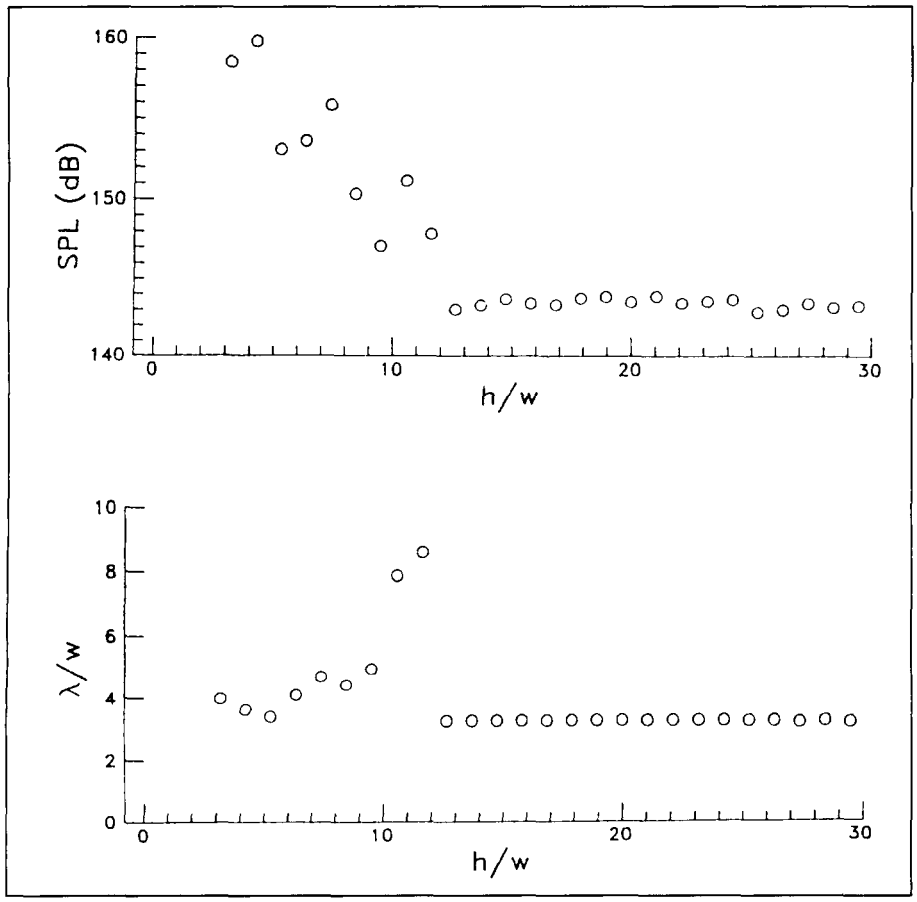

Wavelength and amplitude of dominant tone generated by supersonic rectangular impinging jet.

15 dB and exhibits a level as high as 160 dB.

The increased acoustic loading experienced at small nozzle-to-ground distances may have serious effects on ASTOVL structural design. Further studies of the loads generated by different nozzle configurations are planned. **(T. D. Norum, 2645)**

Axis Switching Phenomenon of Supersonic Elliptic Jets

Supersonic jet plumes that rapidly mix with the surrounding medium produce significantly smaller acoustic and thermal signatures. This property ameliorates fatigue concerns of airframe designers in their use of advanced lightweight composites, and of supersonic propulsion designers in meeting community noise standards for airport operation. The technology associated with rapid plume mixing centers around the issue of azimuthal variation of exit plane boundary-layer momentum thickness. With an appropriately tailored boundary-layer momentum thickness around an elliptic nozzle, enormous growth of the large-scale turbulence can be achieved in one plane of the nozzle. This large growth continues until the initial plume's minor axis becomes the major axis. This process, which is called axis switching, is known to be repetitive and to lead to rapid disintegration of the jet plume.

Previous research studies with low subsonic Mach number elliptic nozzles with aspect ratios of 2 are known to switch axes at least three times, and the plume spread rates are very large. Theory based on the quasi-linear wave modal analysis method predicts that axis switching should also occur with supersonic elliptic jets when the minor axis momentum thickness is at least twice that of the major axis.

A supersonic elliptic nozzle was designed with an aspect ratio of 2 to have shock-free flow at an exit Mach number of 1.5. As shown in the figure, which depicts operation at the nozzle design point, the flow contains only very weak waves. This result is predicted by Kumar's three-dimensional viscous code. The measured boundary-layer momentum thickness for the condition shown in the figure satisfies the theoretical constraint for axis switching. However, measurements reveal that the plume has an equal spread rate along each axis when the nozzle is operated at its design point (as shown in the figure). In sharp contrast to this, a large growth rate of the minor

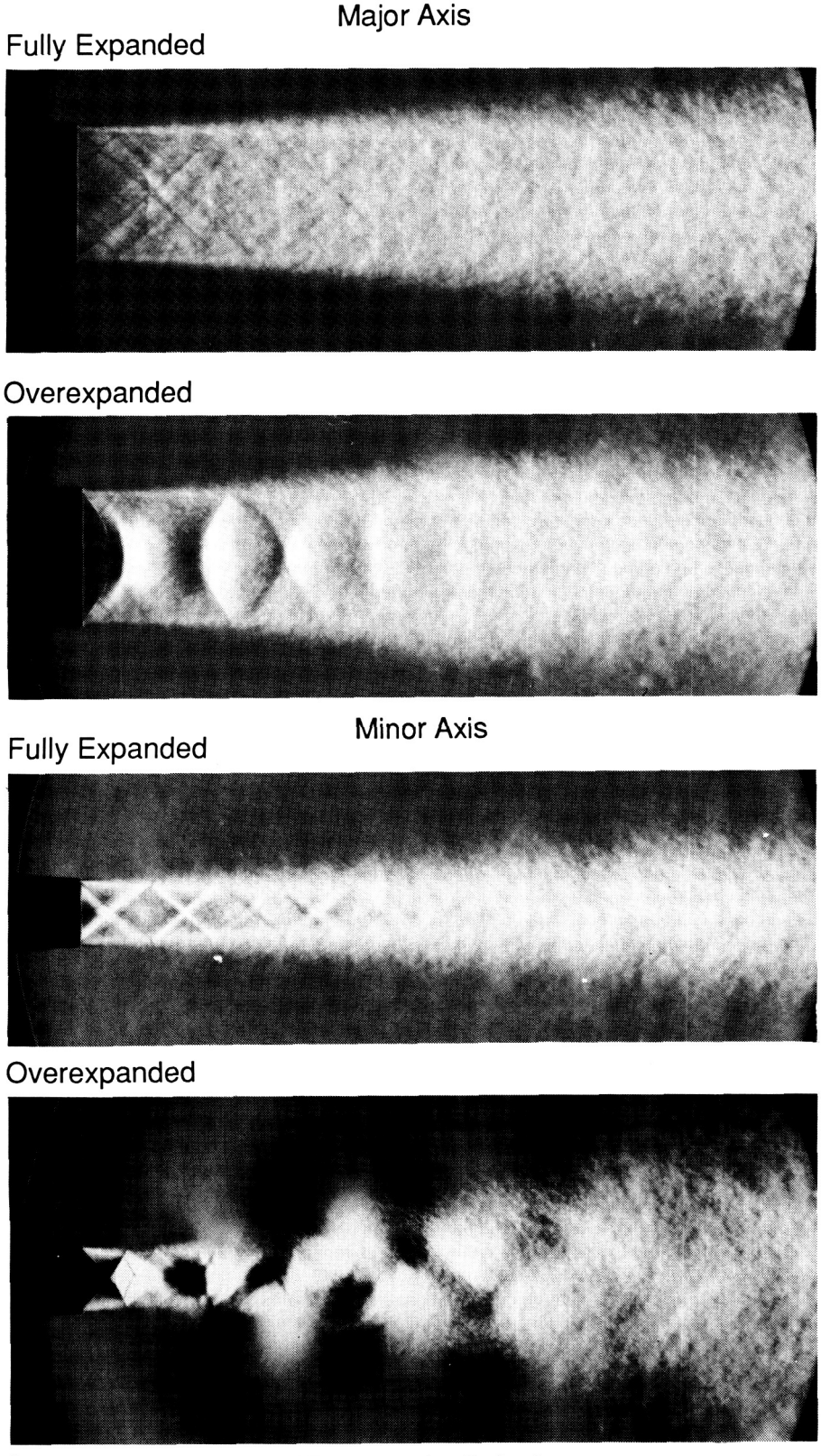

Schlieren records of Mach 1.5 supersonic elliptic plume.

axis shear layer is observed in an off-design operating condition of the same nozzle. The presence of shock cells in the jet plume may play an important role in this case. Further research is in progress for a full explanation of the axis switching mechanism. **(J. M. Seiner, 2645)**

Active Noise Control in Fuselage Environments

Without additional acoustic treatment, the cabin environment in proposed advanced turboprop powered aircraft has been shown to exceed currently accepted standards for passenger comfort and safety. Although the expected fuel economy makes this propulsion system extremely cost effective for the airlines, an acoustic and vibration environment characterized by that of current turboprop aircraft would be deemed unacceptable by the airline industry. In order to provide the needed noise control with minimum weight penalty, alternative methods are being investigated. One such method, termed active noise control, uses additional interior noise sources to provide a more acceptable interior acoustic environment.

To investigate the application of this technology, a finite-length, thin-walled, aluminum cylinder with end caps was used to model a fuselage. Exterior sources provided excitation simulating propellers, and interior

acoustic control was provided by an array of four acoustic sources. The inputs to these control sources were optimized to minimize the sound over an array of 10 interior microphones.

The figure presents the results of interior sound pressure level surveys at two cross sections for the primary field alone and for the operation of the active control system. All pressure levels are referenced to peak levels for the primary field at $x/a = 0$. The primary interior response is seen to be a dominant second-order azimuthal mode both at the source plane and away from the source plane. The operation of the active control system strongly attenuates this mode, thus reducing peak levels over 10 dB. This reduced level occurs not only in the source plane but also over all the interior volume as indicated by the composite pressure map at $x/a = 0.75$. **(R. J. Silcox, 3561)**

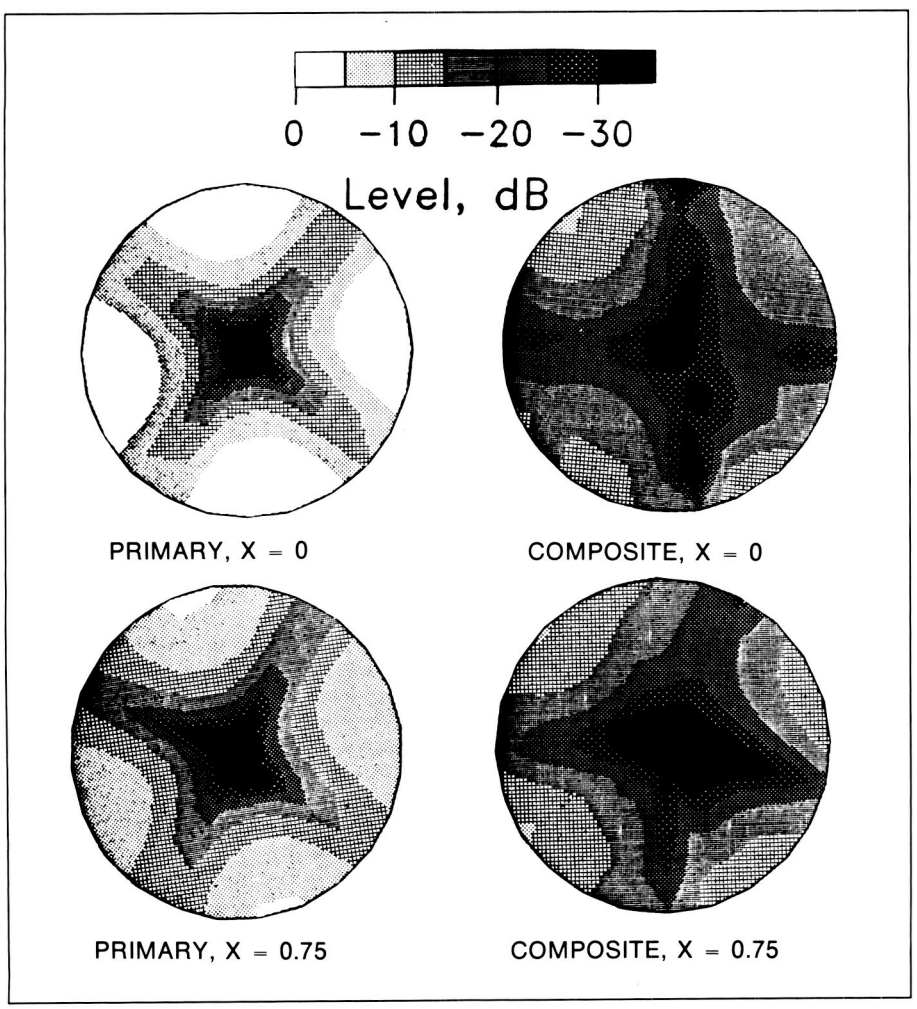

Relative sound pressure level contours with control off/on.

High-Intensity Acoustic Tests of Buckled Panels

Aircraft panels can be curved due to buckling, thermal effects, or the natural shape of the fuselage. Intense acoustic loads can cause a "snap through" behavior that results in large stresses and a potentially shortened fatigue lifetime. "Snap through" was studied experimentally in the Langley Thermal Acoustic Fatigue Apparatus (TAFA), which is capable of controlled, high acoustic levels. A 4-in. by 8-in. by 0.04-in. aluminum panel was buckled in a specially constructed support frame (as shown in the first figure). The compression screw tightened against the movable clamp provided a controlled amount of end shortening u which could be held constant when the support frame was installed in TAFA and the progressive wave acoustic load was applied at grazing incidence. Both static and dynamic components of the strain response of flat and buckled panels were measured for acoustic levels from 140 dB to 165 dB (as shown in the second figure).

Vibratory strain of the flat panel follows a trend of the square root of the acoustic pressure p indicating a nonlinear hardening spring behavior. At the lower sound levels the buckled panel has less strain than the flat panel, due to its curvature. At the higher levels the buckled panel follows a "p-squared" trend of a nonlinear softening

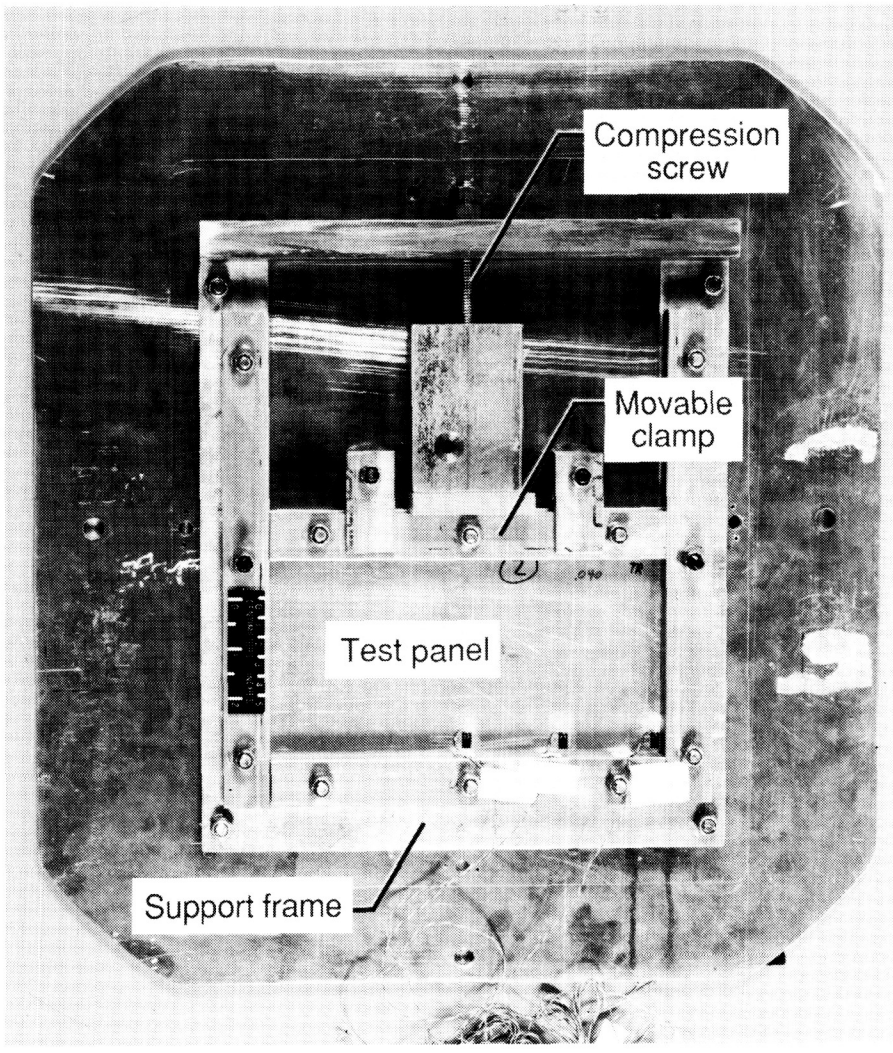

Apparatus for acoustic test of buckled panel. L-87-7814

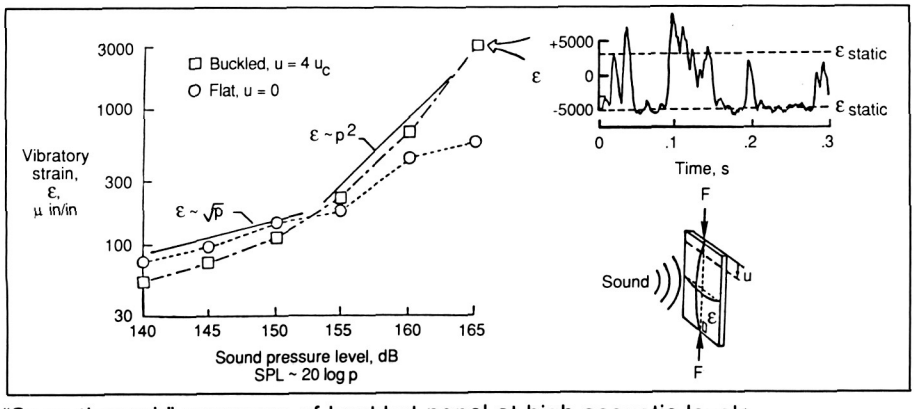

"Snap-through" response of buckled panel at high acoustic levels.

spring, and reaches strain levels of about five times the strain in the flat panel. The time history shows that the high strains result from the "snap through" from the static equilibrium position at $\epsilon = -5000$ to the other position at $\epsilon = +3000$.
(J. S. Mixson, 3561)

Strain Response of Rectangular Panels to Base Excitation

An analytical and experimental research program is under way to investigate the strain response of panels under thermal and/or acoustic loads. The goal of the program is to develop methods for predicting panel stresses and strains to aid in the assessment of sonic fatigue failure in advanced aerospace vehicle structures. Early studies within this program compared measured and predicted responses of composite panels to acoustic excitation. However, strain predictions differed from measurements by factors of 2 or more. Because of this poor agreement, an additional study using base excitation instead of acoustic excitation was conducted. Use of base excitation enabled close control and accurate knowledge of the panel forcing function. Several rectangular metallic panels having cantilever or clamped-free-clamped-free boundary conditions were investigated. The experimental setup for the cantilever panels is shown in

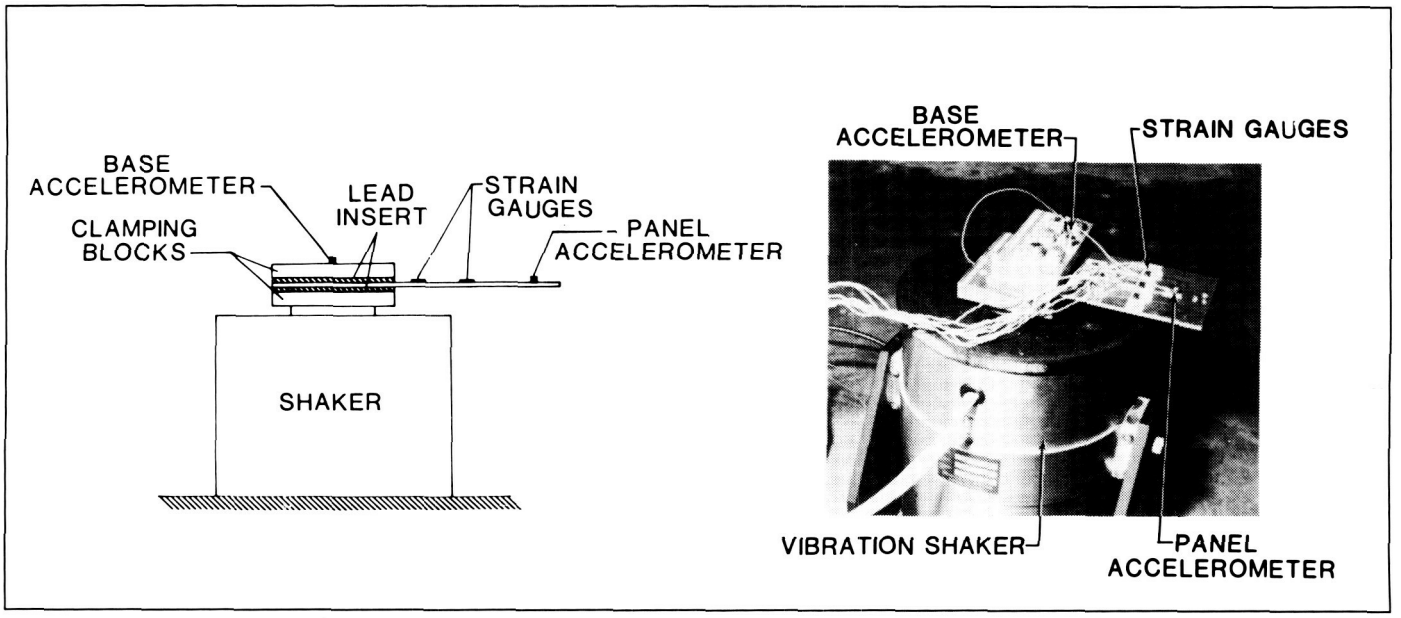

Test setup for dynamic strain response measurements.

the figure. Membrane strain was measured at several locations and panel acceleration at a single location on each panel. Input acceleration at the base was also measured. Panel frequencies and damping values were determined using a standard circle-fit procedure.

The analytical model used to predict panel strain response was based on the Ritz technique. Results indicated that panel dynamics (i.e., frequency and damping), as well as membrane strains in both the longitudinal and transverse directions, agreed well with measurements. However, panel acceleration response was not well predicted due to difficulties in accounting for base acceleration and phase effects. Attempts to modify the analysis to improve acceleration prediction capability are continuing.
(J. D. Leatherwood, 3561)

Advanced Turboprop Aircraft Community Noise Annoyance

Advanced turboprop (ATP) aircraft are expected to have counterrotating propellers (CRP) with thin, highly swept, twisted blades. The noise from these propellers is unique in that its tonal content is a complex mixture of two harmonically

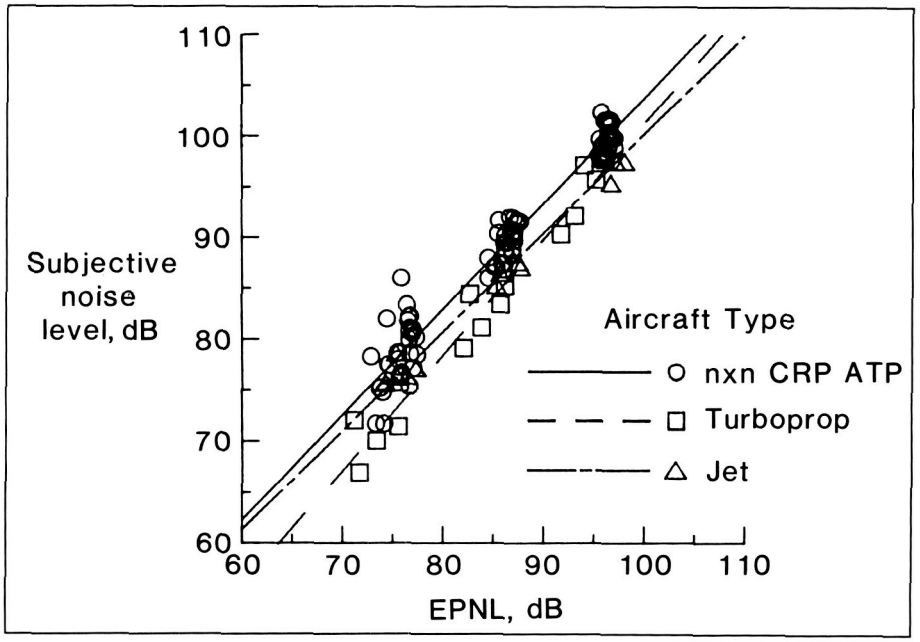

Comparison of annoyance responses using effective perceived noise level (EPNL).

related sets of pure tones, both occurring at frequencies higher than those of the single set of harmonically related pure tones produced by conventional, single-rotating propeller aircraft. The ATP aircraft will come into general usage only if the noise meets standards of community acceptability currently applied to conventional aircraft. Two experiments have been conducted in the anechoic listening room (a human-response-to-noise laboratory) of the Aircraft Noise Reduction Laboratory to compare the annoyance of ATP aircraft flyover noise with the annoyance of conventional turboprop and jet aircraft flyover noise.

The Aircraft Noise Synthesis System was used to generate realistic, time-varying simulations of counter-rotating ATP takeoff noise. For the first and second experiments, respectively, the system generated 27 noises representing CRP configurations with an equal number of blades on each rotor (e.g., 8×8) and 35 noises representing CRP configurations with an equal number of blades on each rotor (e.g., 10×8). In each experiment, 64 subjects judged the annoyance of the synthesized ATP takeoffs along with recordings of five conventional turboprop takeoffs and five conventional jet takeoffs. Each of the noises was presented at three sound pressure levels to the subjects in the anechoic listening room.

Analyses of the judgments examined the effects on annoyance of blade passage frequency, tone-to-broadband noise ratio, and aircraft type. For example, the figure compares the annoyance response to $n \times n$ CRP advanced turboprops with the annoyance responses to conventional turboprops and jets. The annoyance prediction ability of current noise measurement and correction procedures was also examined. The addition of duration corrections and corrections for tones above 500 Hz to the noise measurement procedures improved prediction ability.

(D. A. McCurdy, 3561)

L-87-5709

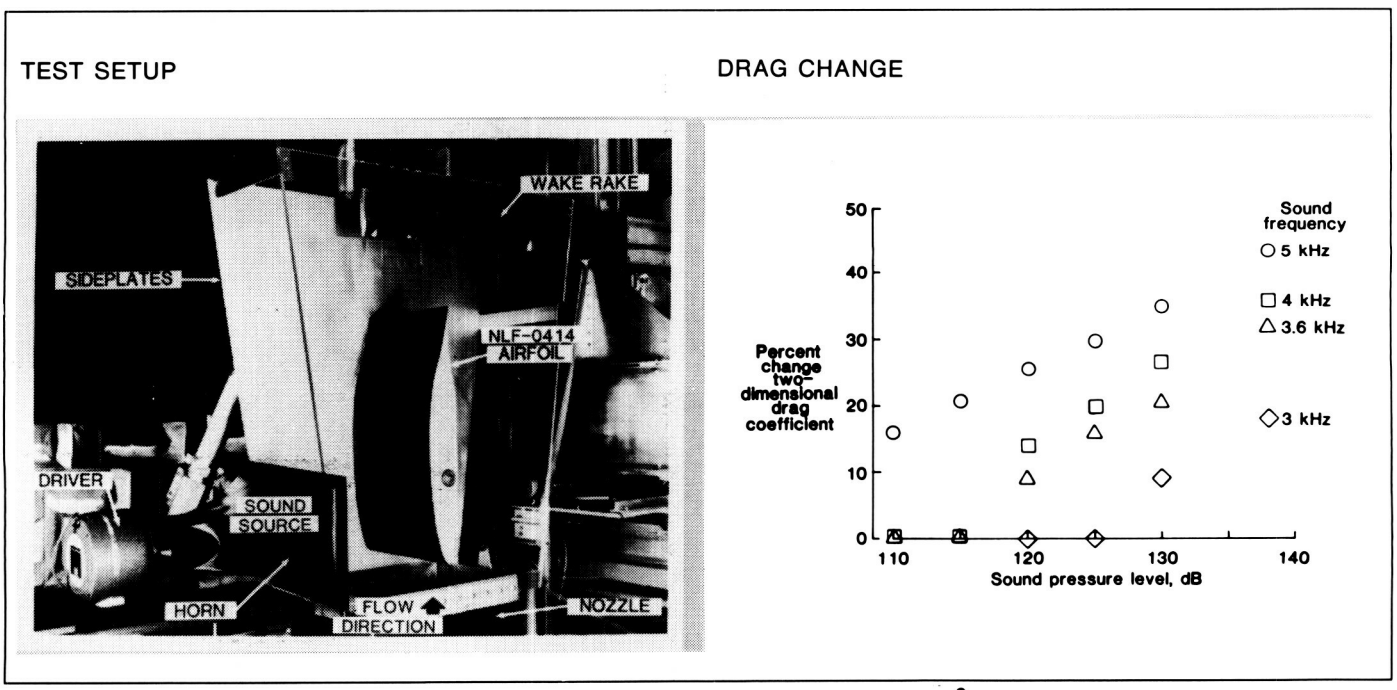

Composite of test setup and drag change due to acoustic source at R_N of 3×10^6 and induced turbulence at 68 percent chord (see text, page 52).

Acoustic Effects on Drag of NLF-0414 Airfoil

A two-dimensional natural laminar-flow airfoil (NLF-0414) was subjected to high-intensity sound over a frequency range from 2 kHz to 5 kHz, while emersed in a flow of 240 ft/s (R_N of 3×10^6) in the quiet flow facility of the ANRL. Using a wake rake, wake dynamic pressures were determined and a simple exchange in momentum was used to produce the two-dimensional drag coefficient.

In the investigation the airfoil was observed, using liquid crystals, to have laminar flow up to a 70-percent chord. Boundary-layer tripping near that chord position assured the absence of any laminar separation bubble, such as has been observed by previous investigations of this airfoil. Acoustic tones having sound pressure levels from 110 dB to 138 dB and varying from 2 kHz to 5 kHz were directed at the airfoil's first 20-percent chord. The resulting wake and free-stream pressures yield the two-dimensional drag coefficient C_D. The figure (page 51) shows a photo of the model and sound source and plots of percent change in drag coefficient as a function of sound pressure level (SPL) at various frequencies. The increase in drag is believed to be due to the sound exciting the flow near the airfoil surface causing the existing turbulence to become more intense and increase the skin friction. Movement of transition location was not observed during the investigation; hence, excitation of the natural instability waves is not believed to be the primary cause of the drag rise. The airfoil was also made fully turbulent (tripped at 5-percent chord) and an increase in drag of 20 percent was observed at an SPL of 138 dB and 5 kHz. Additional drag data should be acquired using a force balance and/or skin friction gauge to validate this initial result on drag change. Measurements of fluctuating surface stresses using hot-film sensors should also be made to better understand the physical phenomena.

(J. G. Shearin, 4911)

Acoustic Scale-Model Propagation Experiment

A scale-model acoustic propagation experiment was performed in the anechoic chamber of the ANRL to investigate long-range sound propagation over soft and hard surfaces when the sound is emitted and travels close to the surface. The experiment, which was performed in the facility from September 1986 through May 1987, consisted of broadcasting tones above a model ground plane and measuring the decrease in sound level with propagation distance. The model ground plane was 6 m by 8 m in size. The test matrix included four ground surfaces: plywood, felt,

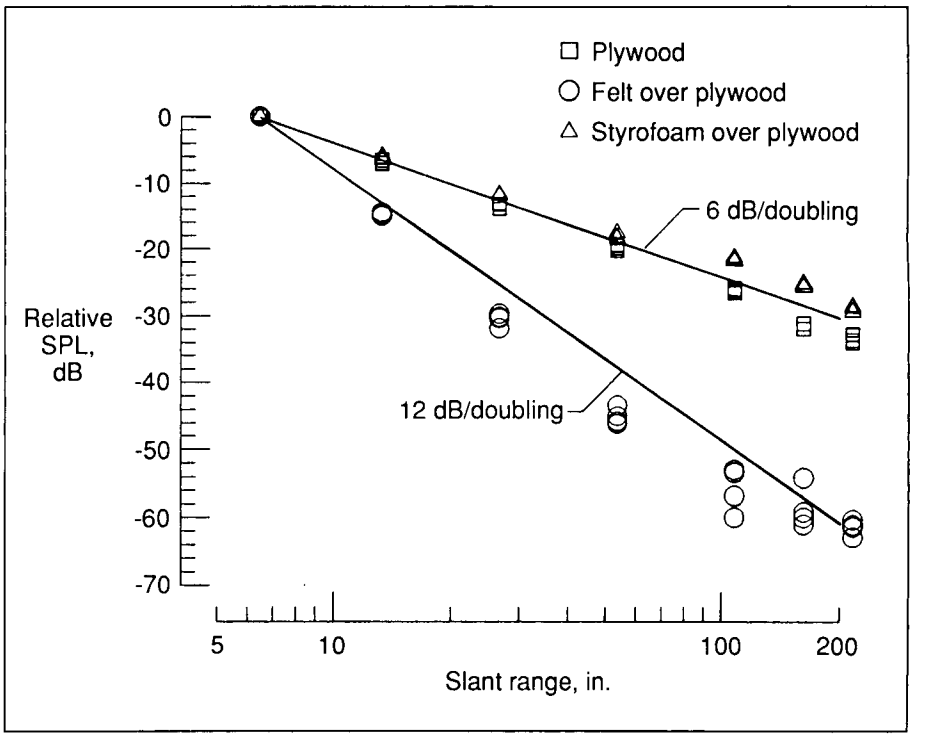

Scale-model propagation experiment at frequency of 9945-Hz source and receivers are flush.

styrofoam, and fiberboard. A scale factor of 100 to 1 was employed. The full-scale frequencies of interest were scaled to test frequencies in the range of 10 kHz to 15 kHz. Probe microphones were mounted underneath the ground plane and were located from 0.1 m to 5.5 m away from the acoustic source.

Typical propagation data are illustrated in the figure for propagation over plywood, felt, and styrofoam for a tone of 9945 Hz. Data are given for four repeat runs for each surface with the source and microphones flush to the test surfaces. Two distinct trends are apparent. The falloff of the plywood and styrofoam data with distance is a nearly spherical spreading (a 6 dB decrease with every doubling of distance), which is characteristic of an acoustically hard surface. The felt data follow a 12 dB per doubling of propagation distance, which is characteristic of a ground wave. When a ground wave exists, the data and theoretical models not included here indicate that the received acoustic level will be much smaller than if a spherical wave were present. Meaningful, high-quality, repeatable acoustic data were measured in a scale-model acoustic propagation experiment. This achievement indicates that scale-model experiments can be used to investigate outdoor, long-range, low-frequency propagation problems.

(W. L. Willshire, Jr., 4310)

Avionics Integration Research Laboratory—AIRLAB

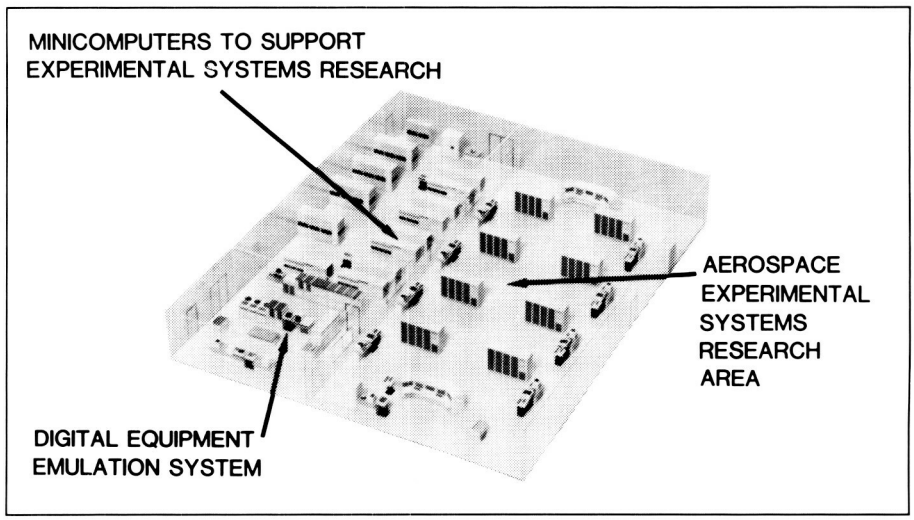

The United States leads the world in the development, design, and production of commercial and military aerospace vehicles. To maintain this leadership role throughout the 1990's and beyond will require the incorporation of the latest advances of digital systems theory and electronics technology into fully integrated aerospace electronic systems. Such efforts will entail the discovery, design, and assessment of systems that can dramatically improve performance, lower production and maintenance costs, and at the same time provide a high, measurable level of safety for passengers and flight crews.

AIRLAB has been established at Langley Research Center to address these issues and to serve as a focal point for United States government, industry, and university research personnel to identify and develop methods for systematically validating and evaluating highly reliable, fully integrated digital control and guidance systems for aerospace vehicles.

The increasing complexity of electronic systems entails multiple processors and dynamic configurations. These developments allow for greater operational flexibility for both normal and faulty conditions, thus impacting and compounding the validation process. Whereas a typical reliability requirement for current electronics systems is a probability of failure of less than 10^{-6} at 60 minutes, the requirement for flight-critical electronic controls is for a probability of failure of less than 10^{-9} at 10 hours. Obviously, a new validation process is essential if this significant increase in reliability (four orders of magnitude) is to be achieved and believed.

Validation research in AIRLAB encompasses analytical methods, simulations, and emulations. Analytical studies are conducted to improve the utility and accuracy of advanced reliability models and to evaluate new modeling concepts. Simulation and emulation methods are used to determine latent fault contributions to electronic system reliability and hence aircraft safety. Experimental testing of physical systems is conducted to uncover the latent interface problems of new technologies and to verify analytical methods.

AIRLAB is a 7600-ft^2 environmentally controlled structure located in the high-bay area of Building 1220. AIRLAB houses a number of microcomputer and minicomputer resources and several special fault-tolerant research hardware test specimens dedicated to the support of validation research. The minicomputer resources consist of 10 Digital Equipment Corporation VAX 11/750 computers, one VAX 11/780 computer, 5 MicroVAX II computers that are used, for example, to control experiments (fault insertions, performance monitoring, etc.); to retrieve, reduce, and display engineering data; to develop and validate simulations; and to develop and validate analytical reliability and performance estimation tools. Also included in AIRLAB are three advanced fault-tolerant computer systems, SIFT (software-implemented fault tolerance), FTMP (fault-tolerant multiprocessor), and

FTP (fault-tolerant processor), which are designed to explore fault-tolerant techniques for future flight-critical aerospace applications. These computer systems serve as research test beds for validation studies in AIRLAB.

Estimating Distribution of Fault Latency in Digital Processors

The reliability analysis of a fault-tolerant computer requires information concerning the fault occurrence and fault recovery behavior of the system. A major component of the recovery processes of a fault-tolerant system is fault latency, which is the time interval from the occurrence of the fault until the fault generates an error. While latent, faults cannot be detected and removed by the system's fault-tolerance mechanisms. Consequently, the longer a fault lies latent, the greater is the probability that a fault will arrive in a second processor, and, at some later time, both faults will produce errors simultaneously. These errors can defeat the voting system and cause system failure.

Since the time-of-error generation is not directly observable in a physical processor, measurements of fault latency in a digital processor were previously unobtainable. Recently, researchers at the University of Michigan (under a NASA Langley Research Center grant) have developed a technique to infer the distribution of fault latency indirectly from the fault detection response of a processor injected with fixed duration faults. The technique is based on the observation that the ratio of the number of faults detected by a fault-tolerant processor to the number of faults injected is an estimate of the latency distribution at a point equal to the duration of the injected fault. By repeating this procedure for values of the fault duration over a wide range of values, the distribution of fault latency is obtained. The University of Michigan technique has been improved by Langley Research Center personnel to obtain better distribution estimates and to provide quantification of the accuracy of the estimates with statistical confidence bounds.

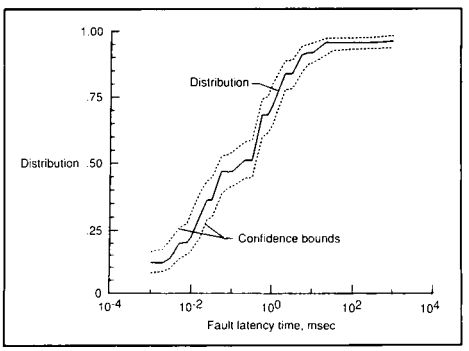

Estimated distribution of fault-latency times with confidence bounds.

Fault latency has been measured in two fault-tolerant computers located in the AIRLAB Facility. Over 15,000 fault injections were performed on FTMP by University of Michigan researchers and over 4500 faults were injected in SIFT by NASA researchers. These tests have demonstrated the viability of the new methodology to measure fault latency in digital processors. **(R. W. Butler and E. L. Ellis, 3681)**

Coincident Error Estimation and High-Speed Simulation

Ultrareliable analog-based computer systems are commonly used in passenger aircraft autoland systems in which failure can lead to loss of human life. Ultrahigh reliability is achieved in these systems by employing multiple redundant computers. A major factor affecting the reliability of such fault-tolerant systems is the ability of the system to rapidly detect a faulty redundant computer. Because of the nature of analog technology, fault detection is virtually instantaneous and, therefore, fault and error latency are essentially nonexistent. In the future, however, digital computer technology will replace analog computer technology in life-critical applications. Although digital technology offers many advantages over analog technology, there is one disadvantage that requires close attention. Digital computers often manifest long fault and error latency times in contrast to analog computers. The danger of these long fault and error latency times is the possibility the fault-tolerant system will accumulate many of these anomalies in mul-

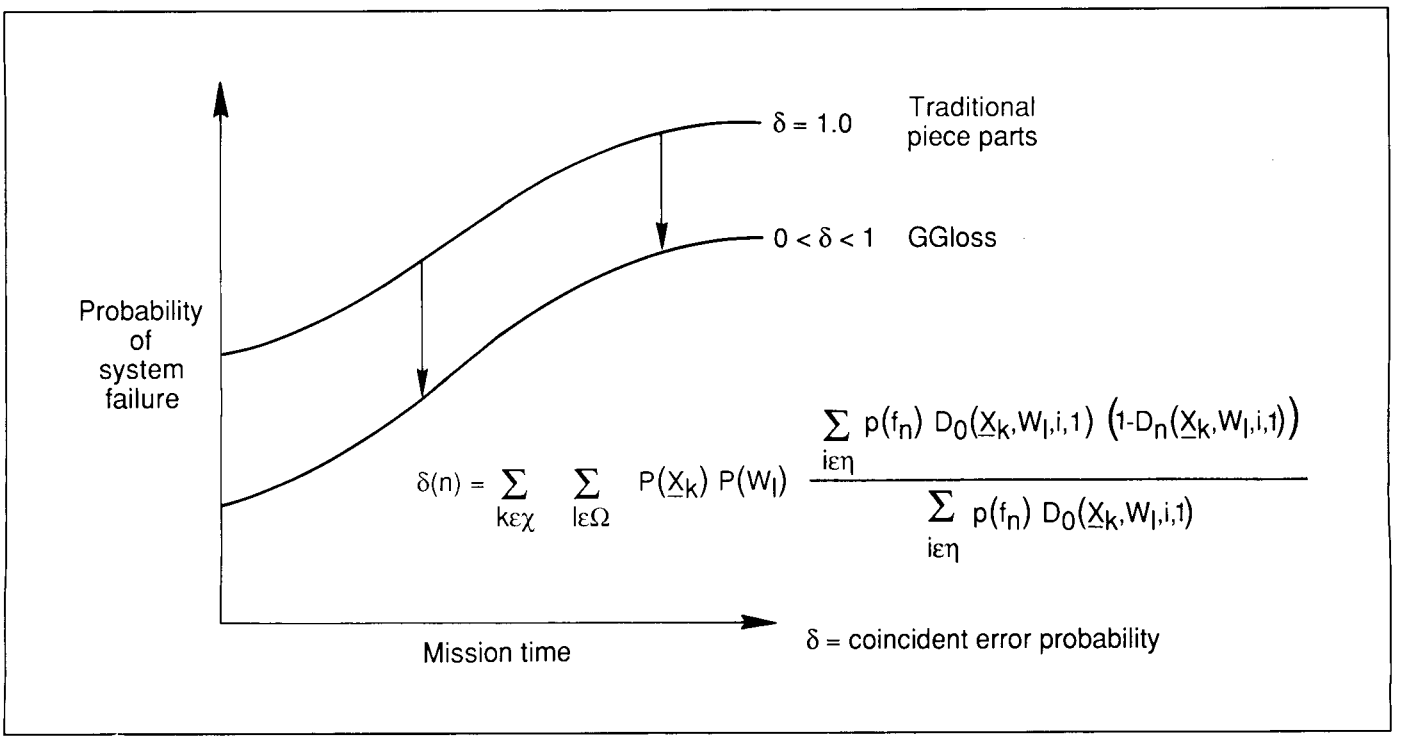

Effect of coincident error estimation on reliability prediction.

tiple computers that rely on comparison or voting to detect faulty computers. It has been postulated that under certain conditions, such as an aircraft mode change, many latent faults or errors could be excited simultaneously. This condition would defeat the error detection capability of the system possibly causing system failure and loss of life.

Because of the high complexity of these electronic systems and the industry's inability to measure the likelihood of defeating the detecting capability of the system, reliability analysts assume conservatively that critical near-coincident faults will necessarily result in system failure. These necessary assumptions are made in the reliability modeling and prediction of all such systems. It turns out that the probability of the occurrence (under this assumption) of critical near-coincident errors is the dominant parameter in reliability prediction and therefore controls the design of the system. (The coincident error probability is the probability that two faulty processors, while executing an identical code, will produce the exact same wrong result that will therefore defeat the system fault detection and recovery mechanisms.) The recent development of a superhigh-speed computer system simulator program has now made it possible to estimate the occurrence probability of the critical near-coincident error probability. Although only preliminary measurements have been made, there is encouraging evidence that indicates that the coincident error probability is considerably less than the 100-percent figure currently used. The result of this important discovery is that much higher reliabilities are possible than previously predicted.

The new tool that makes this measurement possible is called the gate logic software simulator (GLOSS). The GLOSS executes on a DEC VAX computer and utilizes parallel simulation in conjunction with zero and unit delay simulation techniques. This combination makes it economically feasible to inject tens of thousands of gate-level faults while the simulated computer or computer system is executing its application or self-test code.

(S. J. Bavuso, 3681)

Characterization of Fault Recovery Behavior of Fault-Tolerant Systems

Systems achieve fault tolerance, and consequently high reliability, by incorporating fault recovery mechanisms that enable them to continue functioning properly in the presence of faults. To produce credible reliability models and parameter estimates, it is necessary to characterize fault recovery behavior. This characterization can be done by repeatedly injecting a fault into a test specimen and measuring the fault recovery process.

To provide a basis for the development of sampling methods and parameter estimation techniques, pin-level fault injection experimentation was conducted in AIRLAB on the FTMP. The resultant fault detection times were analyzed to discover and identify the sources of variation and to establish the statistical distribution of the detection phenomenon. Detection time was chosen for analysis because it accounted for most of the variation in the total recovery process. Comparisons among the data sets showed that there were distinct groupings of detection time behavior; however, none of the factors varied in the experiment accounted for the groupings. Distribution fitting revealed that none of the well-known statistical distributions tested could be shown to be the overall best.

Of particular importance is the result that the exponential distribution was the worst fit over all data sets investigated, thus refuting the common assumption of reliability modeling that detection times are exponentially distributed. These results suggest that new sampling methods and parameter estimation techniques are required to characterize fault detection.

(G. B. Finelli, 3681)

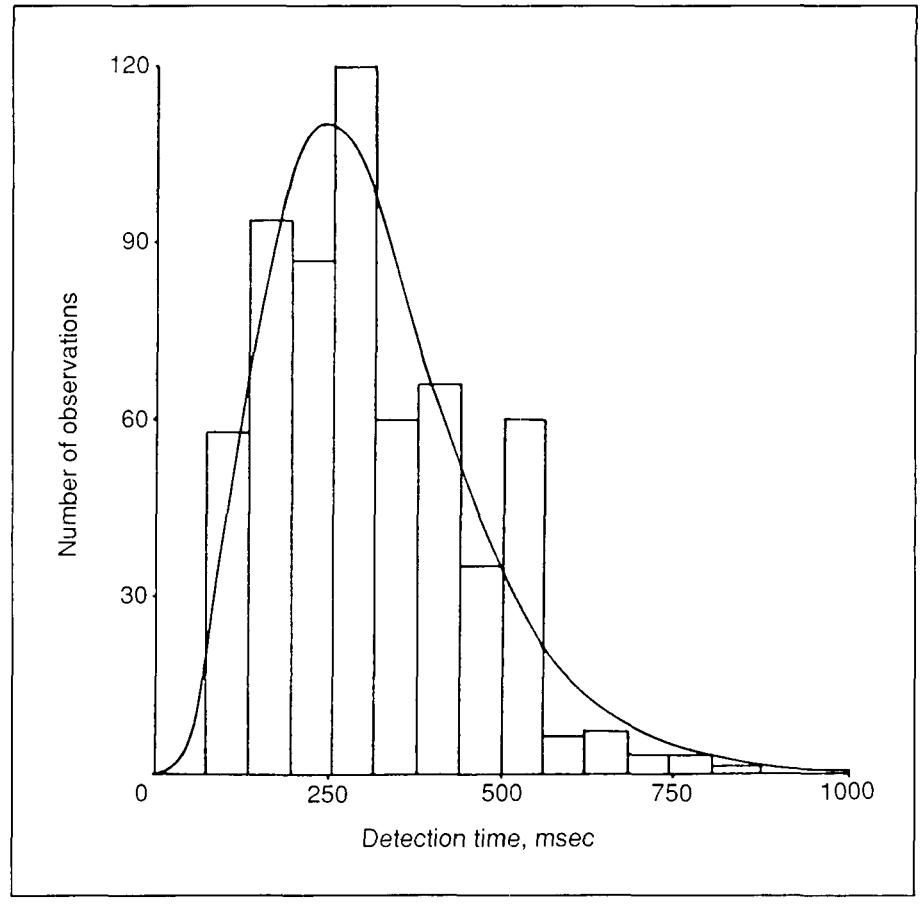

Histogram of fault-detection times and gamma distribution.

Transport Systems Research Vehicle (TSRV) and TSRV Simulator

The Transport Systems Research Vehicle (TSRV) and TSRV Simulator are primary research tools used by the Advanced Transport Operating Systems (ATOPS) Program. The goal of the ATOPS Program is to increase the operational capability of modern aircraft and foster their integration into the evolving National Airspace System.

A comprehensive upgrade has been completed on the TSRV, a specially instrumented Boeing 737 airplane. New capabilities include color cockpit displays and advanced experimental avionics.

The TSRV has two flight decks: a conventional Boeing 737 flight deck provides operational support and safety backup, and the fully operational research flight deck, positioned in the aircraft's cabin, provides the capability to explore innovations in display formats, contents, and in-aircraft operations.

The "all-glass" research flight deck presents information to the crew via eight newly installed 8-in.-square electronic displays representative of the technology to become available in commercial transports in the 1990's. The state-of-the-art color displays are driven by new, onboard computers and, most importantly, specially developed computer software. These new technologies make it possible to more clearly display information presented only partially or in scattered locations on existing electromechanical and first-generation electronic displays in today's aircraft.

In addition to video concepts for primary flight and navigation displays in front of both pilot and copilot, center panel displays provide the capability to monitor engine and system status and to manage aircraft systems operation. The center panel displays will permit research on how ad-

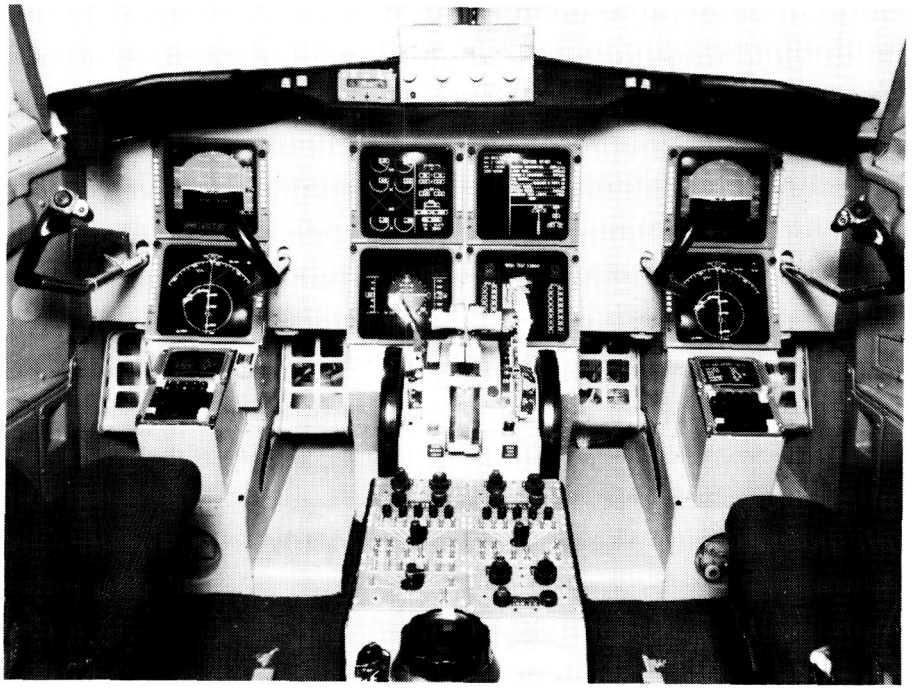

New TSRV aft cockpit configuration. L-87-3645

ditional information can be displayed and used to improve situational awareness, air traffic control communications, flight management options, and traffic awareness.

The TSRV Simulator provides the means for ground-based simulation in support of the ATOPS research program. The Simulator, which is also being modified to duplicate the upgraded aft flight deck located in the TSRV, allows proposed concepts in such areas as guidance and control algorithms, new display techniques, operational procedures, and man/machine interfaces to be thoroughly evaluated. Promising simulation research results become the subjects of actual flight test research.

Concurrent Validity by Flight Simulation Study of SWAT and NASA-TLX Work Load Measures

The Subjective Workload Assessment Technique (SWAT) and the NASA Ames Task Loading Index (NASA-TLX) have been used widely to estimate work load. Each has been used extensively in laboratory and flight simulation studies. Although SWAT and NASA-TLX have been compared in the laboratory, no published flight simulation studies have used both measures in the same experiment.

An investigation of SWAT and NASA-TLX formed part of a larger study that focused on evaluating the benefits, if any, achieved by combining a computer-generated horizontal situation display (HSD) into a primary flight display (PFD), thereby reducing the pilot's visual scan area. One display configuration presented the PFD and HSD information on separate cathode ray tubes (CRT's); a second display configuration had the PFD and HSD information combined on a single CRT. Four United States Air Force pilots were used as subjects. High- and low-work-load tasks were created by varying flight path complexity. The pilot's primary task was to fly the airplane on the assigned path with a minimum of deviation in altitude, airspeed, and cross-track error. Scores for SWAT and NASA-TLX were recorded after every trial. In addition to statistical significance, differences were considered experimentally significant only if the differences in mean values were greater than 20 percent.

Both SWAT and NASA-TLX were statistically and experimentally significant for path complexity, indicating a much higher work load for the high path complexity (as shown in the figure). This result is essentially a flight simulation validation of both techniques. Neither measure was statistically or experimentally significant for display configuration differences, indicating that the one-CRT and two-CRT display configurations had equal work load. SWAT and NASA-TLX subjective work load measures have been compared and validated in a single study and shown to be sensitive to flight path work load.

(M. Nataupsky, 3917)

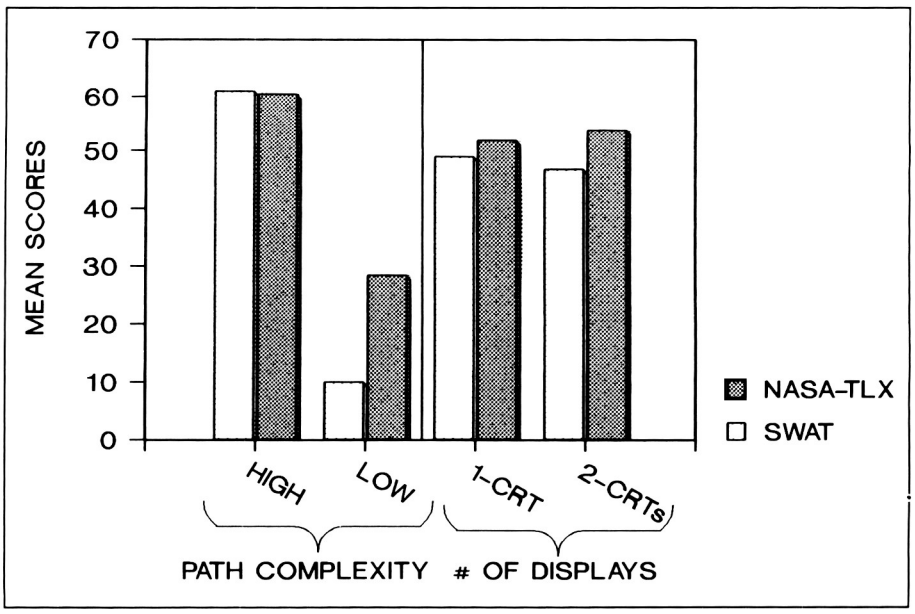

Comparison of work load measures in piloted simulation study.

Four-Dimensional Guidance Concept

A four-dimensional (4-D) Terminal Maneuvering Area (TMA) guidance concept, developed by the DFVLR (Deutsche Forschung- und Versuchsanstalt fuer Luft und Raumfahrt) Institute of Flight Guidance at Braunschweig, Germany, has been flight tested on the Advanced Transport Operating Systems Boeing 737 research aircraft. The concept is an updated version of one that was tested on DFVLR's HFB 320 test aircraft. This version uses lateral flight path stretching to arrive at a traffic merge gate on the extended runway centering within 5 s of a preselected time.

The current flight path is displayed to the pilot on an electronic navigation display (ND) as illustrated in the figure. The planned time of arrival (PTA) at the merge gate is also presented and if changed causes a new (stretched) path to be computed and displayed to the pilot. The path is also recomputed (and displayed) during the approach to null any time errors that may have accumulated. The associated vertical profile is based on fuel-efficient idle thrust descent segments and incorporates both a top-of-descent (TOD) cue at the beginning of the approach and a deceleration (DEC) cue to indicate when the aircraft begins slowing to the final approach speed.

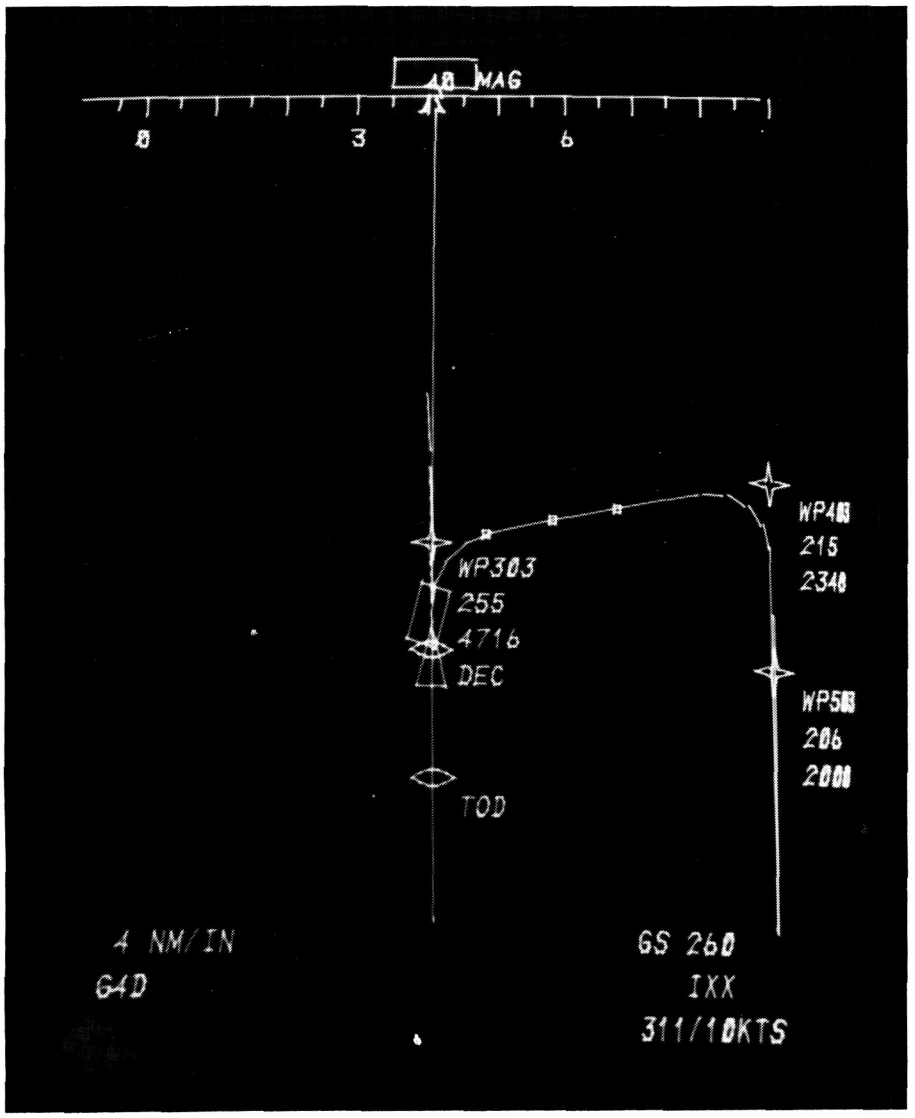

Navigation display showing planned time-accurate flight path. L-84-9869

The 20-hr test program covered a variety of conditions including several to test algorithm sensitivity to poor initial conditions and wind model update errors. The flight test results indicated that all but 3 of the 43 approaches flown crossed the merge gate within 6 s of the PTA, and many of these were within the 5-s goal despite the intentional input errors.
(J. R. Kelly, 2541)

Takeoff Performance Monitoring System

A Takeoff Performance Monitoring System (TOPMS) has been developed to provide pilots with graphic/numeric information pertinent to their decision to continue or abort a takeoff. To convey this information, head-up and head-down dis-

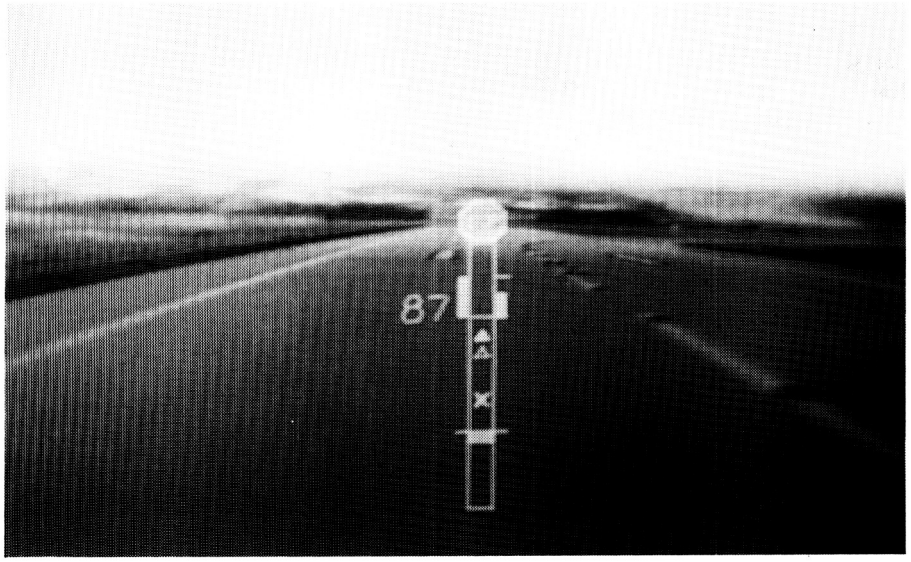

TOPMS head-up display for failed right engine. L-87-11,228

plays have been configured and evaluated on the Transport Systems Research Vehicle (TSRV) Simulator. Emphasis in 1987 was placed on improving the head-down display developed and evaluated (by 32 invited pilots) in 1986 and on creating a head-up display (HUD) for the pilot making the takeoff. (The HUD was a primary recommendation by the pilots who performed the 1986 evaluation.)

The TOPMS HUD uses a somewhat simpler graphic than the head-down display that appears on cathode ray tubes on the instrument panel in front of each pilot. The HUD is shown in the figure for a case when the right engine of a B-737 failed at an 87-kn airspeed. The HUD is superimposed on a projected real-time television picture of the runway. The symbols indicate the present position (as shown in the lower solid rectangle with a horizontal line across its front), calibrated airspeed (87), predicted stop point (X), initial and current prediction of where the rotation speed V_R will be reached (open and solid triangles, respectively), engine pressure ratio (the vertical bars beside the runway graphic; the bar on the right had dropped from its reference line), and a red stop sign (which recommended an abort) at the end of the graphic.

Seventeen invited pilots evaluated the head-up and head-down TOPMS displays and generally rated them "good" to "very good." The pilots particularly liked the system because it provided information they had long desired and displayed it in a format that was quickly and easily comprehended. A flight test of the head-down display on the TSRV is planned for 1988.

(D. B. Middleton and R. Srivatsan, 3595)

Autopilot Path Redefinition Algorithms for Transition From RNAV to MLS

In providing a transition from radio navigation (RNAV) to the more precise Microwave Landing System (MLS) data, large guidance errors can be input to the autopilot because of accuracy differences between RNAV sensors and the MLS. These errors can result in large undesirable aircraft pitch and roll maneuvers as the autopilot acts to drive the errors to zero. Because the transition can happen at a critical time in the landing approach and may cause passenger discomfort, research was conducted to develop methods of reducing these maneuvers. Algorithms were developed, implemented, and flight-tested in the flight control computers of the Transport Systems Research Vehicle. The approach used to reduce the large maneuvers was to appropriately redefine the desired path, which for this research was a three-dimensional (3-D) path, such that the new path would begin at the best aircraft position estimate (the MLS position) and rejoin the original path in a smooth way.

This research resulted in three algorithms that are called the zero cross-track (ZCT), tangent path (TP), and continued track (CT). The redefined path starts at the current aircraft position, as determined by the MLS, and merges with the original path in one of three ways depending on the algorithm

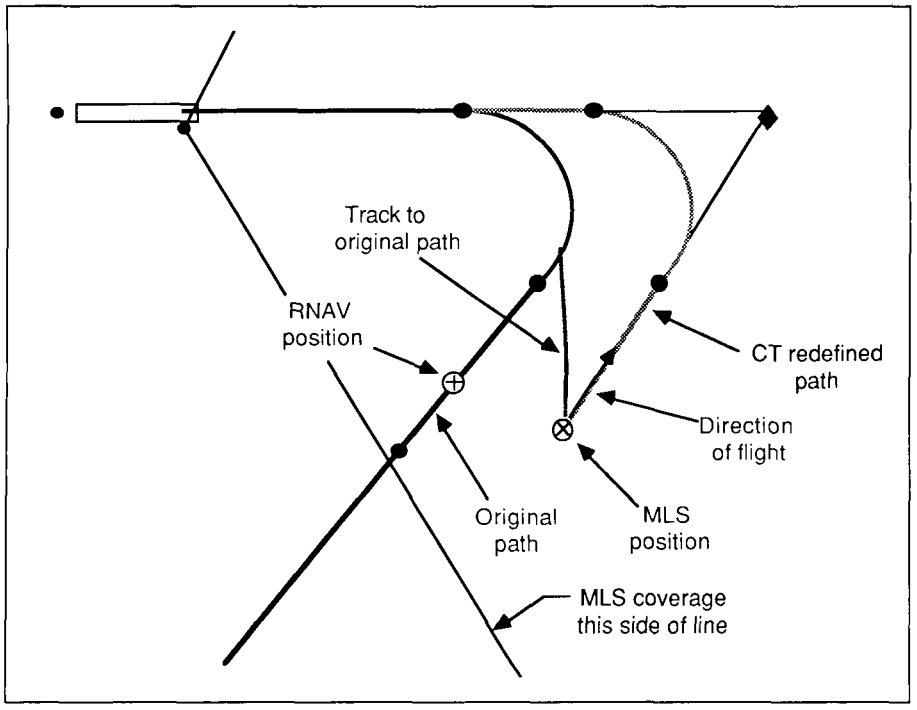

Aircraft flight path with and without path redefinition.

being used. The ZCT algorithm constructs the path to merge with the original path at the next waypoint (the intersection of the current and the next straight-line segments). The TP algorithm merges with the original path at the tangency point on the next turn. The CT algorithm merges where the aircraft's current ground track intersects the next straight-line segment. The first figure shows the original flight path on which the algorithms were flight-tested and the redefined path using the CT algorithm. The second figure shows aircraft flight test roll attitude data and compares roll maneuvering without path redefinition and with CT path redefinition during the transition to MLS navigation under nearly identical position errors between the MLS and RNAV. The data show that without the algorithm the roll attitude reaches 25° (the autopilot limit) during the transition to MLS and that with the algorithm no roll maneuvering occurs during the switch to MLS. All of the algorithms were flight-tested, and each significantly reduced roll maneuvering for the transition to MLS. The use of the CT algorithm results in the least maneuvering. However, the algorithm to use for a particular situation remains a subject of future research. **(R. M. Hueschen, 3540)**

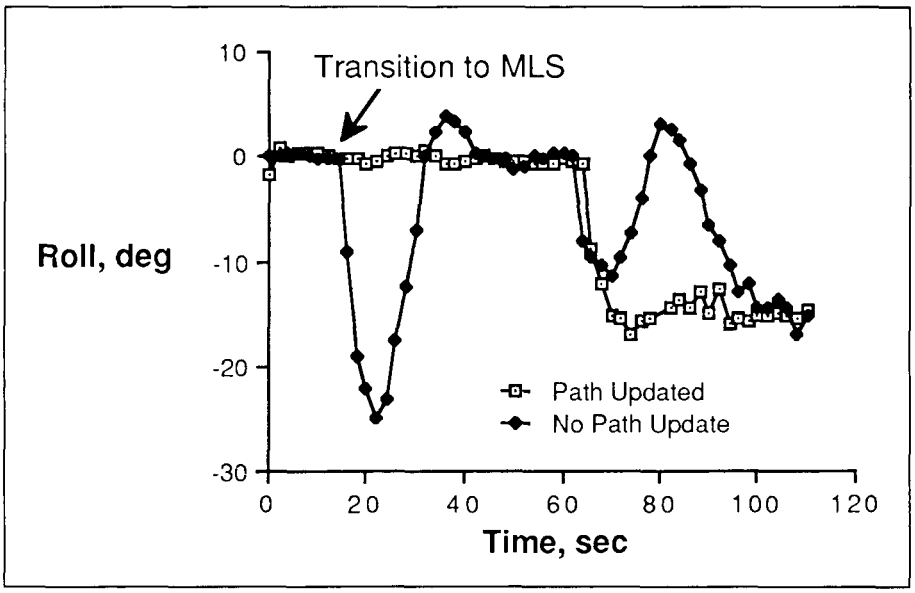

Aircraft roll attitude with and without path redefinition.

Human Engineering Methods Laboratory

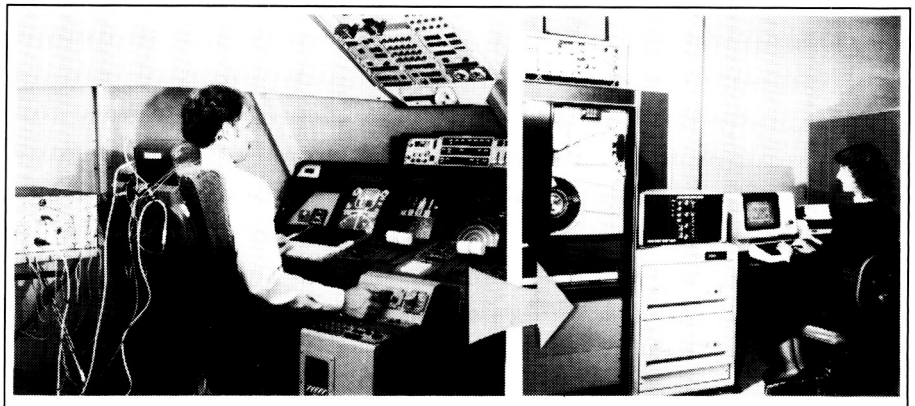

SIMULATOR WITH BIOINSTRUMENTATION

DATA ACQUISITION & ANALYSIS

The Human Engineering Methods (HEM) Laboratory has been established to develop measurement technology to assess the effects of advanced crew station concepts on the crew's ability to function without mental overload, excessive stress, or fatigue. The laboratory provides the capability for measurement of behavioral and psychophysiological response of the flight deck crew.

The facility comprises state-of-the-art bioinstrumentation as well as computer-based physiological data acquisition, analysis and display, and experiment control capability. Software has been developed which enables the demonstration of work load effects on the steady-state evoked brain response and transient evoked response signals as well as the monitoring of electrocardiographic (EKG), electromyographic (EMG), skin temperature, respiration, and electrodermal activity.

The Langley-developed oculometer capability has been integrated with the other physiological measurement techniques. Subjective rating and secondary task methods for assessing mental work load have also been implemented. A computer-based criterion task battery is available for preliminary testing (with human subjects) of work load techniques that are being validated prior to evaluation and application in the simulators. Satellite physiological signal conditioning and behavioral response capture stations are located at the simulator sites to provide human response measurement support for flight management and operations research.

Eye Blink Physiological Measures Applied to Work Load Estimation

The visual system is the primary information-gathering system of most humans, and study of visual behavior reveals effects that reflect the complexity of information being processed. For instance, there are two occasions during which information is not being taken in through the visual system: when the eyes are shut (blinks) and when the eyes are moving from one location to another (saccades). It is known that the human reduces these noninformation-gathering times as the information gathering becomes more difficult.

A series of simulator tests were conducted to evaluate the sensitivity of eye blink measures to changes in work load. Three landing approach path/guidance-mode combinations were used to provide three levels of work loads under which to evaluate various eye response measures. The instrument landing system (ILS) condition, which was a straight-in landing approach, had been subjectively rated previously by the test subjects as the lowest work load condition. The River approach, which involved several small heading changes, had been rated as a medium work load condition. The Hook approach, which involved a few large heading changes as well as using raw guidance information instead of command guidance information, had been rated as the highest work load. Three eye response

measures were evaluated: half- and full-closure durations were measured by electrooculogram (EOG) recordings, and the percentage of eye blinks during which a saccade occurred was calculated from the EOG recordings.

There were no statistical differences in the three eye response measures for the ILS and River approaches. However, for all three eye response measures, there was a difference between the ILS/River approaches and the Hook approach conditions, indicating higher visual work load. During the Hook approach, for example, the blink duration was shorter (85 ms versus 93 ms), the half-closure duration was shorter (105 ms versus 108 ms), and the number of blinks with saccades increased (as shown in the figure) as compared to the ILS and River approaches. Thus, as visual work load increased, the eyes blinked faster and blinks were "scheduled" to occur coincident with saccades.

(A. T. Pope and R. L. Harris, Sr., 4685)

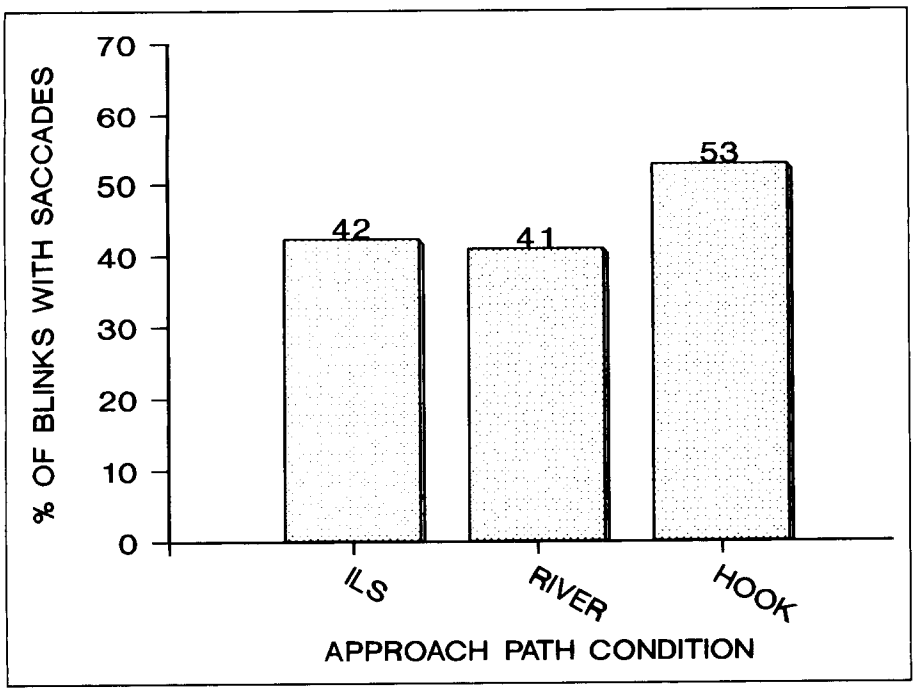

Visual work load of three approach paths indicated by blinks with saccades.

General Aviation Simulator

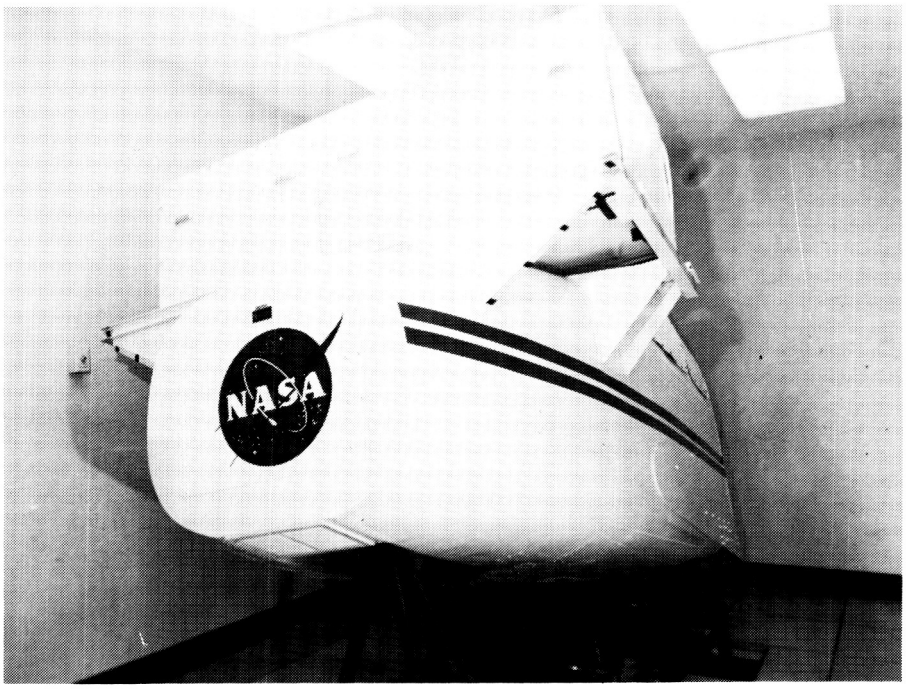

The General Aviation Simulator (GAS) consists of a general-aviation aircraft cockpit mounted on a three-degree-of-freedom motion platform. The cockpit is a reproduction of a twin-engine propeller-driven general-aviation aircraft with a full complement of instruments, controls, and switches, including radio navigation equipment. Programmable control force feel is provided by a "through-the-panel" two-axis controller that can be removed and replaced with a two-axis side-stick controller that can be mounted in the pilot's left-hand, center, or right-hand position. A variable-force-feel system is also provided for the rudder pedals. The pilot's instrument panel can be configured with various combinations of cathode ray tube (CRT) displays and conventional instruments to represent aircraft such as the Cessna 172, Cherokee 180, and Cessna 402B. A collimated-image visual system provides a 60° field-of-view out-the-window color display. The visual system can accept inputs from a terrain model board system and a computer-generated graphics system. The simulator is flown in real time with a CDC CYBER 175 computer to simulate aircraft dynamics.

Research conducted in the GAS on the single-pilot instrument flight rules (SPIFR) has identified the pilot interface with cockpit controls and displays as a critical factor in reducing pilot work load and blunders. The air traffic control (ATC) Mode-S transponder, planned for operational use in the next decade, will add the capability of a digital ground-air ground data link to the general-aviation (GA) SPIFR cockpit. A research program is under way to evaluate the impact of various levels of data link capability on GA SPIFR operations. The levels tested will vary from uplink only of short ATC messages to uplink and downlink of complex messages. Messages to be considered will include weather data, initial instrument flight rules (IFR) clearances, and ATC tactical instructions. Initial tests will utilize current ATC procedures and conventional aircraft avionics suites. Follow-on tests will consider advanced ATC procedures and the interface of the airborne data link device with flight management system computers for execution of ATC clearances. Another research application using the GAS is the investigation of flight control problems encountered in recovering a twin-engine GA aircraft to normal flight after one engine fails.

Ride Quality Augmentation System

Improving the ride quality of general-aviation airplanes has been identified as one of the top priorities for revitalizing the depressed

general-aviation marketplace. In response to this need, NASA has initiated a program to develop and validate design methodology for gust-alleviation systems for this class of airplanes. The University of Kansas, under a grant from NASA, has developed candidate control laws for an experimental system to be tested on a modified Cessna 402B Businessliner, shown in the figure. These control laws were developed using modern control theory and a linear aerodynamic mathematical model for the Cessna 402B.

The candidate control laws were tested on the General Aviation Simulator. This simulator incorporated a nonlinear aerodynamic mathematical model and allowed realistic pilot-in-the-loop evaluations of the maneuvering characteristics. The simulation evaluation demonstrated the effectiveness of the system in reducing the airplane response to turbulence and indicated that the modified airplane would have generally good flying characteristics. A few potential problem areas in the control algorithms were uncovered. These problems could not be evaluated using the linear, pilot-out-of-the-loop simulations at the University of Kansas. In addition, the effects of system failures, including failure of an engine, on the airplane flight characteristics were evaluated by the project pilot. Most of the failures were benign, but a few failures that warrant further analysis were identified. **(E. C. Stewart, 3274)**

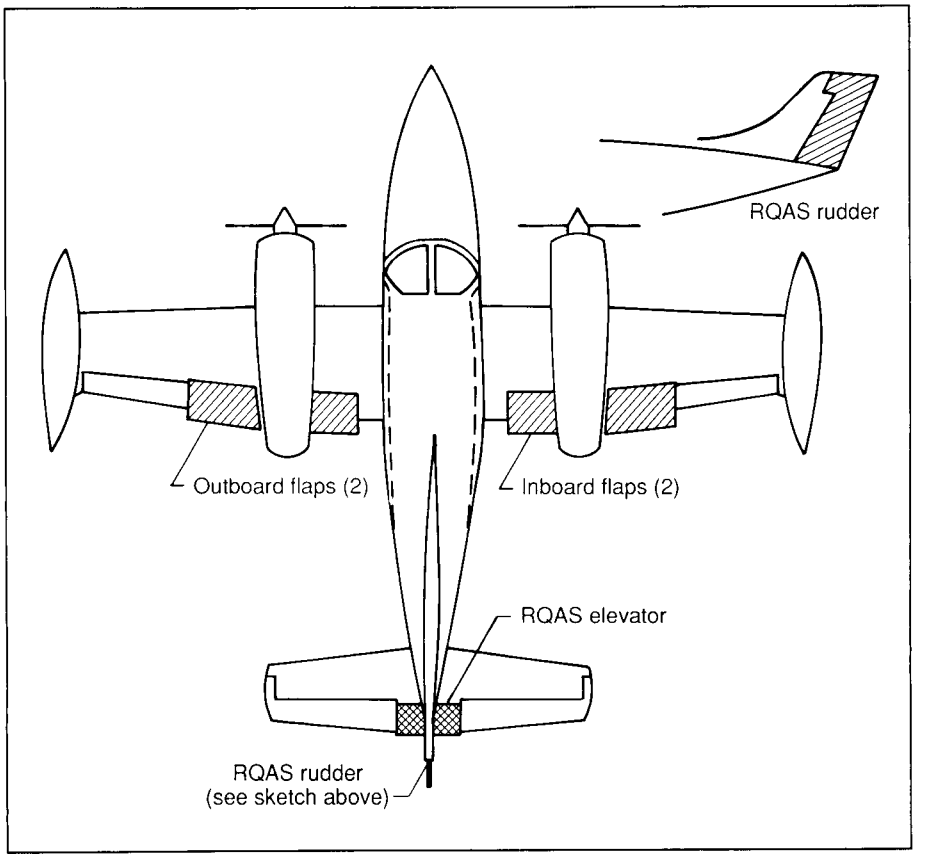

Ride Quality Augmentation System (RQAS) on Cessna 402B Businessliner.

Mission Oriented Terminal Area Simulation—MOTAS

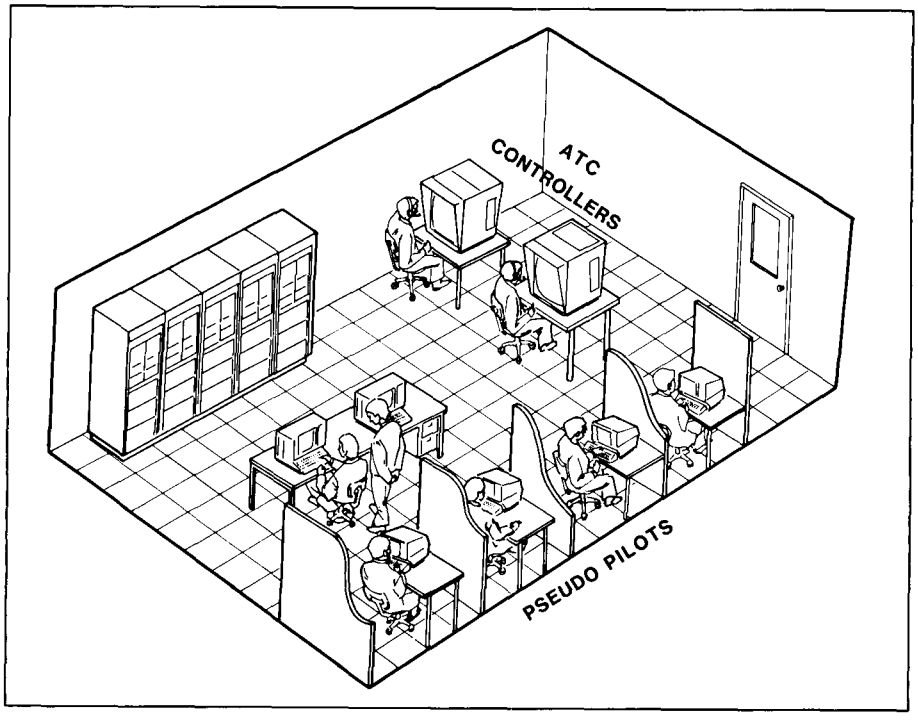

The Mission Oriented Terminal Area Simulation (MOTAS) facility is an advanced simulation capability that provides an environment in which flight management and flight operations research studies can be conducted with a high degree of realism. This facility provides a flexible and comprehensive simulation of the airborne, ground-based, and communications aspects of the airport terminal area environment. The major elements are an airport terminal area environment model, several aircraft simulators, pseudo pilot stations, air traffic controller stations, and a realistic air-ground communications network. The airport terminal area represents today's Denver Stapleton International Airport and surrounding area with either an advanced automated air traffic control (ATC) system or a present-day vectoring ATC system using air traffic controllers.

The MOTAS facility combines the use of several aircraft simulators and pseudo pilot stations to fly aircraft in the airport terminal area. The facility is presently operational with the Transport Systems Research Vehicle (TSRV) Simulator, the DC-9 Full-Workload Simulator, and the General Aviation Simulator. The Advanced Concepts Simulator will be interfaced to the facility once it becomes operational for research studies. These aircraft simulators allow full crews to fly realistic missions in the airport terminal area. The remaining aircraft flying in the airport terminal area are flown through the use of the pseudo pilot stations. The operators of these stations can control five to eight aircraft at a time by inputting commands to change airspeed, altitude, and direction. The final major components of the facility are the air traffic controller stations, which are presently configured to display and control the two arrival sectors, the final approach sector, and the tower and/or departure sectors.

Because of its flexibility in reconfiguring according to research requirements, the MOTAS facility can support a variety of flight vehicle and/or air traffic control system research studies that would not be possible in the real world due to safety, economic, and repeatability considerations. Two aircraft/ATC data link message transfer studies (one addressing civil transports and the other addressing general aviation) are examples of studies that are under way. In both cases, operational issues and experimental equipment involved in the data link transfer of ATC information and advisories are being studied. Examples of studies under development are a baseline controller study to obtain data on manual ATC operations to be used for comparison with results from advanced automatic ATC systems, and development of a tieline from the Wallops Flight Center (WFC)

to Langley Research Center (LaRC) to allow the Transport Systems Research Vehicle to be flown at WFC as one of the aircraft in the simulated ATC environment at LaRC.

Development of Time-Based Terminal Flow Control Concept

A time-based concept, called TIMER (traffic intelligence for the management of efficient runway scheduling), has been developed, implemented, and evaluated. TIMER embodies, in an evolutionary manner, an extended terminal area flow control system by integrating en route metering, cruise speed control, fuel-efficient profile descents, and terminal sequencing and spacing together with computer-generated controller aids. The goals are to achieve full use of runway capacity and to improve the fuel efficiency through planned delay absorption. The concept has been implemented in the Mission Oriented Terminal Area Simulator and coupled to both aircraft simulators and flight vehicles.

Fast-time and real-time computer simulation results have identified and shown the effects and interactions of key variables, such as horizon of control, metering fix and final approach delivery time errors, aircraft separation criteria, wind, and knowledge of aircraft expected-final-approach speed. Among the major findings is the idea that en route metering fix delivery-error standard deviations should be at or below approximately 45 s to achieve full runway capacity. It was also determined that, with computer aid, the runway interarrival-error standard deviation for non-four-dimensional equipped traffic can be reduced to the region of 8 s to 12 s if expected-final-approach speed is known (as shown in the figure). However, if the expected-final-approach speed is unknown, the standard deviation rises to the region of 16 s to 20 s. Flight test data are presently being analyzed for comparison to the fast-time and real-time simulation results.

(L. Credeur and W. Capron, 3621)

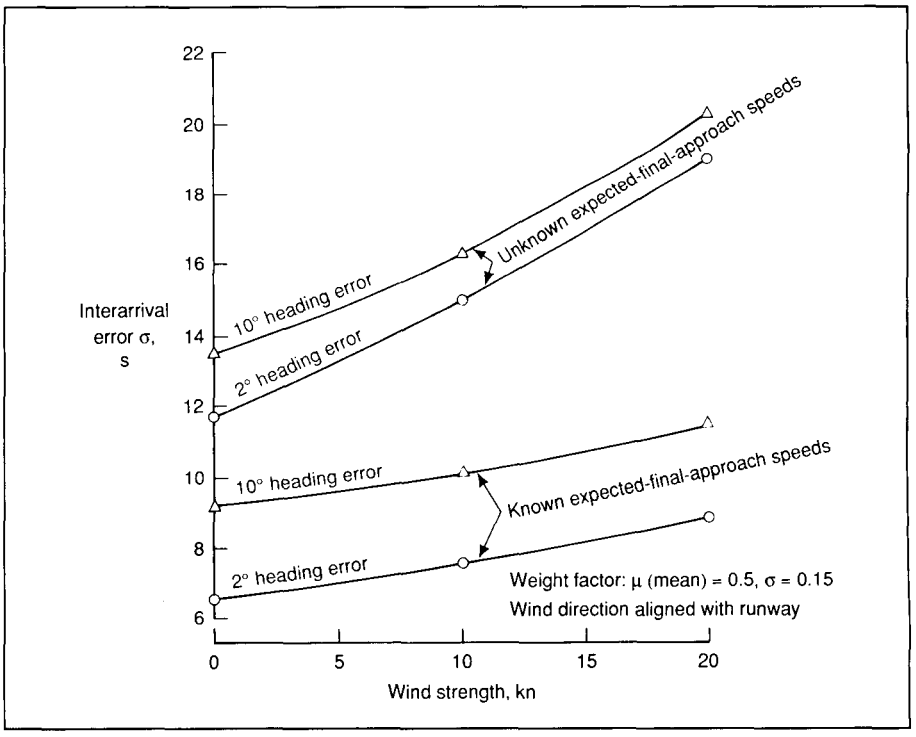

Wind strength, heading error, and unknown final approach speed effect on system arrival error.

Differential Maneuvering Simulator

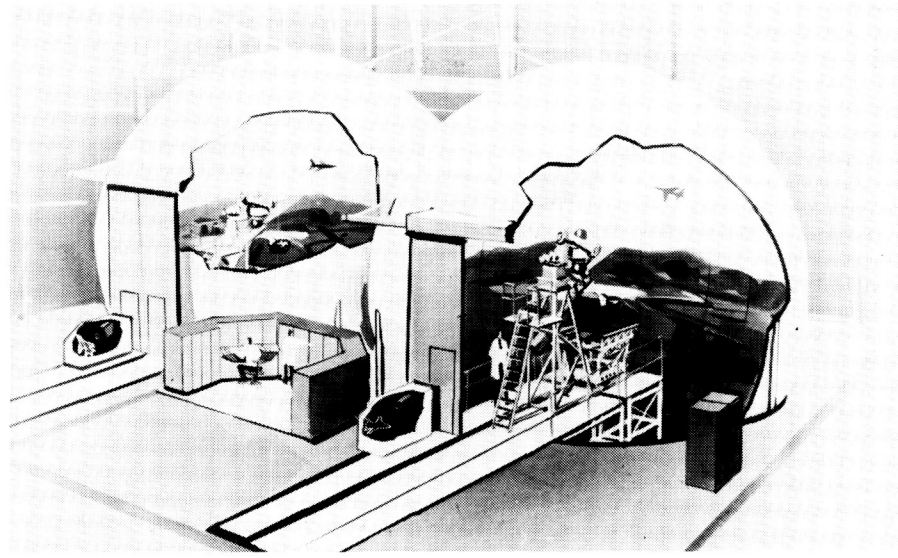

The Langley Differential Maneuvering Simulator (DMS) provides a means of simulating two piloted aircraft operating in a differential mode with a realistic cockpit environment and a wide-angle external visual scene for each of the two pilots. The system consists of two identical fixed-based cockpits and projection systems, each based in a 12.2-m-diameter (40 ft) projection sphere. Each projection system consists of a sky-Earth projector to provide a horizon reference and a system for target image generation and projection. The internal sky-Earth scene provides reference in all three rotational degrees of freedom in a manner that allows unrestricted aircraft motions. The present sky-Earth scene has no translational motion. The internal visual scene also provides continuous rotational and bounded (300 ft to 45,000 ft) translational reference to a second (target) vehicle in six degrees of freedom. The target image presented to each pilot represents the aircraft being flown by the other pilot in this dual simulator. Each cockpit provides three color displays with a 6.5-in. square viewing area and a wide-angle head-up display. Kinesthetic cues in the form of a g-suit pressurization system, helmet loader system, g-seat system, cockpit buffet, and programmable control forces are provided to the pilots consistent with the motions of their aircraft. Other controls include a side arm controller, dual throttles, and a rotorcraft collective. Research applications include studies of high-angle-of-attack flight control laws, evaluation of evasive maneuvers for various aircraft and rotorcraft, and evaluations of the effect of parameter changes on the performance of several baseline aircraft.

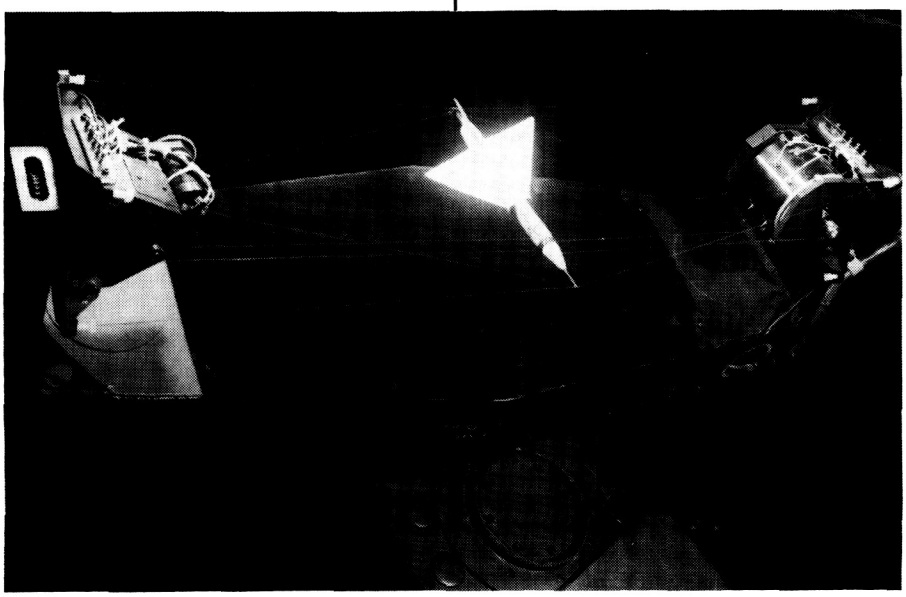

Target model. L-71-2579

Advanced Controls Research

Air combat studies have shown the importance of providing future fighter aircraft with extreme levels of agility and maneuverability throughout their flight envelope. A key to achieving this capability is the development of advanced control concepts that provide significant improvements in effectiveness, particularly at high-angle-of-attack conditions. Recent research efforts have focused on two classes of concepts: (1) multiaxes vectoring of the engine thrust, and (2) unconventional aerodynamic control devices such as movable forebody strakes. The investigations have included both wind tunnel testing as well as piloted simulation studies on the Differential Maneuvering Simulator.

The primary objectives of the simulation studies are to evaluate the enhancements in maneuverability provided by the advanced control concepts under realistic combat conditions and to define control law requirements to maximize these benefits. The investigations are being conducted using a full-envelope simulation model of the F-18 airplane. To this baseline simulation have been added representations of a multiaxes thrust vectoring system and deflectable forebody strake yaw control devices developed using wind tunnel test data. Evaluation methodology has ranged from simple maneuvering tasks to simulated one-on-one air combat. The results to date show that these advanced control concepts can provide maneuvering enhancements that are very advantageous in air combat. However, the results also show that achieving these gains requires advancements in several related technology areas including multieffector control law design to meet critical flying qualities requirements and cockpit information systems for improved pilot simulation awareness and maneuver guidance.
(M. E. Ogburn, 2184)

View of cockpit and visual display. L-87-8822

Visual/Motion Simulator

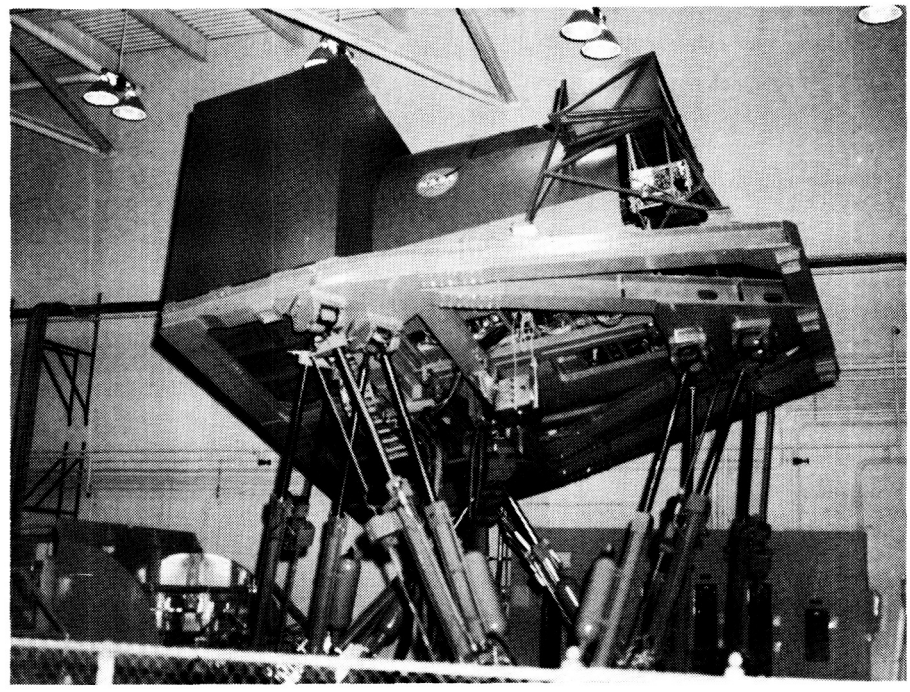

The Visual/Motion Simulator (VMS) is a general-purpose simulator consisting of a two-man cockpit mounted on a six-degree-of-freedom synergistic motion base. A collimated visual display provides a 60° out-the-window color display for both left and right seats. The visual display can accept inputs from several sources of image generation. A programmable hydraulic-control loading system is provided for column, wheel, and rudder in the left seat. A second programmable hydraulic-control loading system for the right seat provides roll and pitch controls for either a fighter-type control stick or a helicopter cyclic controller. Right-side rudder control is an extension of the left-side rudder control system. A friction-type collective control is provided for both the left and the right seats. An observer's seat was installed in 1986 to allow a third person to be in the cockpit during motion operation.

A realistic center control stand was installed in 1983 which, in addition to providing transport-type control features, provides auto-throttle capability for both the forward and reverse thrust modes. Motion cues are provided in the simulator by the relative extension or retraction of the six hydraulic actuators of the motion base. Washout techniques are used to return the motion base to the neutral point once the onset motion cues have been commanded. In addition, a g-seat is provided which can be interchanged between the left and right seats to augment the motion cues from the base.

Research applications have included studies for transport, fighter, and helicopter aircraft. These studies addressed problems associated with wake vortices, high-speed turnoffs, microwave landing systems, energy management, multibody transports, and maneuvering stability flight characteristics. Numerous simulation technology studies have also been conducted to evaluate the generation and usefulness of motion cues.

Effect of Motion Cues During Complex Curved Approach and Landing Tasks

NASA is participating with the Federal Aviation Administration in the Microwave Landing System Advanced Applications Program. This is a multiphase program that uses both fixed-based and motion-based aircraft simulators to define envelopes of usable approach path geometry by considering aircraft instrumentation, path tracking performance, pilot acceptance, and work load. There was concern that both quantitative and subjective measures being used to indicate pilot performance, acceptance, and work load might be affected by motion or lack of motion. The objective was to determine the effects of motion

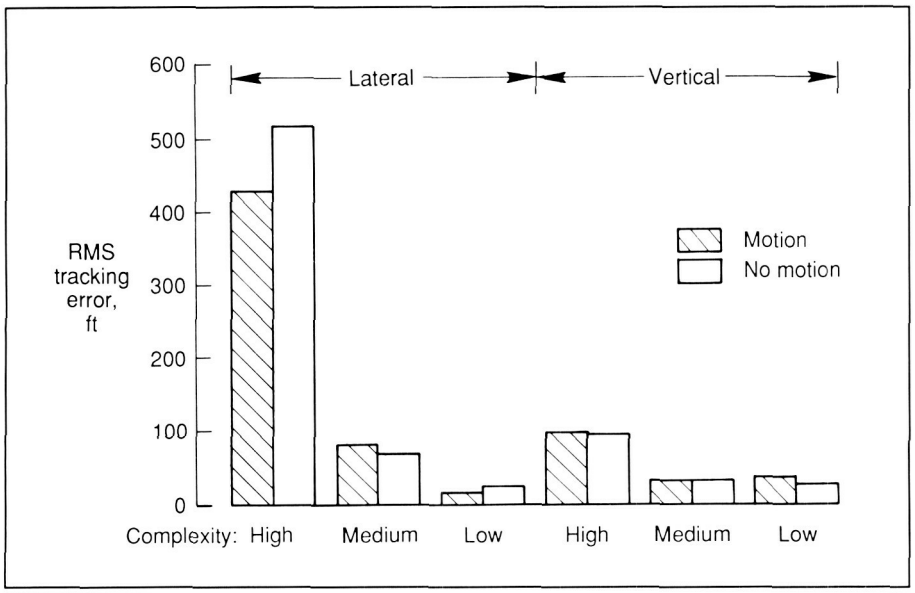

Effect of motion on pilot-in-the-loop simulation results (tracking performance).

cues during manually flown, curved approach-and-landing tasks.

Seven pilots, who were used as test subjects, flew a test matrix of 36 approach-and-landing tasks in a high-fidelity motion-based aircraft simulator that was equipped with electro-mechanical flight displays. The test matrix contained tasks of high, medium, and low complexity, with and without turbulence, with three wind models, and with and without motion. Analysis of variance (ANOVA) tests were conducted on pilot tracking performance and work load measures, and statistical summaries of subsets of the data set were computed to determine the effects of motion. As an example, root mean square (RMS) lateral and vertical tracking errors, with and without motion, are shown in the figure for several levels of task complexity. Statistically significant motion effects were found only for one of the six comparisons shown; for the high-complexity task, "motion-on" resulted in a smaller lateral tracking error. "Motion-on," however, resulted in a higher work load than "motion-off" as measured by the Subjective Workload Assessment Technique (SWAT) ratings, pilot control activity, and pilot eye scan rate.

These results suggest that reliable performance results are obtainable from fixed-base simulation for low-to-moderate-complexity tasks but for high-complexity tasks, the performance results obtained in fixed-based simulations are conservative, i.e., the fixed-base simulation predicts somewhat poorer performance than would be achieved in the real world.
(C. E. Knox, 3621)

Space Simulation Facility

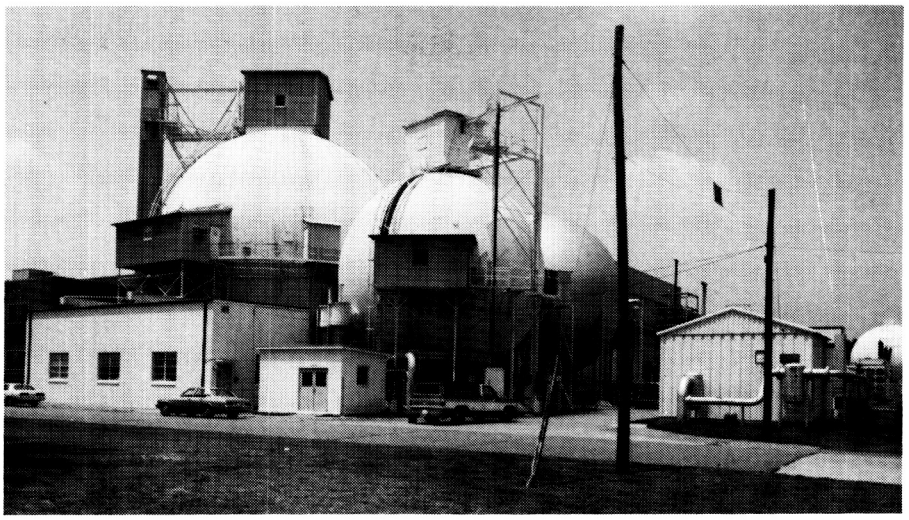

The 60-ft-diameter Space Simulation Facility can simulate an altitude of 320,000 ft (2×10^{-4} mm Hg). This vacuum level is attainable in 7 hours with a three-stage pumping system. The carbon steel sphere is accessible through a personnel door, a 12-ft-diameter specimen door, and a 4-ft maintenance door at the top. A 2-ton hoist located at the top enhances specimen handling inside the sphere. Sight ports are located both at the top and at the equator. Two closed-circuit television cameras, a video cassette recorder, and an oscillograph are available. Firing circuitry and a programmer are available for the use of pyrotechnics, and a system of flood lights is installed in the sphere to facilitate high-speed photography. The sphere is used primarily for dynamic testing of aerospace components and models at near-space environment.

Thermal vacuum testing has long been a prerequisite to the active deployment of space experiments. A series of experiments that optically sense characteristics of the Earth's atmosphere from outer space necessitated the creation of an ultrahigh-cleanliness thermal facility. The optical components of these experiments would be severely degraded by contamination by oils or other vaporous materials commonly found in thermal chambers and vacuum pumping systems. Langley Research Center created the 8- by 15-Foot Thermal-Vacuum Chamber facility by repeated vacuum bakeout and solvent wipedown of a previously used chamber. Two 35-in. cryogenic pumps were installed, and cold traps were inserted in the roughing pump lines to eliminate back contamination from the pumps. The chamber is capable of $-300°F$ to $+1000°F$ temperatures and has glass ports for solar illumination simulation. A one-unit flux solar simulator is installed with the chamber.

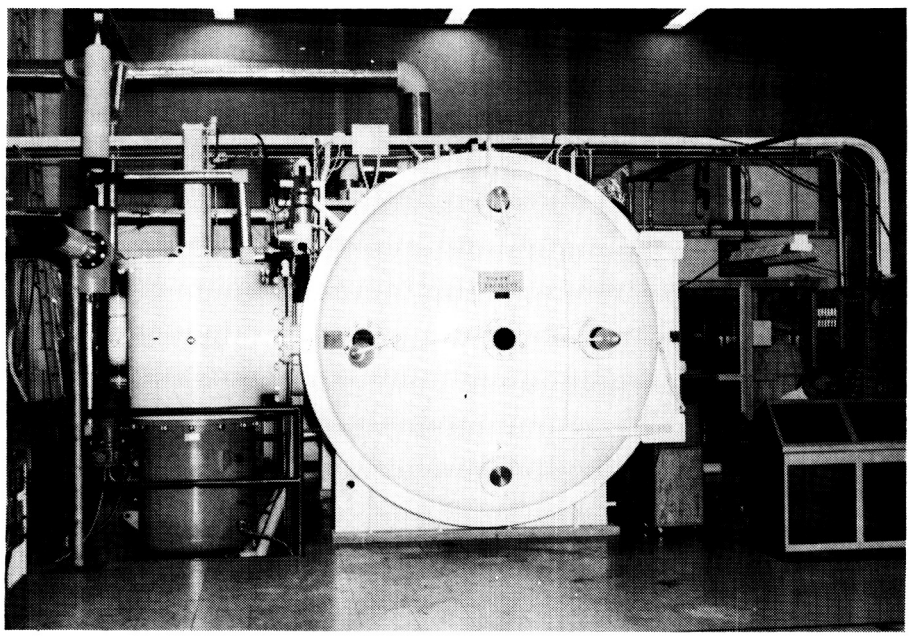

8- by 15-Foot Thermal-Vacuum Chamber. L-82-9,672

Halogen Occultation Experiment Chopper Motor Lifetime Test

The Halogen Occultation Experiment (HALOE) uses a chopper wheel to chop the incoming optical beam as well as the onboard blackbody beam. A projected lifetime test of a HALOE chopper motor/wheel assembly is being conducted to demonstrate that the motor will perform satisfactorily during a 2-year period of continuous operation in a vacuum environment. The motor is a hysteresis synchronous motor (Schaeffer Magnetics Incorporated, part number 102975, serial 104) purchased as a spare by the HALOE Project. A simulated inertia wheel was fabricated and attached to the motor, which was then balanced to flight specifications. The motor/wheel assembly was attached to a bracket that simulated flight heat flow and then placed in a vacuum chamber capable of pumping to 1×10^{-6} torr. Eight temperature sensors, motor current, and motor speed are monitored. Additionally, the voltage and current of the power supplies and the pressure of the chamber are monitored.

The data are taken using an IBM PC-AT with a Techmar interface card installed with the computer. A data sample is taken every 10 s and compared to preset limits. If the data are within limits, they are stored in a first-in-first-out buffer and written over when data from the last hour has been stored. If the data are out of limits, they are stored in a permanent buffer until the out-of-limit condition is cleared. Additionally, a sample taken every hour is printed and stored in a long-term file.

The photograph shows the test setup. The vacuum chamber is the large stainless-steel bell-shaped container. The HALOE chopper motor has operated inside the vacuum chamber since November 1986. Information showing the condition of the motor, the chamber, and test equipment has been collected at the beginning of each month for analysis and plotting. To date, over 200,000 samples of data have been reviewed without any detectable degradation of the motor.

(V. S. Laney, 4621)

MAPS Characterization Tests

The Measurement of Air Pollution From Satellites (MAPS) Experiment is a single-channel thermal infrared instrument operating at 4.3 μm designed to provide remote measurements of total tropospheric carbon monoxide (CO) burden from near-Earth orbital altitudes. Following the OSTA-1 and OSTA-3 missions, an instrument modification was completed at Langley Research Center to minimize polarization errors resulting from in-flight balance and calibration operations. Subsequent to that modification, extensive instrument thermal vacuum survival and characterization testing was conducted on the MAPS flight system. This testing was conducted in Langley's 8- by 15-Foot Thermal-Vacuum Chamber,

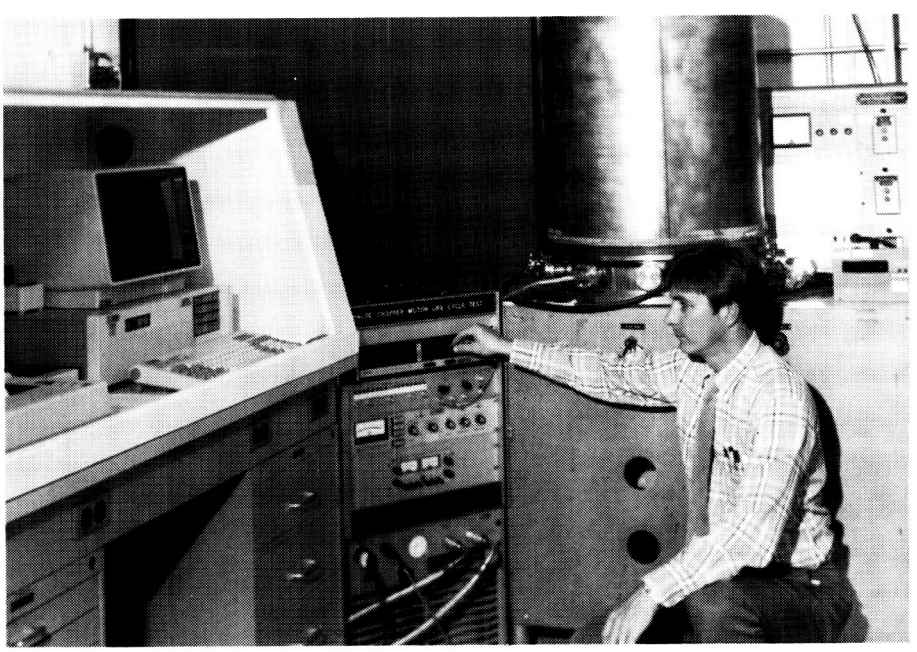

Instrumentation arrangement. L-86-11,135

as shown, in June and July of 1987.

During the initial phase of that test program, a matrix of 260 test conditions was utilized to characterize instrument performance in a simulated space environment. These test conditions were selected on the basis of instrument temperature, source temperature, and simulated tropospheric composition and temperatures. During the second phase of the test, instrument performance was evaluated as a result of a variation of the instrument temperature through the survival and operational temperature ranges of 263 K to 316 K. Successful operation of the instrument throughout these tests demonstrated that all functional design requirements were met. Post-test data reduction confirmed that polarization errors were minimized as predicted. **(R. T. Sherrill, 4621)**

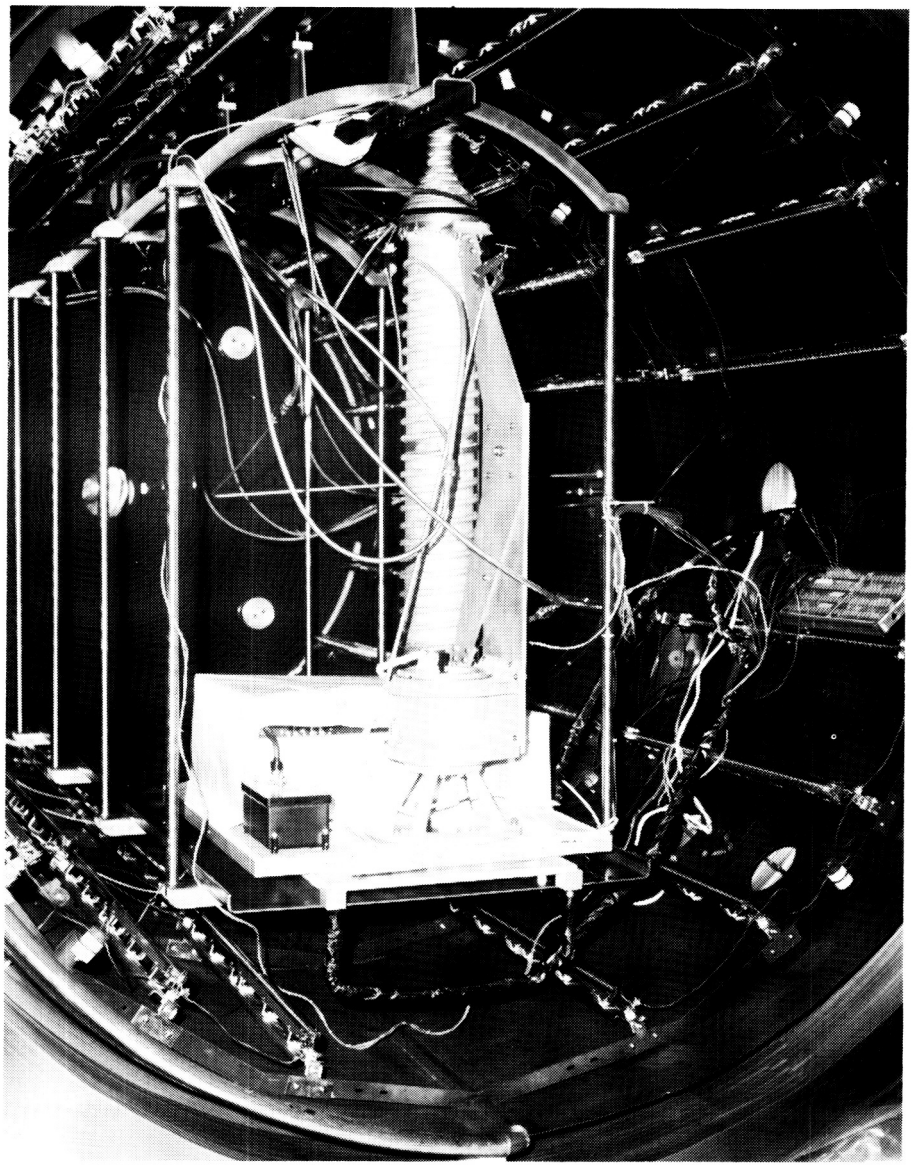

MAPS Thermal-Vacuum Chamber test installation. L-87-06992

HALOE Thermal Sensitivity Tests

A series of thermal sensitivity tests were performed on the HALOE instrument in the 8- by 15-Foot Thermal-Vacuum Chamber to determine the cause of serious performance problems when the mainframe (optical bench) temperature was changed. Temperature changes of 1°C to 2°C caused significant changes in the electronic signal from the photovoltaic gas channel detectors. The automatic gain control (AGC) electronics could not maintain the required difference signal stability for thermally changing environments expected when the instrument was put into Earth orbit. The thermal environment inside the 8- by 15-Foot Thermal-Vacuum Chamber was varied to induce temperature changes on the instrument mainframe.

Individual optical components were modified, and the effects of each change were monitored during the sensitivity tests. Primary solutions developed from the tests were to increase the aperture size on the instrument internal blackbody and baffles located along the optical path. In addition, during refurbishment of the instrument,

refined detector alignment procedures will be used to locate the energy beam on the most uniform response area of the detector. Temperature sensitivity tests will be repeated in the 8- by 15-Foot Thermal-Vacuum Chamber after the refurbishment of the HALOE instrument has been completed.
(L. Gordley, 2719)

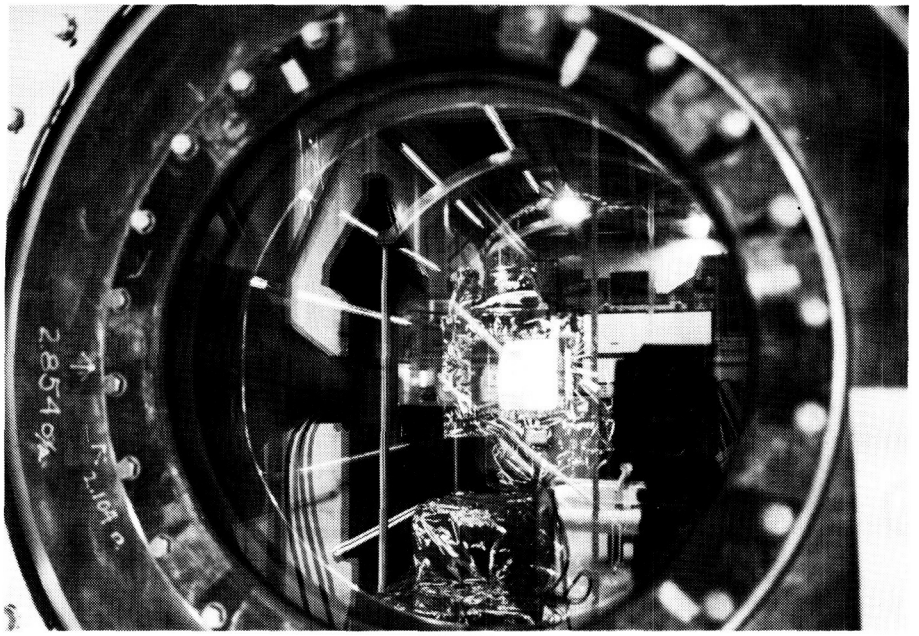

L-86-8109

HALOE instrument in Thermal-Vacuum Chamber during thermal sensitivity tests.

Structural Dynamics Research Laboratory

The Structural Dynamics Research Laboratory is designed for the conduct of research on the dynamic behavior of spacecraft and aircraft structures, equipment, and materials. It offers a variety of environmental simulation capabilities, including acceleration, vacuum, and thermal radiation.

A main feature of the laboratory is the 16-Meter Thermal-Vacuum Chamber. It has a 55-ft diameter hemispherical dome with a removable 5-ton crane, a 65-ft high dome peak, flat floor, and option for a large centrifuge or a rotating platform. Access is by an airlock door and an 18-ft high by 20-ft-wide test specimen door. There are ten 10-in.-diameter view ports that are randomly spaced for visually monitoring tests. A vacuum level of 10 torr can be achieved within 120 minutes and, with diffusion pumps, 10^{-4} torr vacuum can be achieved in 160 minutes. The centrifuge attached to the floor of the chamber is rated to 100 g with a 50,000-lbf capacity and a maximum allowable specimen weight of 2000 lb. Six-ft mounting faces for test articles are available at 16.5-ft and 20.5-ft radii. The tables can accommodate electromagnetic and hydraulic excitation devices. A temperature range of 100°F is obtained from 250 ft^2 of portable radiant heaters and liquid-nitrogen-cooled plates.

The other dominant feature of the Main Laboratory (room 106) is a 38-ft-high backstop of I-beam construction. Test areas available around this facility are 15 ft by 35 ft by 38 ft high and 12 ft by 12 ft by 95 ft high.

A new feature is the Large Component Test Room (room 123). It is an open room with nominal dimensions of 75 ft by 84 ft by 84 ft high. There is a 7-ton monorail hoist and a full environmental control system. This laboratory room has

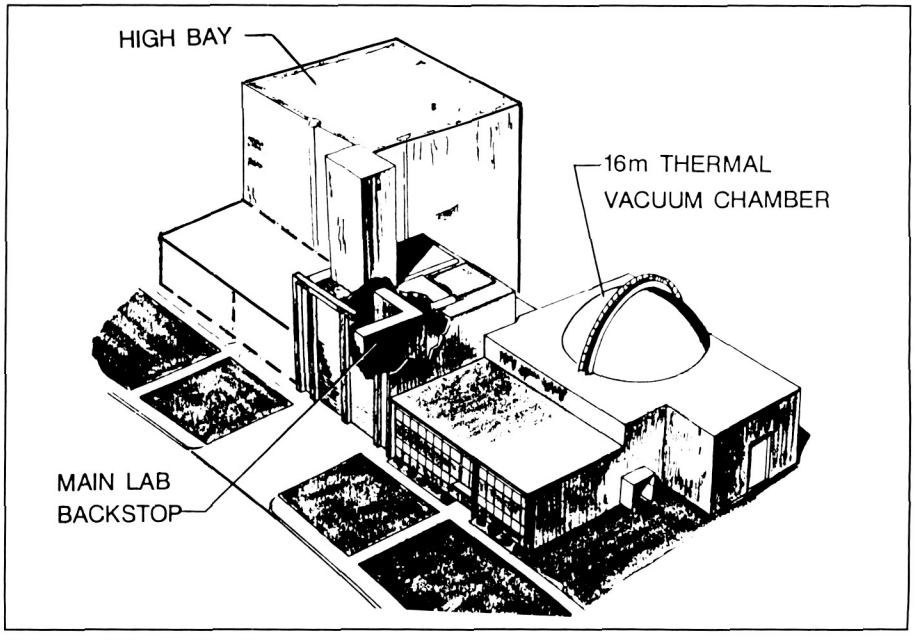

Structural Dynamics Research Laboratory.

various platforms accessible for viewing and instrumentation.

Available excitation equipment includes several types of small shakers. The largest shaker is a hydraulic with a maximum of 1200-lbf, 6-in. stroke, and a 0-Hz to 70-Hz range. All areas are monitored by closed-circuit television cameras, connected by voice, and hard-wire connected to a central data acquisition and processing room. This room contains signal-conditioning equipment and analog and digital data recording capability for up to 220 channels of data. A GenRad 2515 digital signal processing system is available along with a VAX 11-780/EAI 2000 hybrid computer system for simulation and on-line test control. A variety of auxiliary data logging and signal processing equipment is also available.

Feasibility of Scaling Structural Joints for Erectable Space Station

Many future spacecraft such as the Space Station are expected to be much too large to obtain accurate structural test data in the Earth's gravity. Therefore, preflight verification of analyses and design must be obtained using tests on components and, possibly,

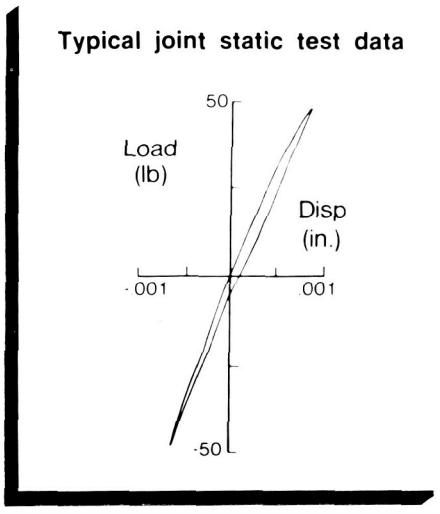

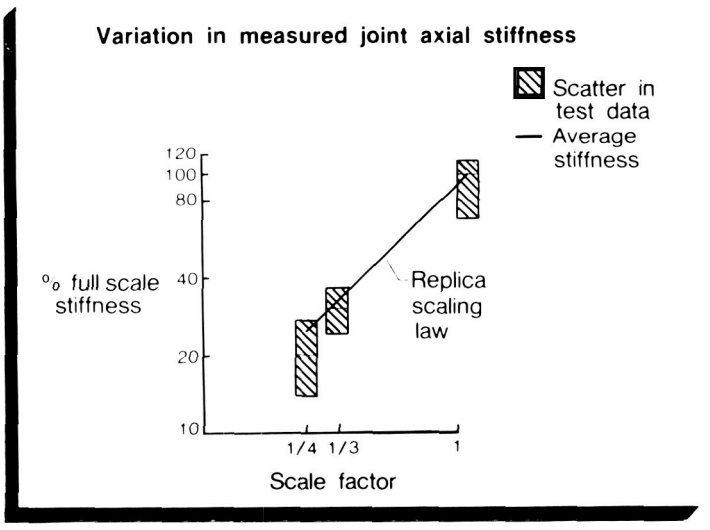

Examples of joint specimen

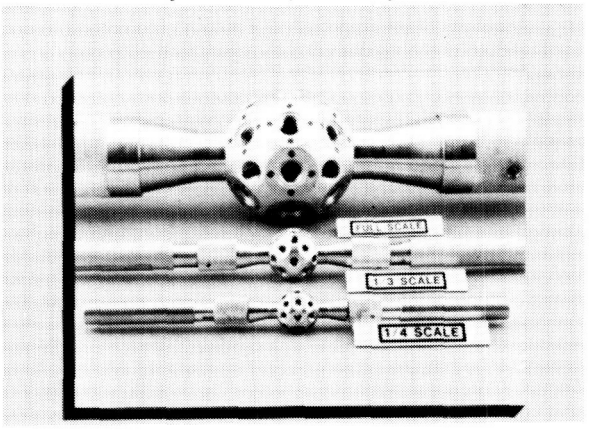

ORIGINAL PAGE IS
OF POOR QUALITY

Typical joint static test data (top, left), variation in measured joint axial stiffness (top, right), and examples of joint specimen (bottom). L-87-4232

scale models of the full system. Studies are being conducted to examine the feasibility of geometrically scaling structural joints applicable to an erectable Space Station and to predict their behavior according to replica scaling laws.

An interim joint design for an erectable Space Station was selected as the basis for the scaling studies. Test joints were fabricated under contract at 1/3 and 1/4 scales by geometrically scaling from the full-scale joint. Certain full-scale features could not be practically scaled within the scope of this study (i.e., machining tolerances and screw threads). Static tests were conducted on full-scale and subscale joints at approximately scaled test conditions. Joint axial stiffness was calculated based on the measured load-deflection test data.

Relatively good correlation between the results of the subscale and full-scale tests was achieved considering the quality of replication. Shown in the figure are the scaled axial stiffness values measured for the various joints as a percentage of the average full-scale stiffness. The test data showed there is appreciable scatter in the measured axial stiffness among each size of joint (depicted as the shaded areas in the graph, page 78). This is probably due to variability in machining tolerances from joint to joint leading to misalignment of mating surfaces and variability in preload introduced when assembling the joint. It is realistic that a certain amount of scatter will be present; yet, in practice, this scatter can be reduced by more stringent quality control over the fabrication process. Theoretically, if the subscale joints are completely replicated, the axial stiffness should scale linearly with the scale factor. Thus, a 1/4-scale joint would have 1/4 the axial stiffness of the full-scale joint. It was found that the average stiffness of the scaled joints appropriately multiplied by the theoretical scale factor was close to the predicted value based on replica scaling laws. The 1/3- and 1/4-scale joints were about 8 percent and 18 percent lower, respectively, than the predicted values. A major factor in the difference is attributed to the tolerances that were not scaled. The 1/3-scale joints could be machined with tolerances more like the full-scale joints; thus, they performed better.

A major challenge in conducting a successful test-analysis program on a scale model of the Space Station is the ability to fabricate subscale joints that behave according to replica scaling laws. This initial attempt to scale joint stiffness is extremely encouraging and indicates that with improved manufacturing precision, the stiffness of the full-scale joint can be replicated to 1/4 scale. These results also emphasize that scaling is more practical with large-scale models in which the machining process can be better controlled.

Additional tests are planned using scaled replicas of a more current erectable joint design with tighter control over the machining tolerances. Analytical models that describe nonlinear joint behavior are being developed. **(P. E. McGowan, 3615)**

Initial Test Results for Mini-Mast

NASA Langley Research Center is conducting tests on a deployable, 20-m truss beam known as the Mini-Mast to learn how to efficiently test large truss structures, to relate component testing (joints and tubes) to the overall behavior of the structure, and to update the associated analytical model based on experimental data.

The stowed structure is about 5 percent of the fully deployed 20-m length. A total of 111 titanium joints are used in deploying the 18-bay structure. To minimize the effect of instrumentation on the truss beam, noncontacting proximity probes are used to measure displacements. One probe is located at each vertex of the triangular cross sections to measure displacements. The sensed data are then transformed to a global coordinate system to recover the displacements at each bay. Bending and axial strain gauges are used to monitor reaction forces at the base. The structure was statically loaded at the tip of the beam by a cable-pulley-

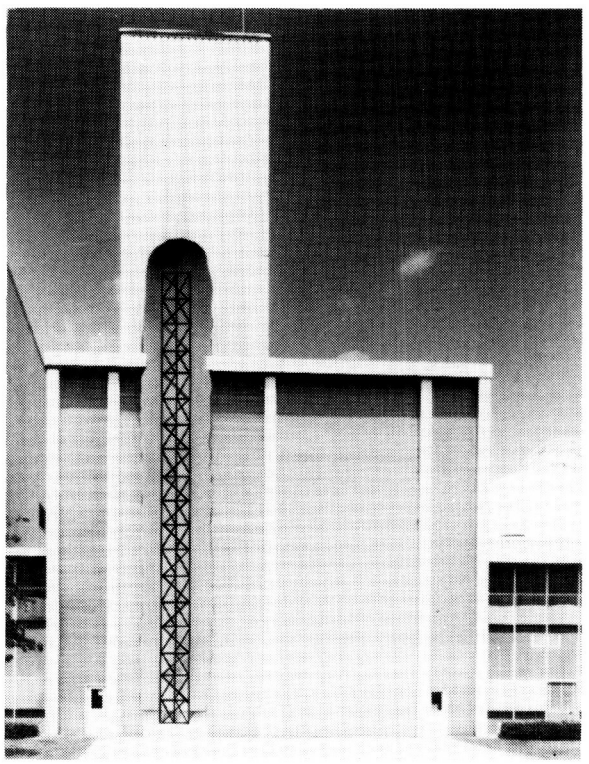

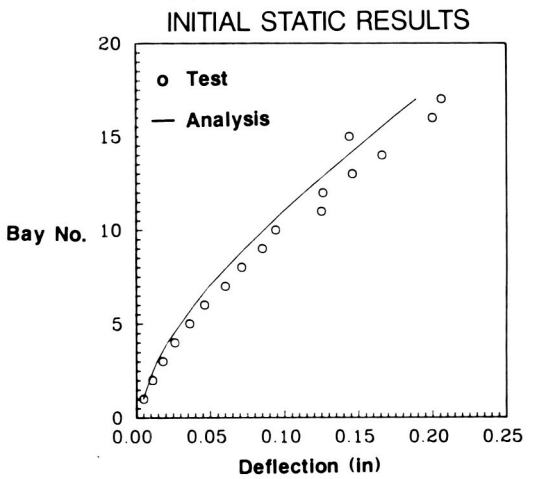

INITIAL DYNAMIC RESULTS

	ANALYSIS		TEST	
	FREQ. (HZ)	DAMPING (%)	FREQ. (HZ)	DAMPING (%)
1ST BENDING	1.44	*	1.45	0.6
1ST TORSION	7.11	*	8.54	0.4
2ND BENDING	9.66	*	9.47	0.5

Mini-Mast test configuration and results. L-87-5745

weight arrangement. Impact testing was used for the initial dynamic test.

Initial testing of the beam includes verification of the measurement system which is, in itself, a major task. The data acquisition program reads 51 probes each time to recover the motion for 17 bays. The figure depicts a sketch of the truss beam overlayed on a picture of the Building 1293B test tower to show its relative size. The beam is supported at the base and loaded at the tip with 5 lb. The right-hand plot shows the measured deflection (circles) of the center of gravity (CG), and the solid line shows the predicted values from the finite-element model as a function of the bay number. The analytical model appears to be stiffer than the measured response. To examine the fidelity of the finite-element model, a dynamic test was performed. The beam was impacted with a rubber hammer at a point seven bays above the base support, and data from 15 probes were analyzed. Because of the low energy imparted to the beam, only the first three modes were identified. The identified modal frequencies and damping values are shown in the table (at the bottom right in the figure) along with the predicted values. Initial results show good agreement in the frequencies for the bending modes. The torsion mode is higher than the predicted value. The measured modal damping is below 1 percent.

The work shows the fidelity of the 20-m deployable truss beam when compared to the existing analytical model and the capability of the existing measurement. In addition, this joint-dominated structure exhibited low damping values, an indicator of high quality of the joints.
(G. C. Horner, 3699)

Structures and Materials Research Laboratory

Built in 1939, this laboratory has been contributing significantly to the development of aircraft structural designs and validation since World War II. Work conducted in this laboratory includes the characterization and application of advanced materials and the development of novel structural concepts. Static testing, environmental testing, and material analysis are performed using the unique capabilities of this laboratory. Results of the testing and analysis are directly applicable to the structures and materials technologies development required for future advanced subsonic aircraft, high-speed transports, high-performance military aircraft, and large space systems. Research performed here focuses on the development of structural mechanics technology and advanced structural concepts required to enable the verified design of efficient, damage-tolerant advanced composite aircraft structural components subjected to complex loading and environmental conditions and on space-durable advanced materials and structural designs for future large space systems with significant improvements in performance and economy.

The main feature of the laboratory is its static testing equipment. A 1,200,000-lb-capacity testing machine is used for tensile and compressive tests of specimens up to 6 ft wide by 18 ft long. This machine has been used to test full-scale, compression-loaded cover panels for aircraft structures. Lower capacity testing machines of 300,000-, 120,000-, 100,000-, and 10,000-lb capacity also are used for smaller specimens. These machines have been used for a wide range of tests that examine both material properties and structural response. Capability exists for testing large structural specimens such as the trusses used for the Space Station development and future large space structures. Test data are recorded using a high-speed automated data acquisition system, and these data are reduced and analyzed using on-site computers.

Environmental testing for materials is performed using inert atmosphere furnaces with temperature capabilities up to 4500°F. A 3200°F inert atmosphere dilatometer/thermogravimetric analyzer also is used. A hypersonic materials environmental system is capable of continuous operation at Mach 5 to 150,000 ft altitude to simulate operating conditions for future high-speed and hypersonic aircraft. The system is used to study the effects of environment on the materials used for future high-speed and hypersonic aircraft applications. Polymer films are studied using two 30-in.-diameter electron irradiation chambers capable of pressures to 10^{-8} torr and of energy levels to 100 keV.

Material analysis of fiber-reinforced composite materials and of new alloys is performed using a scanning electron microscope, an electron probe analyzer, X-ray equipment, and an electron microscope. This equipment is used for fundamental material science studies of emerging materials for aerospace applications.

Postbuckling Strength of Graphite/Epoxy Panels

Aircraft structures have been traditionally designed to carry load without buckling. A fuselage or wing panel may be more structurally efficient and less expensive if buckling occurs at loads less than the design ultimate load. However, a panel's postbuckling behavior may affect its strength. The strength of metal panels is predicted empirically using a large experimental data base. Composite materials have a limited data base because of the wide variety of laminates and many possible local failure modes, and the strength of a composite structure is difficult to predict. The objective of this research is to conduct experiments that identify and provide understanding of the local failure modes limiting the postbuckling performance of composite structures. These experiments are also used to verify predictions.

The specimen shown in the 1,200,000-lb capacity testing machine was designed and tested to study the postbuckling behavior of graphite/epoxy panels. The panel was manufactured by the Lockheed Aeronautical Systems Company-Georgia Division. This stiffened panel is 60 in. long by 42 in. wide and has a 143-in. radius. The panel is stiffened by five J-stiffeners spaced approximately 7 in. apart and by three frame sections spaced approximately 20 in. apart. The panel has fail-safe straps and skin padding under the stiffeners to suppress the skin-stiffener separation failure mode common to postbuckled stiffened panels.

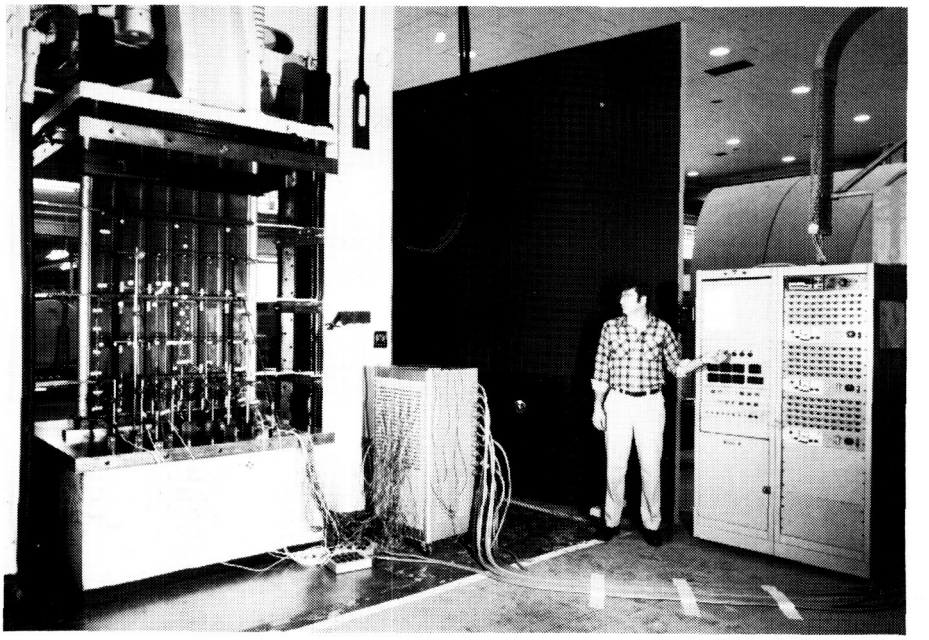

Graphite/epoxy fuselage panel prepared for postbuckling test. L-85-2036

The experimental buckling and ultimate loads were approximately the same as the predicted buckling and ultimate loads, respectively, but the panel failed due to a different failure mode than predicted. Failure occurred at a fail-safe strap and appears to be related to the thickness and stiffness discontinuities between the panel skin and the fail-safe strap. Additional studies of thickness and stiffness discontinuities of compression-loaded panels are under way, and a detailed nonlinear analysis of the panel is planned.
(J. H. Starnes, Jr., 2552)

Stiffness of Erectable Space Station Truss Joint

The baseline Space Station structure, which supports and connects all attached habitat modules, laboratory modules, and payload platforms, has been chosen to be an erectable 5-m truss. While a large number of reasons affected the truss selection decision, two extremely important features in favor of the erectable truss were the large achievable truss depth and demonstrated joint stiffness. These two features result in an extremely stiff structure that greatly enhances control of the large Space Station in orbit.

The Space Station truss structure and attached components will be assembled on orbit by astronauts in extravehicular activity (EVA). In order to enhance astronaut

efficiency and safety, a goal was to develop a joint design that did not require tools to assemble, yet demonstrated the required structural qualities and low effort assembly. Such a joint is shown being structurally tested in tension and compression in the photograph. This photograph shows a truss node with two attached strut joints. Testing a "complete" joint/node combination permits developing an effective extensional stiffness for this combination and greatly reduces analysis complexity for large truss structures. The joint/node combination, as shown in the figure, developed an extensional stiffness that was approximately 50 percent of the target strut stiffness to which the joint is to be attached. Other necessary features that were also demonstrated were linear load-displacement behavior and zero joint free play. Further joint developments, not shown in the figure, include the addition of grip enhancement features for astronaut gloves, a redundant lock/unlock feature, and a visual indication of joint position.

(H. G. Bush, 2498)

L-86-5930

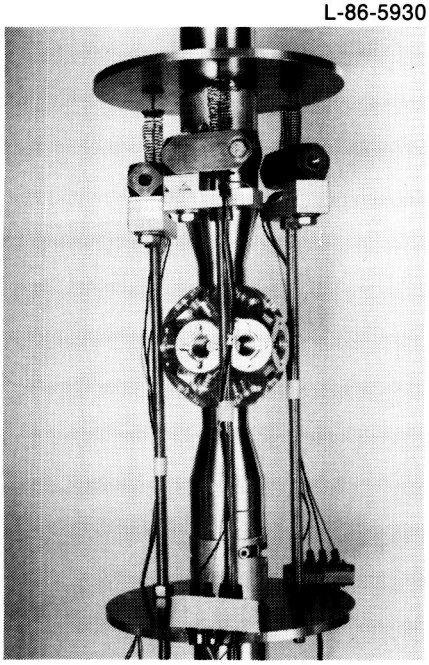

Load displacement test setup for Space Station node and joint.

NDE Research Laboratory

The reliability and safety of materials and structures are of paramount importance to NASA. The assurance of reliability must be based on a quantitative measurement science capability that is nondestructive. The Langley Research Center NDE Research Laboratory has as its prime focus the development of new measurement technologies that can be directly applied to ensuring material integrity. Furthermore, the laboratory activity is strongly directed toward developing physical properties required for structural performance.

The NDE Research Laboratory is a combination of research facilities providing advanced nondestructive evaluation (NDE) capabilities for NASA and is an important resource for government and industry technology transfer. The laboratory is the Agency's focal point for NDE and combines basic research with technology development and transfer. Construction is presently under way to add 16,000 ft^2 of additional laboratory space. The activity concentrates on NDE materials measurement science for composites and metals with emphasis in materials characterization as well as impact damage, fatigue, applied and residual stress, and structural NDE with smart sensors/materials.

The facility is a state-of-the-science measurement laboratory linking 16 separate operations to a central computer consisting of a VAX-750 with 10 megabytes of internal memory and over 500 megabytes of fast storage tied to staff desktop microcomputers. The system interfaces with a real-time video input-output so that NDE images can be obtained, processed, and analyzed on-line. The major laboratory operations include a 55-kip and a 100-kip load system for stress/fatigue NDE research, a magnetics laboratory for residual stress, three computer-controlled ultrasonic scanners for imaging material properties, a technology transfer laboratory, an electromagnetic impedance characterization laboratory for composite fiber integrity, a composite cure monitoring laboratory for process control sensor development, a nonlinear acoustics laboratory for advanced NDE research, a laser modulation applications laboratory for remote sensing and smart materials, a pressure and temperature derivative laboratory for higher order elastic constant measurements, a thermal NDE laboratory, and a signal processing laboratory for improved image resolution and information transfer. An X-ray tomography system is under construction to provide the first view of material or structural failure under load and will be on-line in 1990.

Ultrasonic Characterization of Age-Hardening in 18Ni Maraging Steel

The 18Ni maraging steel (VascoMax) has found increasing applications in the aerospace industry primarily because of its unique property (an extraordinary combination of structural strength and fracture toughness) which can easily be achieved by a

simple maraging heat treatment. This maraging process typically consists of aging at 900°F for 3 hours followed by air cooling and results in a substantial increase (by 50 to 70 percent) in the hardness as measured by the conventional destructive method.

The feasibility of an ultrasonic technique as a nondestructive method of evaluating material hardness has been investigated. Specifically, the acoustic nonlinearity parameter was determined for 200- and 300-grade Vasco-Max samples from the measurements of absolute amplitudes of the fundamental and harmonic ultrasonic waves by the capacitive detector technique. Data were obtained prior to and after

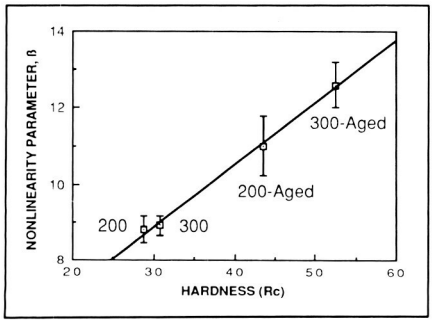

Linear correlation between ultrasonic, nonlinearity parameter and the Rockwell hardness for 18Ni maraging steel.

the maraging treatment for each sample. As shown in the figure, the measured nonlinearity parameter is found to increase almost linearly with increasing hardness values of the Rockwell C hardness.

This experimentally found, linear correlation between hardness and nonlinearity parameter is in qualitative agreement with the theoretical prediction based on interatomic interactions, and indicates that ultrasonic measurements show promise as a nondestructive method to evaluate material hardness. **(W. T. Yost and J. H. Cantrell, 3036)**

Ultrasonic NDE Effort for Solid Rocket Motor

In solid rocket motor (SRM) systems, the attachment of the internal insulation layer to both the case and the fuel is a critical region to be assessed for flight safety. An ultrasonic technique to test the integrity of the bond between the insulation and the case and the insulation and fuel is actively being developed. Analytical models predict that certain frequency resonances of the system are sensitive to the presence of disbonds. Based on this model, measurements have been made on samples from SRM casings with representative cross sections of the actual layers and regions of disbonds. Shown in the top part of the figure is a drawing of the SRM sample with the area of disbond shaded in. The bottom part of the figure shows an image derived from an experimental ultrasonic system that was developed to demonstrate the applicability of the model. Efforts are now

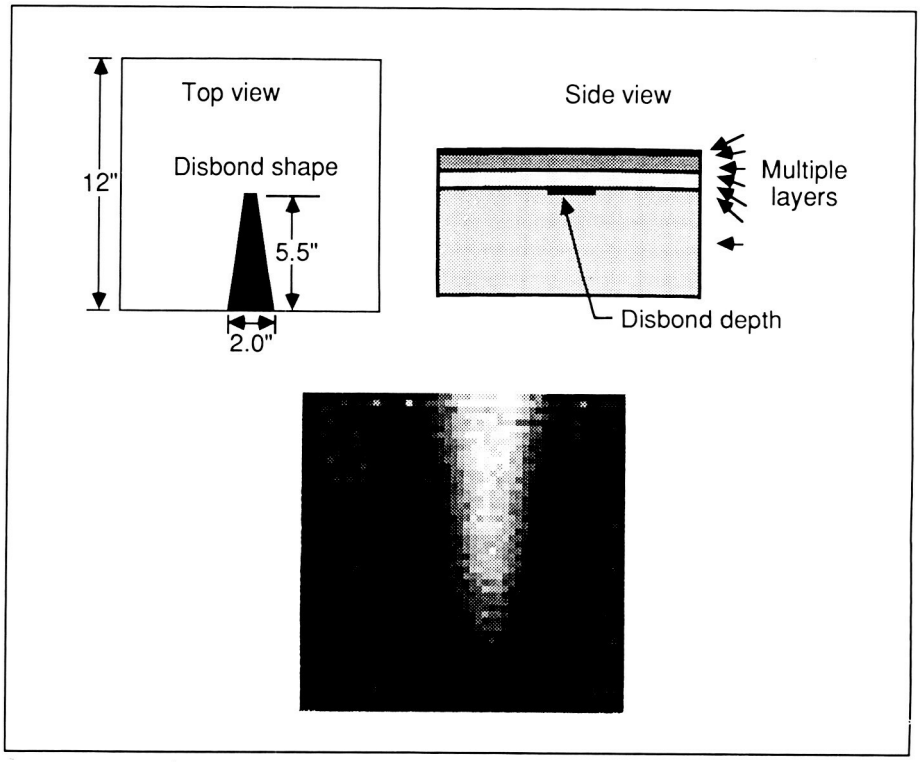

Disbond relative shape and location (top) and corresponding ultrasonic image that highlights disbond region (bottom).

under way to transfer this laboratory technique to a factory setting for verification on actual hardware.
(E. Madaras, 3249)

Ultrasonic Preload Determination of Space Shuttle Wheel Bolts

Application of correct preloads to critical fasteners during the tightening process is undoubtedly one of the key elements related to the safety of flight missions. Conventional torque wrenches used for this purpose often produce erroneous results by measuring the mechanical surface state-dependent frictional forces at the contact areas. Measurement of true tensile stress-induced elongation of fasteners is thus needed and is possible by using the acoustic interferometer developed previously at Langley Research Center. This instrument, called the pulsed-phase-locked loop, measures the stress-induced acoustic velocity changes that result in the frequency changes of the phase-locked waves. Both ultrasonic and torque measurements were performed while tightening the bolts in the rim of a Space Shuttle wheel using different types of lubricants.

As seen in the figure, the torque values show loads with errors in excess of a factor of 2. In contrast, the slope of acoustic frequency shift as a function of applied load is almost independent

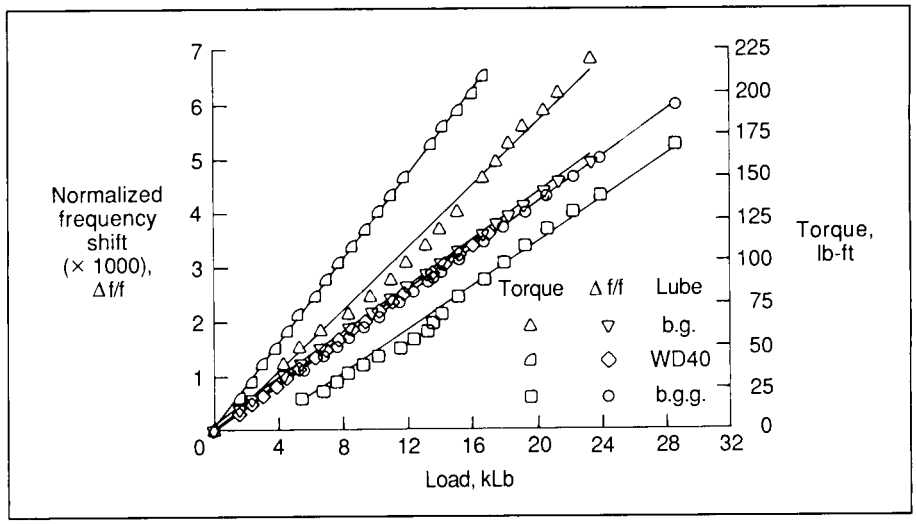

Results of ultrasonic and torque measurements against load applied to Space Shuttle wheel bolt in which three different types of lubricants were used; bearing grease (b.g.), WD 40, and bearing grease containing graphites (b.g.g.).

of lubricant. It has been confirmed that the slope of frequency shift is reproducible within the range shown in the figure for different individual bolts. Therefore, accurate preloading of critical fasteners is achieved with this Langley Research Center technology. Applications of this approach are already in practice and are having significant impact on the safety and reliability of critical structures in aerospace as well as industry.
(J. S. Heyman, 3036)

Smart Structures

The concept of "smart structures" involves a new class of materials containing internal sensors for monitoring structural integrity and actuators for structural control. Smart structures are possible because of a congruence of several diverse technologies, including advanced composite materials, fiber optics, acoustic waveguides, piezoelectrics, and diode lasers. Research is being conducted at the Langley Research Center NDE Research Laboratory to develop fiber optic sensors that can be embedded in composite materials to monitor strain, temperature, pressure, and other parameters affecting structural integrity. This new technology provides a means for assessing impact damage, fatigue, chemical degradation, and feedback information important in the control and guidance of aerospace structures.

A fiber optic sensor has been developed which measures phase modulation in an optical fiber. The device, an optical phase-locked loop, measures the phase of an amplitude-modulated laser signal propagating in the fiber. The figure indicates the major

components of the system. A diode laser is amplitude modulated by a voltage-controlled oscillator, which also serves as a reference oscillator for a mixer. The laser signal passes through the optical fiber, which is exposed to the environment that is to be monitored, and is detected, amplified, and compared to the reference at the mixer. Any modulation of the phase by the environment causes an error voltage at the mixer which drives the voltage-controlled oscillator to a new frequency corresponding to a measure of the phase change.

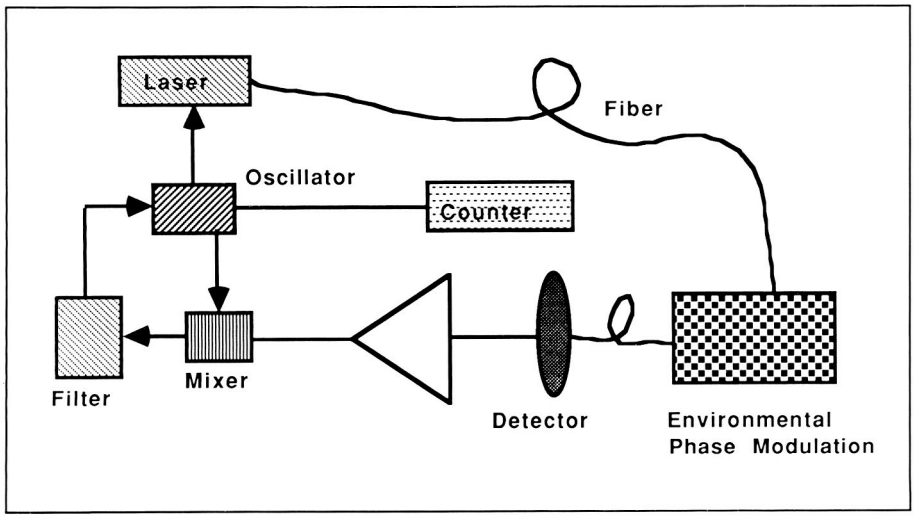

Optical phase-locked loop fiber optic sensor.

Phase changes can be induced in the fiber in many ways. One example is simple elongation, which changes the optical path length. This effect is used to measure strain with an optical fiber attached or embedded in a structure. Dynamic strain measurements have been made with an optical fiber attached to a graphite/epoxy panel arranged as a cantilever beam. If the panel is set into motion, the phase of the modulation oscillates in conformity with the vibration of the structure. Thus, the device can be used to measure the modes of vibration in a structure and could be useful for modal analysis of large flexible structures, such as the Space Station.
(R. S. Rogowski, 3036)

Vehicle Antenna Test Facility

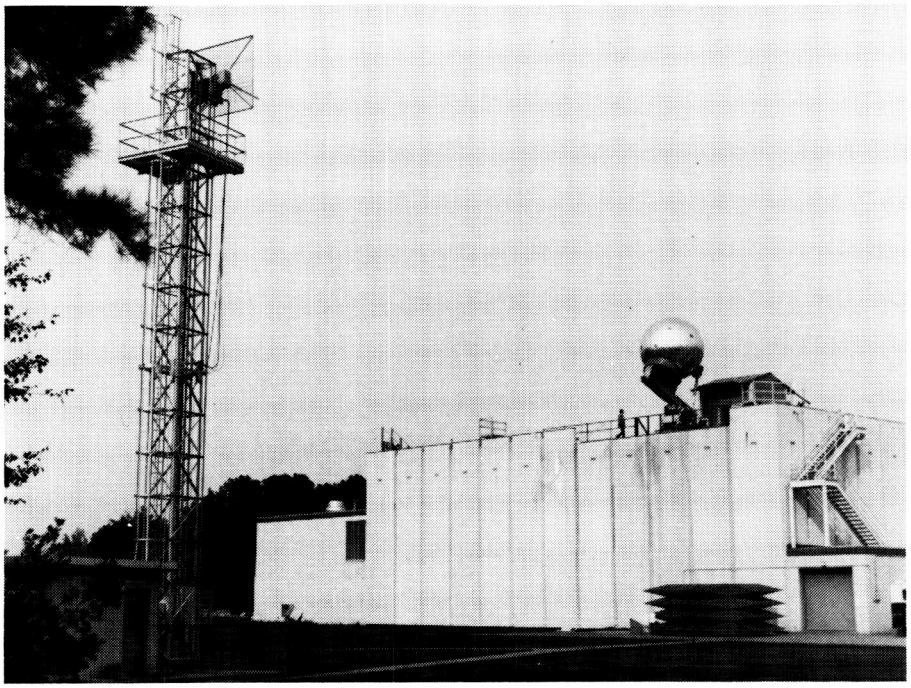

The Vehicle Antenna Test Facility (VATF) is a research facility used to obtain data for new antenna performance and electromagnetic scattering data in support of various research programs. The VATF consists of two indoor radio frequency anechoic test chambers and an outdoor antenna range system. The anechoic chambers provide simulated free-space conditions for measurements from 100 MHz to greater than 40 GHz. The anechoic chambers, which are shaped like pyramidal horns to reduce specular reflections of the walls, are over 100 ft long and have test area cross sections approximately 30 ft by 30 ft.

A spherical near-field (SNF) measurement capability was added to the low-frequency anechoic chamber. A precision antenna positioning system, antenna source tower, and optical alignment system designed for SNF measurements were installed in the low-frequency chamber, and the capability now exists for automatic performance of precision SNF measurements up to at least 18 GHz. Antennas with diameters up to 12 ft can be measured if their electrical size is no greater than 100 wavelengths (i.e., diameter/wavelength ≤100). This limitation is imposed by the SNF system software, which transforms the near-field data to obtain the desired far-field data. Measured data stored on disc can be processed to provide antenna directivity, polar or rectangular plots of the radiation patterns, and three-dimensional contour plots of the antenna radiation characteristics.

The high-frequency anechoic chamber was used to establish a Compact Range Facility. The compact range is an electromagnetic measurement system used to simulate a plane wave illuminating an antenna or scattering body. The plane wave is necessary to represent the actual use of the antenna or scattering from a target in a real-world situation. The compact range utilizes an offset-fed parabolic reflector to create the simulated plane wave test conditions. The standard commercially available compact range is limited to the measurement of antennas or models with maximum dimensions of 4 ft over the frequency range of 4 GHz to 100 GHz.

The outdoor antenna range system is available for use when the antenna or test model size or frequency precludes the use of the anechoic chambers. The outdoor range consists of two remote transmitting towers that are spaced 150 ft and 350 ft from the test positioner mounted on the VATF roof. The VATF has several electronic laboratories with the extensive measurement capability needed to support the design of unique antennas prior to their evaluation in the antenna chambers or on the outdoor antenna range system.

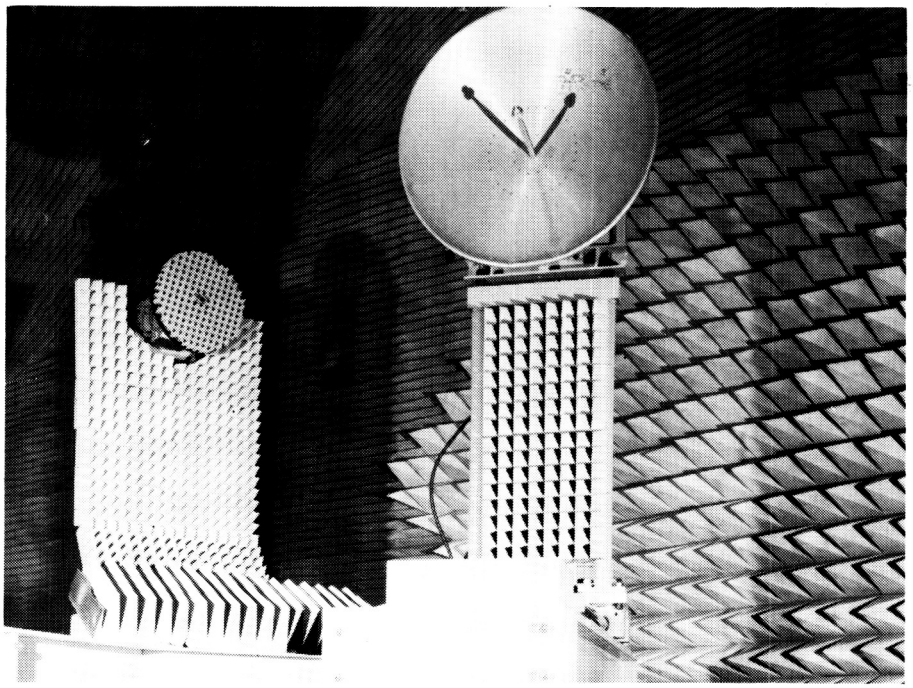

Spherical near-field equipment. L-85-2143

United States Army Doppler Navigation System Antenna Measurements

The United States Army Avionics Research and Development Activity (AVRADA) at Ft. Monmouth, New Jersey, recently solicited for contractor development of a new Lightweight Doppler Navigation System (LDNS) for Army aircraft under the Form, Fit, and Function (F^3) avionics upgrade program. Under this program, two qualified contractors submitted prototype systems for evaluation leading to a competitive award of production contracts. A cooperative agreement was reached with the Joint Research Programs Office (JRPO) to conduct volumetric antenna measurements for subsequent evaluation of the navigation systems.

Test objectives were to determine the radio-frequency (rf) radiation characteristics of the LDNS antenna during normal system operation for performance verification and to provide data for assessment of the detection probability. To accomplish this objective, a series of far-field rf measurements were made at 13.325 GHz in the low-frequency anechoic chamber (as shown in the first figure) for each prototype system and for the existing AN/ASN-128 LDNS currently in use on Army aircraft (as shown in the second figure). Antenna pattern measurements were made over the entire radiating hemisphere to fully characterize the radiating volume of each system.

Radar antenna performance is measured, in part,

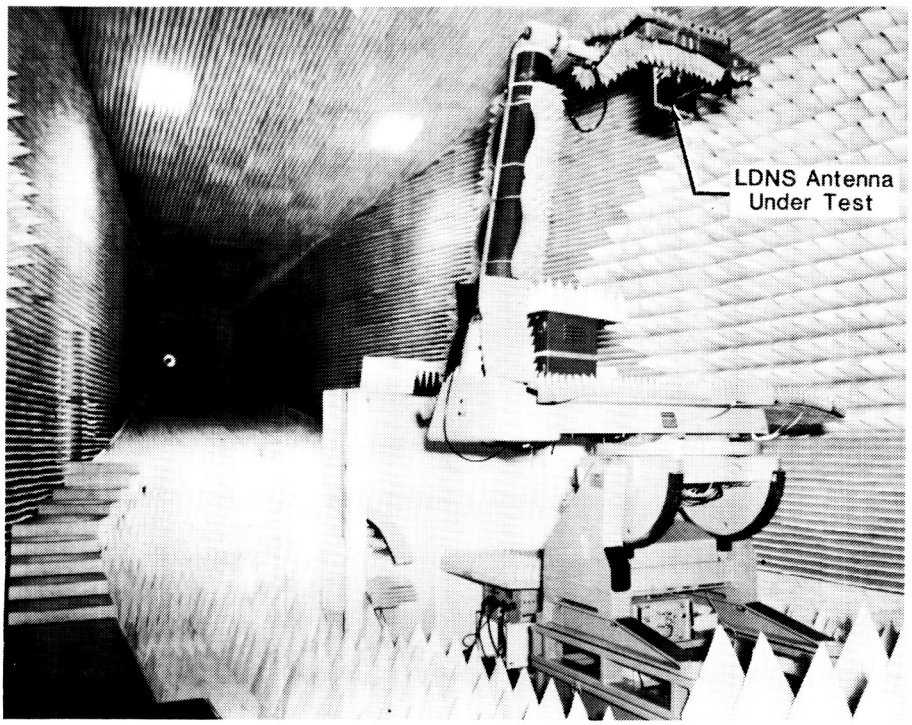

LDNS test configuration in low-frequency anechoic chamber. L-87-11,331

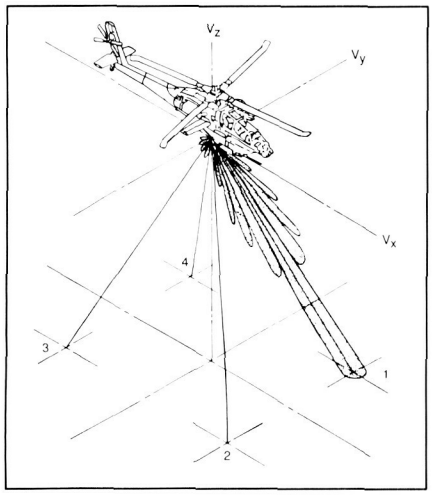

Typical LDNS antenna beam arrangement.

by how the volumetric radiation pattern is distributed. Any radiation not in the main beam structure results in lower antenna efficiency, reduced system performance, and generation of stray signals in undesired directions. By obtaining detailed quantitative measurement information on the relative power levels of the radiating systems, several significant off-main beam levels of radiation, or side lobes, were identified. The third figure shows the relative volumetric radiation levels for a typical LDNS antenna system with identification of a significant side lobe.

With the spatial orientation and magnitude of the side lobes accurately known, design improvements can be implemented and new antenna radiation pattern specifications developed to enhance antenna performance and to lower the probability of detection for all Army aircraft.

(G. C. Barber, 3631)

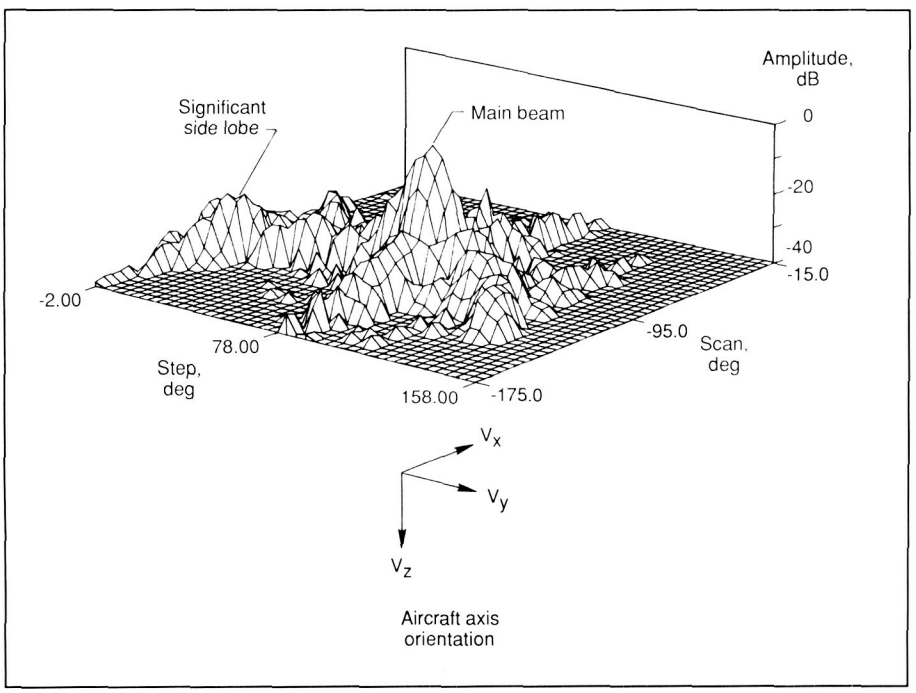

LDNS volumetric antenna pattern.

Impact Dynamics Research Facility

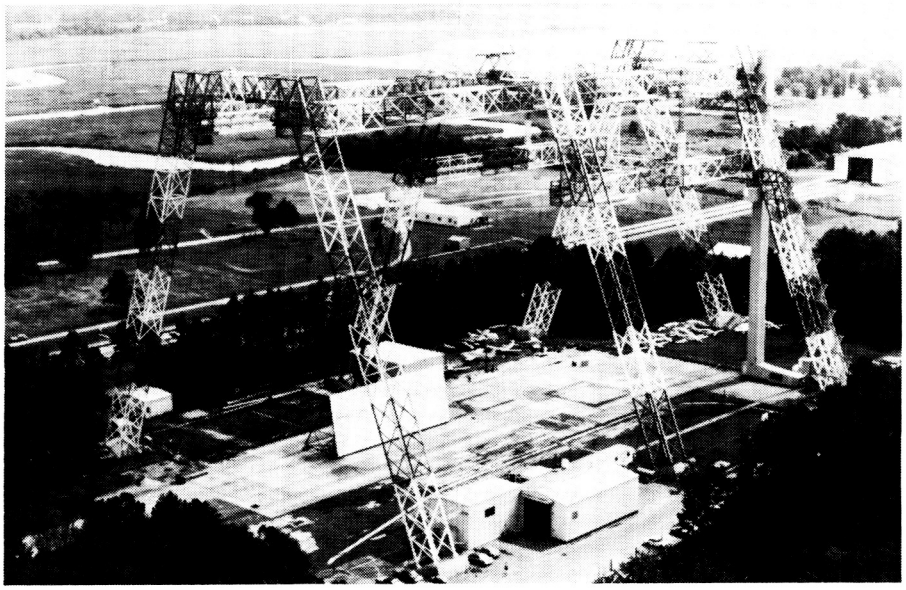

This facility, which was originally used by the astronauts during the Apollo Program for simulation of lunar landings, has been modified to simulate crashes of full-scale aircraft under controlled conditions. The aircraft are swung by cables, pendulum-style, into the concrete impact runway from an A-frame structure approximately 400 ft long and 230 ft high. The impact runway can be modified to simulate other ground crash environments, such as packed dirt with trees. In the past the impact runway has been modified with soil to meet a specific test requirement.

The aircraft is suspended by swing cables from two pivot points 217 ft off the ground. It is then pulled back along an arc to a predetermined height by a pullback cable from a movable bridge on top of the A-frame, released from the pullback cable, and allowed to swing, pendulum-style, into the ground. An instant before impact, the swing cables are separated from the aircraft by pyrotechnics. The length of the swing cables regulates the aircraft impact angle from 0° (level) to approximately 60°. Impact velocity can be varied up to approximately 65 mph (governed by the pullback height) and to 90 mph with rocket assist. Variations of aircraft pitch, roll, and yaw can be obtained by changes in the aircraft suspension harness attached to the swing cables. Onboard instrumentation data are obtained through an umbilical cable attached to the top of the A-frame. Data are transmitted by hard wire to the control room at the base of the A-frame. Photographic data are obtained by ground cameras and cameras mounted on top of the A-frame. Maximum allowable weight of the aircraft is 30,000 lb.

F-111 Crew Module Drop Test

A total of nine impact tests were successfully conducted on an F-111 crew module during a sequence of three separate test series. The impact tests were conducted at the Impact Dynamics Research Facility in support of a United States Air Force program to upgrade the air bag impact attenuation system to correspond to a new parachute system. Impact attitude parameters varied for the different sequences to evaluate the new air bag cushioning attached to the bottom of the crew module. Typically, the impact attitude involved pitch, roll, and yaw of the module under a targeted vertical impact velocity of 25 ft/s with either a 42 ft/s or 32 ft/s horizontal velocity component. Onboard instrumentation and high-speed cameras along with ground-based motion picture cameras recorded the loads and response of the structure, dummy crew, and air bag performance during the impact sequence. The photograph shows a typical F-111 crew module just prior to ground contact on the dirt impact surface.

F-111 crew module prior to impact. L-87-6865

Analysis of the impact data for the test sequences was evaluated to determine whether the loads on the crew members were acceptably low enough based on the Dynamics Response Indices criteria established by the Air Force for the three mutually perpendicular load axes on the spinal column. The responses of the crew under the various attitude situations of the test series resulted in only two occasions wherein the Dynamic Response Index was above the criteria level. **(H. D. Carden, 3795)**

Full-Scale Crash Tests of Two All-Composite Helicopter Structures

Two fully instrumented, all-composite, full-scale helicopter drop tests were conducted to evaluate the composite structural crash behavior in support of the United States Army's Advanced Composite Airframe Program (ACAP). A Bell Helicopter Textron version and a Sikorsky Aircraft helicopter version shown in the photograph were used in the crash tests conducted at the Impact Dynamics Research Facility. These vehicles are experimental utility helicopters designed to demonstrate the technology advancement achievable with advanced composite materials when used in both primary and secondary airframe structure. The ACAP vehicles are configured to meet or exceed military requirements of the United States Army and include in their design crashworthiness, ballistic tolerance, radar signature reduction, enhanced reliability and maintainability, and militarized crew and troop accommodations. Test parameters are shown in the table.

Initial evaluation of recorded data and motion picture coverage of the response of the structure and dummy occupants' behavior indicates that survivable loads and critical structural integrity of the all-composite aircraft structures were achieved in the crash event. Additional evaluation and analytical studies of structural response and load-limiting crew and troop seating behavior are under way. **(H. D. Carden, 3795)**

L-87-08053

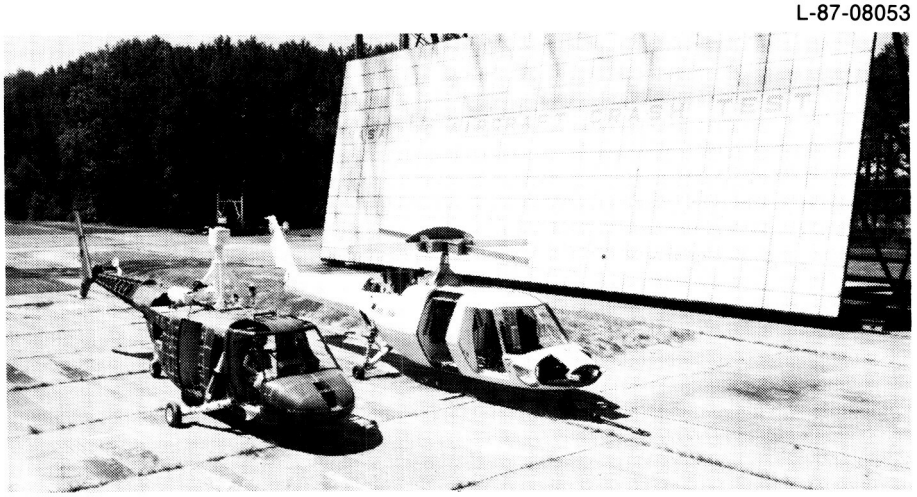

Bell Helicopter Textron ACAP (left) and Sikorsky Aircraft A helicopter (right) used in crash tests.

Bell Helicopter ACAP		Sikorsky Aircraft ACAP	
Flight path angle	= -57.0°	Flight path angle	= -90°
Flight path velocity	= 48.1 ft/s	Flight path velocity	= 38 ft/s
Roll angle (right)	= 10°	Roll angle (right)	= 10°
Pitch angle (up)	= 10°	Pitch angle (up)	= 10°

Test parameters.

Aircraft Landing Dynamics Facility

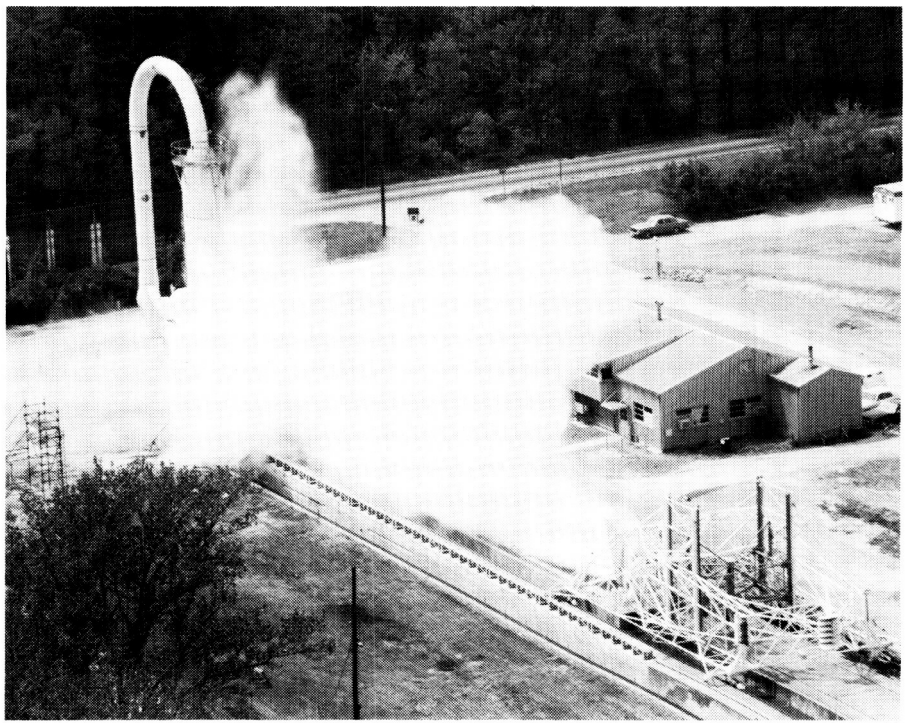

Langley Research Center has recently updated the landing loads track to the Aircraft Landing Dynamics Facility (ALDF) to improve the capability of low-cost testing of wheels, tires, and advanced landing systems. The main features of the updated facility are the propulsion system, the arresting gear system, the high-speed carriage, and the track extension.

The ALDF uses a high-pressure water jet system to propel the test carriage along the 2800-ft track. The propulsion system consists of an L-shaped vessel that holds 28,000 gallons of water pressurized to 3150 lb/in^2 by an air supply system. A timed, quick-opening shutter valve is mounted on the end of the "L" vessel and releases a high-energy water jet, which catapults the carriage to the desired speed. The propulsion system produces a thrust of 2×10^6 lb maximum pressure, which is capable of accelerating the 108,550-lb test carriage to 220 knots within 400 ft. This thrust creates a peak acceleration of approximately 20 g. The carriage coasts through an 1800-ft test section and decelerates to a velocity of 175 knots or less when it intercepts the five arresting cables that stretch across the track. The arresting system brings the test carriage to a stop in 600 ft or less. Essentially any landing gear can be mounted on the test carriage, including those exhibiting new concepts, and any runway surface and weather condition can be duplicated on the track. Research on slush drag, hydroplaning, tire braking, steering performance, and runway grooving has been conducted in the past.

Future research programs include the Space Shuttle orbiter main and nose gear tire spin-up wear characteristics and cornering force measurements at high speeds as well as frictional properties of radial and H-type aircraft tires for comparison with conventional bias ply tires. A surface traction program to study the effect of different runway surface textures and various runway grooving patterns on the stopping and steering characteristics of aircraft tires will be conducted. Finally, tests associated with the National Tire Modeling Program will also be conducted.

Corduroy Solution to Spin-Up Wear Damage Problem at Space Shuttle Landing Facility

The test objective of this research was to define a texture modification for the touchdown zones of the Kennedy Space Center (KSC) Shuttle Landing Facility which reduces spin-up damage to an acceptable level while still maintaining adequate cornering friction when wet. Tests were conducted

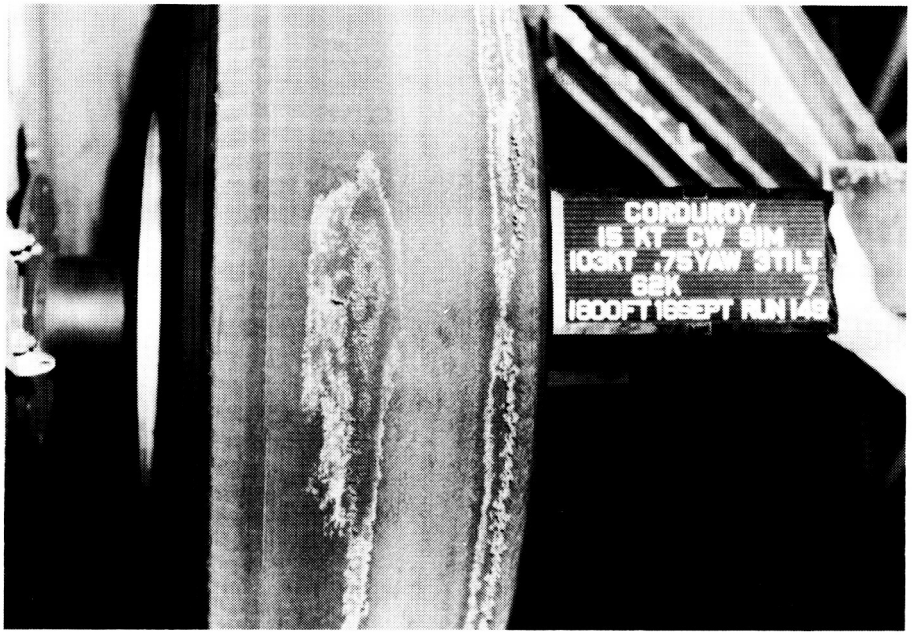

Space Shuttle tire wear for 15-kn crosswind landing with spin-up on corduroy-smoothed touchdown zone and rollout on high-friction KSC surface.

at the Aircraft Landing Dynamics Facility (ALDF) to investigate the spin-up wear and cornering behavior for touchdowns on smooth concrete, smooth-grooved concrete, and grooved and ungrooved corduroy surfaces. The corduroy surface tested was produced by smoothing the existing KSC runway with a cutter utilizing a blade spacing of 4.5 blades per inch, a similar technique to that used for smoothing highways. In addition to the spin-up tests, a simulated landing rollout was performed at the ALDF to predict tire wear for spin-up on the 4.5 blades per inch ungrooved corduroy surface and subsequent rollout on the existing KSC surface texture.

Test results showed that spin-up damage caused by the 4.5 blades per inch ungrooved corduroy surface is no worse than that caused by a smooth ungrooved surface, and friction on the corduroy surface is acceptable. The figure shows the tire wear that can be expected from a spin-up on a corduroy touchdown zone and a simulated 15-kn crosswind rollout on the existing KSC runway. The corduroy spun-up tire shown had two cords worn through at the end of the rollout as opposed to four cords worn through on the KSC spun-up tire (not shown). This benefit translates into an improved safety margin at the present crosswind limits, or a crosswind capability increase of 3 kn to 5 kn at present safety margins.

(R. H. Daugherty and S. M. Stubbs, 2796)

Basic Aerodynamics Research Tunnel

Computational methods are progressing rapidly toward the prediction of the three-dimensional flow field about complex geometries at high angles of attack. These computational methods require a large number of grid points to adequately model the flow field, and they produce large amounts of information. To validate these methods, detailed experimental flow field measurements are required. The Basic Aerodynamics Research Tunnel (BART) is a flow diagnostic facility dedicated to the task of acquiring the detailed data required for code validation and investigating the fundamental character of complex flow fields.

BART is an open-return wind tunnel with a closed test section 28 in. high, 40 in. wide, and 10 ft long. The maximum test section velocity is 220 ft/s, which yields a Reynolds number per ft of 1.4×10^6. The airflow entering the test section is conditioned by a honeycomb, four antiturbulence screens, and an 11 to 1 contraction ratio. These flow manipulators, coupled with an excellent speed controller, provide a low-turbulence, uniform flow in the test section. The level of the longitudinal component of turbulence intensity ranges from 0.05 percent at low speeds to 0.08 percent at a test section dynamic pressure of 45 lb/ft^2.

The timely acquisition of the detailed data required for code validation dictates the use of a highly integrated and fully automated Data Acquisition and Control System (DACS). BART DACS consists of a computer system that monitors and controls all test instrumentation. BART instrumentation includes a three-dimensional probe traverse system, an electronic scanning pressure system, a three-component hot wire, and a three-component laser Doppler velocimeter.

Forward view of BART. L-85-3069

BART three-component laser velocimeter.

A dedicated orthogonal three-component, fringe-type laser velocimeter was designed and installed in the BART. The system had a nominal focal length of 1.2 m with the receivers located orthogonal to the transmitted laser beams. This configuration resulted in a spherical sample volume, 150 μm in diameter, which could be placed to within 200 μm of the unprepared model surface. Color separation was used to distinguish the scattered light from each of the three components. Bragg cells were placed in all three components to provide full directionality measurement capability. The optical system was placed on a three-component mechanical traversing system that provided computer-controlled positioning within a 1-m cube with a resolution of 10 μm.

The seed particles were 0.8-μm-diameter polystyrene spheres. These particles were suspended in ethanol, which served as a carrier for dispersal from an atomizer spray nozzle located at the tunnel inlet. As the spray traveled down the tunnel, the ethanol evaporated, leaving the polystyrene spheres to pass through the sample volume. No evidence of particle agglomeration was found based on oscilloscope observations.

The signals from the laser velocimeter were processed using high-speed burst counters with their output acquired with a laser velocimeter autocovariance buffer interface (LVABI). The LVABI was set up and controlled by a minicomputer that then accepted the data and performed on-line data processing and storage of the raw and converted data on magnetic tape. An on-line display was performed by a graphics workstation attached to the computer. The minicomputer also controlled the traversing mechanism to complete the automated data acquisition and control of the test.

(J. F. Meyers, 2791)

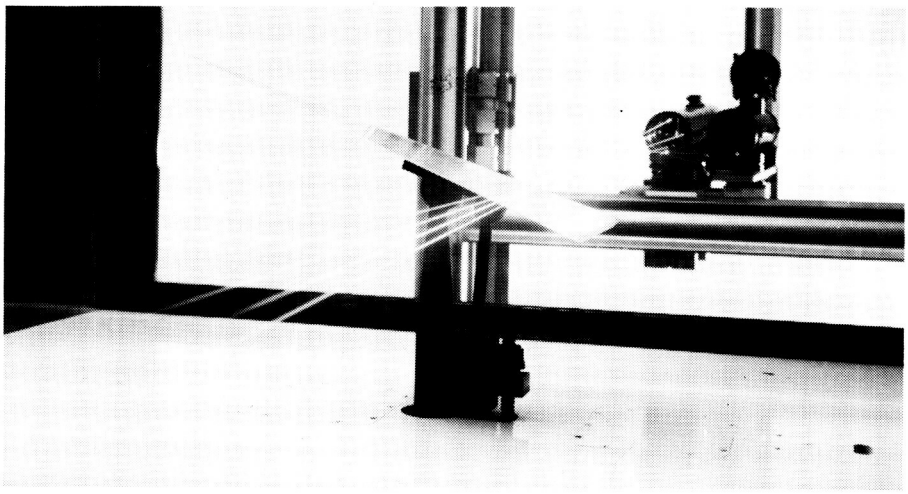

Laser Doppler velocimeter system in operation during delta wing flow field testing in BART. L-87-05035

Flow Field Measurement of Vortex Phenomena on YF-17 Model

There is an increasing interest in providing modern fighter aircraft with the capability of operating at high angles of attack. The flow fields generated by these aircraft are complex and typically consist of multiple interacting vortex flows. The vortices are shed by the sharp wing leading edges, slender fuselage forebodies, or by the wing leading-edge extensions (LEX's). These vortex systems provide a substantial increase in lift and can improve the yaw control of the aircraft if they are properly integrated into the design. The vortices are also subject to a phenomenon called vortex bursting, or breakdown, in which the flow at the core of the vortex abruptly stagnates, then rapidly expands into a highly turbulent state. When breakdown occurs ahead of the empennage, the vertical tails of the aircraft may be subject to increased wear from structural fatigue due to the buffeting from the turbulent flow.

A NASA Langley Research Center/Northrop Corporation cooperative research program to measure the flow field over a twin-tailed fighter configuration at high angles of

attack was conducted in the BART facility. All three components of the velocity field were measured with a laser Doppler velocimeter (LDV) at two angles of attack. The lower angle ($\alpha = 15°$) represented the case where the vortices over the body are unburst. The higher angle ($\alpha = 25°$) represented the burst case and a condition where the buffet loads on the tail increase dramatically. Two longitudinal stations were surveyed at two different Reynolds numbers. A typical survey plane consisted of approximately 230 measurement locations and required 6 hours to complete. Laser light sheet flow visualization, as shown in the figure, was used to obtain a global view of the flow field. At $\alpha = 25°$, the burst point was moving back and forth through the forward station, and the vortices were completely burst at the station just ahead of the twin tails. Reverse velocities up to 20 percent of the free-stream flow were measured in the core of the vortex ahead of the twin tails. The root mean square (RMS) of the velocity fluctuations reaches values of approximately 30 percent of free-stream flow in the burst vortex.

(W. L. Sellers, 2543)

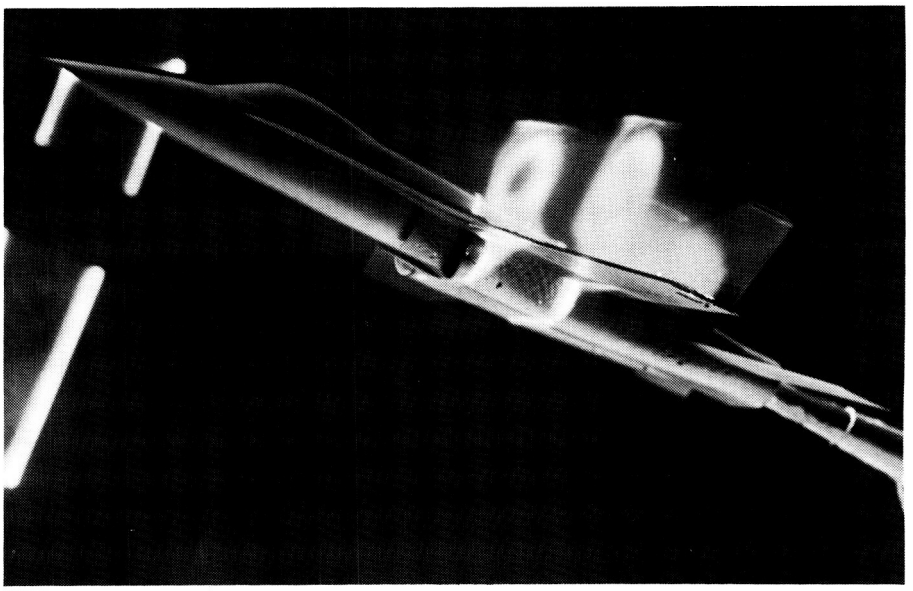

F-17 model at angle of attack of 25°. L-87-7877

Image Processing Laboratory

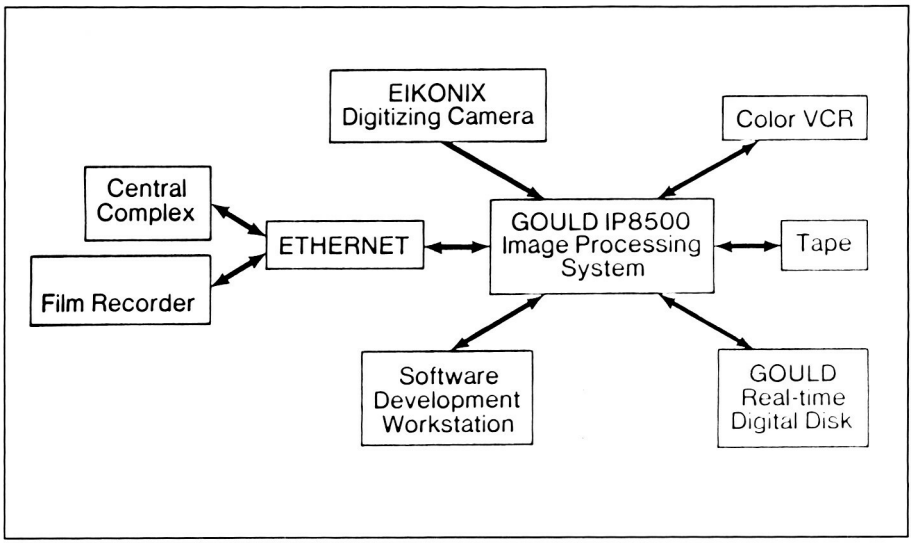

The Image Processing Laboratory (IPL) is a versatile, stand-alone image processing system that allows researchers to enhance and analyze digital images. These images arise from a wide range of applications including wind tunnel flow field experiments, computational fluid dynamics solutions obtained on the VPS-32 supercomputer, nonintrusive aerodynamic heat-transfer measurements, and modeling of satellite imaging systems. Because such images often have very low contrast or spatial resolution, the usual manual methods of analysis and publication of results are time consuming and inaccurate, if not impossible. The IPL provides researchers new analysis tools that allow enhanced images and accurate results to be generated in minutes rather than days.

The IPL is based on a Gould IP8500 image processing system, featuring a digital video processor that is specifically designed to process large arrays of image data fast enough to support interactive work. The system is supported by a number of input/output peripherals in the laboratory. For instance, images on photographic media are input to the IP8500 using the Eikonix digitizing camera, which converts visual information into a digital array of numbers (digital image) that can be quantitatively processed by the system. Also, digital images generated on any computer in Langley Research Center's local area network can be transferred to the system via an Ethernet connection, and a nine-track magnetic tape unit can read digital images created at remote locations. The digital images are then analyzed and interactively enhanced on the IP8500 and subsequently transmitted over the Ethernet connection to either a Dicomed or CELCO film recorder. Both of these devices convert the enhanced digital images into photographic media for a hard copy of results. A sequence of images and individual frames on videotape can be input to the system using the color

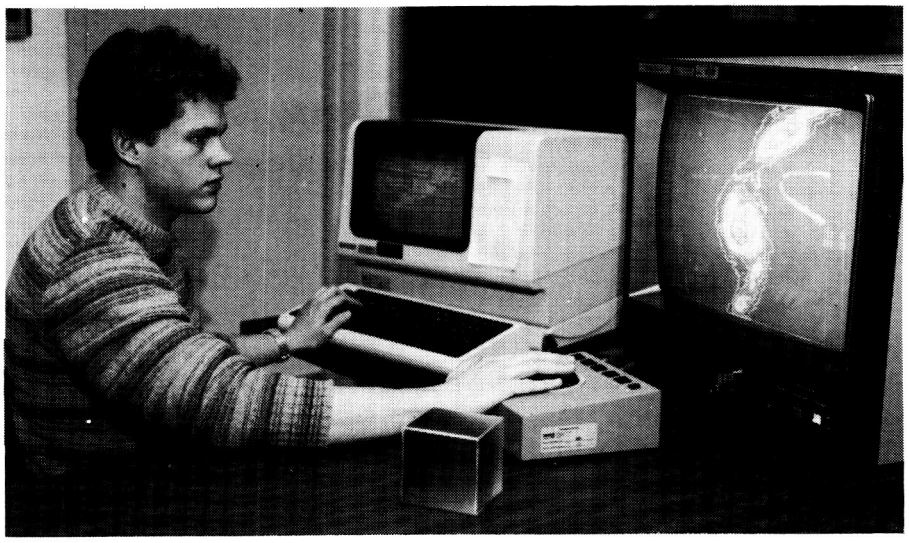

Track ball used for interactive enhancement of flow field images. L-86-2268

videotape recorder. Images can be placed on the real-time disk, which is capable of reading and writing a sequence of digital images at video rates, thus allowing dynamic enhancement of a sequence of images (i.e., wind tunnel tests) recorded on videotape and previewing of computer-generated movies. Enhanced sequences of images can then be recorded back onto videotape or used to produce a sequence of photographic images.

The IPL provides researchers with enhanced images that increase their ability to accurately interpret image data in a wide variety of applications. The interactive nature of the system allows researchers to use their experience and judgment to quickly analyze and process their image data. The enhanced images provide an effective means of presenting research results for analysis, publication, and presentation. IPL provides a practical and interactive environment for users to process image data quickly and to obtain a variety of outputs to meet their needs.

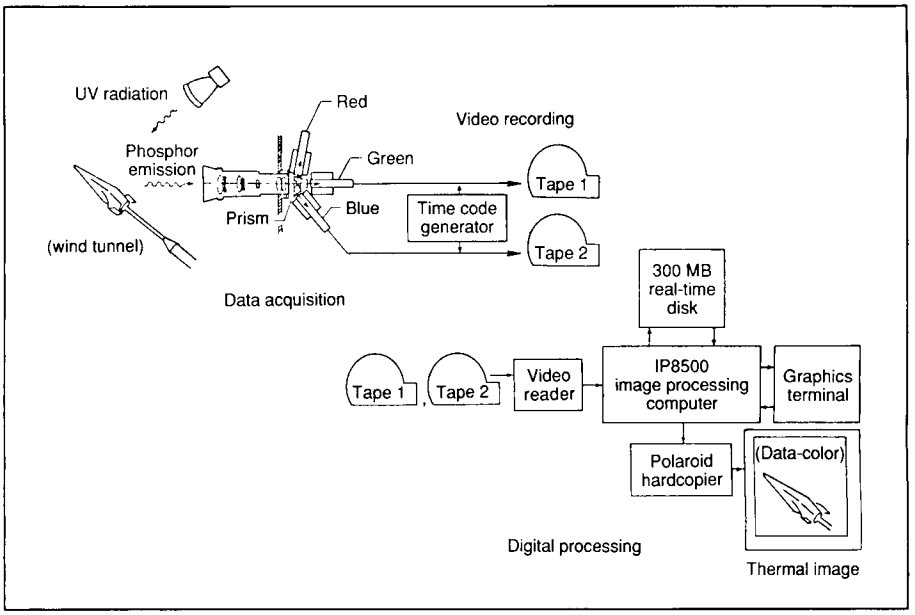

Thermal imaging system using two-color thermographic phosphors.

Development of Thermal Imaging System

A thermal imaging system for wind tunnel surface heating experiments was recently developed at Langley Research Center by the application of digital image processing techniques to spectral image data. Quantitative surface temperature mappings are generated from dual optically filtered video images using the Gould IP8500 image processor.

The thermal imaging technique (shown in the above figure) is based on the ratio of measured blue to green (450, 520 nm) emission from a phosphor coating excited by an ultraviolet (365 nm) source. Separately filtered images are recorded from a three-tube color camera, utilizing off-the-shelf front-end video optics to discriminate wavelengths. As opposed to the variety of image enhancement techniques already employed at the Image Processing Laboratory (IPL), the system is used as a quantitative data-array processor to calculate surface temperature from video data. The technique provides ideal surface temperature-time data necessary in calculating heat-transfer coefficients.

A simple method was developed to calibrate system components used in digitizing data. Data are originally recorded on 3/4-in. analog videotape and then digitized into a 512 by 512 pixel image, which has an 8-bit gray-level resolution per pixel. A 24-bit image calculation plane is used to avoid round-off errors. Using the real-time digital disk, up to 6 seconds of thermal data or 360 image frames are fed into the system at one time and processed. In this mode it takes approximately 1 hour to feed data from videotape and to set up the program and 15 minutes to process the data. Existing contrast and enhancement software are used to display data in a single frame or movie format with color-temperature lookup tables for quantitative reference. After processing,

arbitrary line profiles can be defined and plotted.

The study was initiated to develop a method for obtaining simultaneous heat-transfer measurements and aerodynamic force and moment measurements on hypersonic wind tunnel models. The study approach was to develop a thermal imaging system using an appropriate optical measurement technique providing quantitative surface temperature data. Using the hardware and programming capabilities of the staff at IPL, a quantitative thermal imaging system was developed. This work enables future development of a dedicated digital acquisition/image processing system. Tests demonstrating the thermal imaging system (also discussed on page 32 describing the Hypersonic Facilities Complex) were performed in the 31-Inch Mach 10 Tunnel using phosphor-coated cast ceramic models (as shown in the figure below).
(G. M. Buck, 3984)

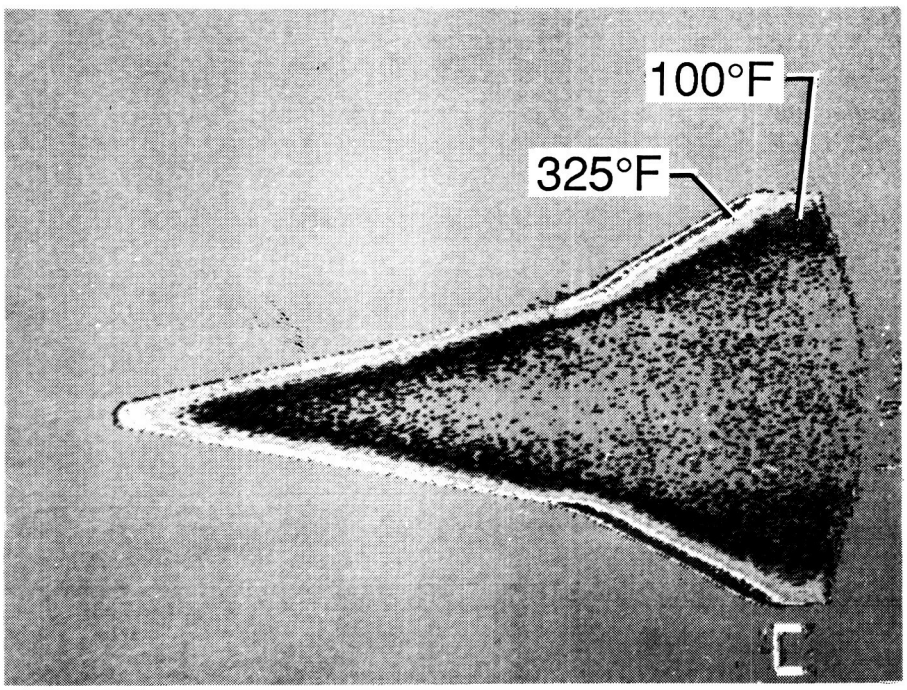

Windward surface temperature mapping on a transatmospheric model in 31-Inch Mach 10 Tunnel.

Flight Research Facility

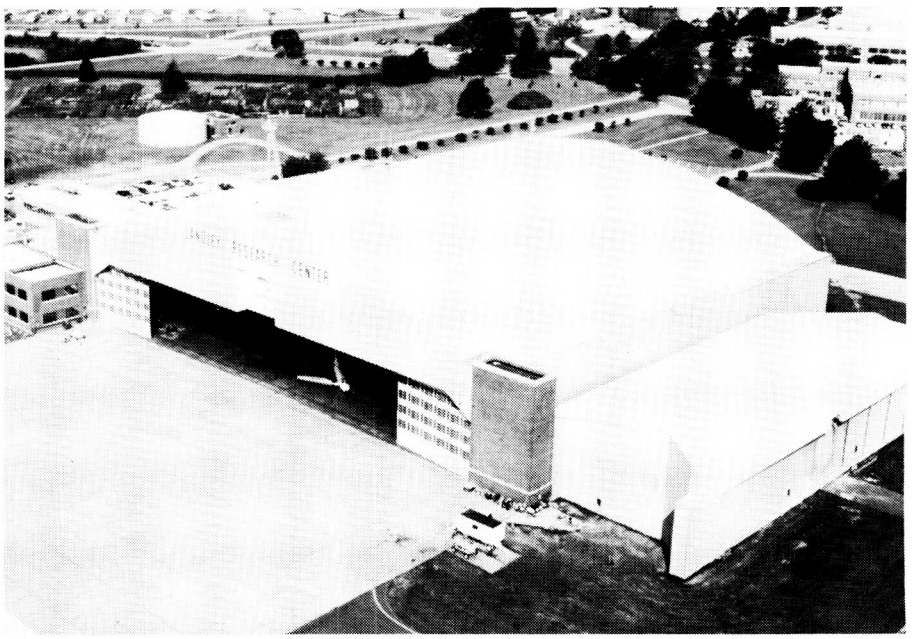

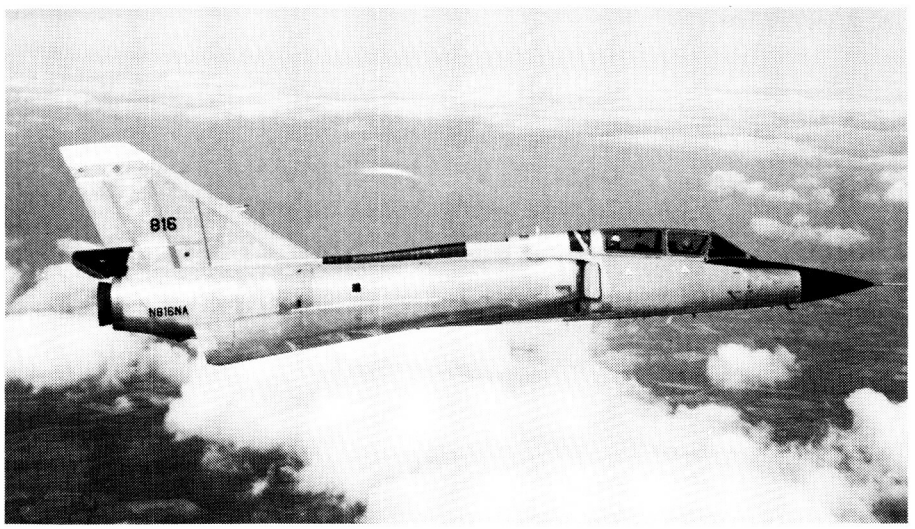

Convair F-106B configured for Storm Hazards Program. L-83-2747

The truss-supported roof of the huge hangar of the Flight Research Facility provides a clear floor space with nearly 300 ft in each direction (over 87,000 ft^2).

Door dimensions will allow entry of a Boeing 747. Features such as floor air and electrical power services, radiant floor heating to eliminate corrosion-causing moisture, a modern deluge fire suppression system, energy-saving lighting, modern maintenance spaces, and entry doors and taxiways on either side of the building make this structure equal or superior to any hangar in the country. Extensive and modern maintenance equipment makes it possible to maintain, repair, and modify aircraft ranging in sophistication from modern metal and composite airliners, fighters, and helicopters to fabric-covered light airplanes. Surrounding the hangar are ramp areas with load-bearing capacity sufficient to handle the largest current wide-body jet. The high-power turnup area can also handle a wide variety of aircraft.

The present array of research and research support aircraft includes an airliner, military fighters, trainers, experimental one-of-a-kind designs, helicopters, and single- and multi-engine light airplanes. This variety enables research to be carried out over a wide range of flight conditions, from hover to Mach 2 and from the surface to 60,000 ft. Research pilot currency in this wide spectrum of aircraft is important in conducting credible in-flight experiments as well as in-flight simulator assessments. A variety of research can be conducted in such areas as terminal traffic flow, Microwave Landing System (MLS) approach optimization, airfoil properties, single-pilot instrument flight rules (IFR), engine noise, turbulence research, natural laminar flow, winglet studies, stall/spin, and severe storm hazards.

One of the support helicopters is used to drop unpowered remotely controlled models of high-performance airplanes to study high-angle-of-attack control characteristics. The Radio-Controlled Drop Model Facility is used to study the low-speed flight dynamic behavior of aerospace vehicles with particular emphasis on high-angle-of-attack characteristics of combat aircraft. The technique consists of launching an unpowered, dynamically scaled, radio-controlled model into gliding flight from the support helicopter, controlling the flight of the model from the ground, and recovering the model with a parachute. The models are constructed primarily of molded fiberglass and are typically about 10-ft long with weights in the range of 200 lb to 300 lb. A comprehensive onboard instrumentation system provides measurements of key flight dynamics parameters that are transmitted to the ground via telemetry and recorded for analysis. The model control loop involves a combination of ground-based and onboard equipment and the required communication links. The heart of the system is a ground-based digital computer into which the control laws are programmed. The processor accepts downlinked feedback signals from the model and commands from the pilot and computes the control surface commands that are then transmitted to the model. Very-high bandwidth electromechanical servoactuators are used to drive the model control surfaces. The

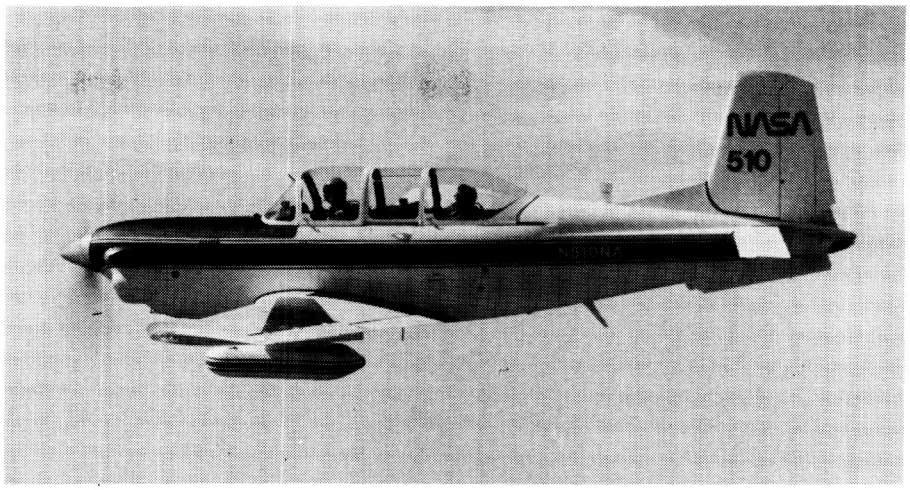

Beech T34C used for flight support. L-80-3923

Bell 204B configured for model drop mission. L-76-6425

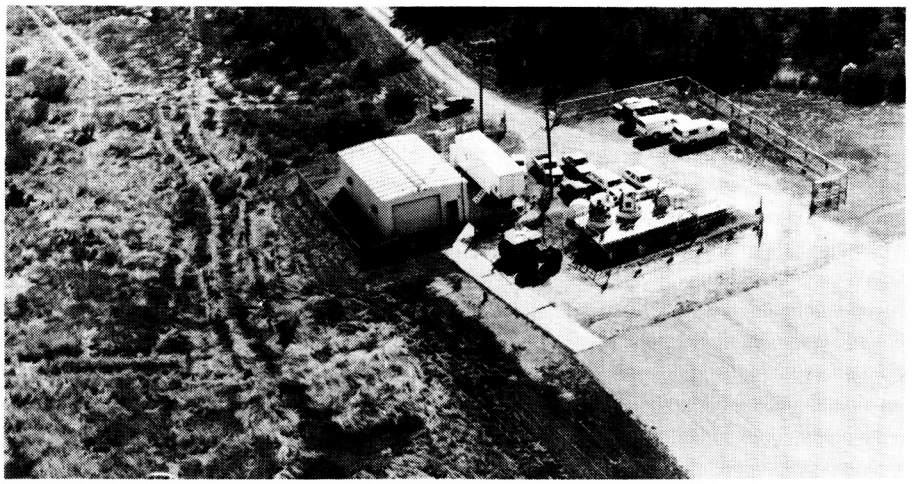

Radio-Controlled Drop Model Facility. L-83-11,167

pilot flies the model from a ground station that provides the required information on a number of displays. These displays include a high- resolution video image of the model, a map display showing model ground track, and conventional analog instruments presenting key parameters such as angle of attack and airspeed.

The tests are conducted at the Plum Tree Test Site located approximately 5 miles from Langley Research Center. The test site is a marsh approximately 2 miles long and 1 mile wide.

Natural Laminar-Flow Engine Nacelle Flight Experiments

Flight experiments have been conducted on a natural laminar-flow (NLF) engine nacelle to determine the locations and causes of laminar boundary-layer transition within an acoustic environment simulating engine and operational noise. The aircraft used for the tests was a NASA-operated Grumman OV-1B Mohawk fitted with a full-scale flow-through NLF nacelle.

The nacelle was highly instrumented with static and fluctuating pressure transducers. Sound sources were located on the inside of the nacelle and outboard of the nacelle in a streamlined pod containing a noise source and a small video camera. Sublimating chemicals were used on the nacelle surface to establish the location of the transition front. The flow patterns were observed from the video camera and by an observer in a chase aircraft. The right-hand turboprop was feathered for zero rotation, and pressure data were measured with the sound source off and with it radiating toward the nacelle.

The acoustic sources were designed to provide excitations between 500 Hz and 4000 Hz at levels up to 132 dB on the nacelle surface. For the flight conditions of these tests, laminar flow was observed as far back as 30 percent of the nacelle length. The effect of the noise was not as detrimental as had been predicted. The boundary-layer transition location moved forward on the order of 3 to 5 percent of the nacelle length. The results of these tests can be used for correlation with predictive criteria at subsonic speeds. **(C. Obara, 3274)**

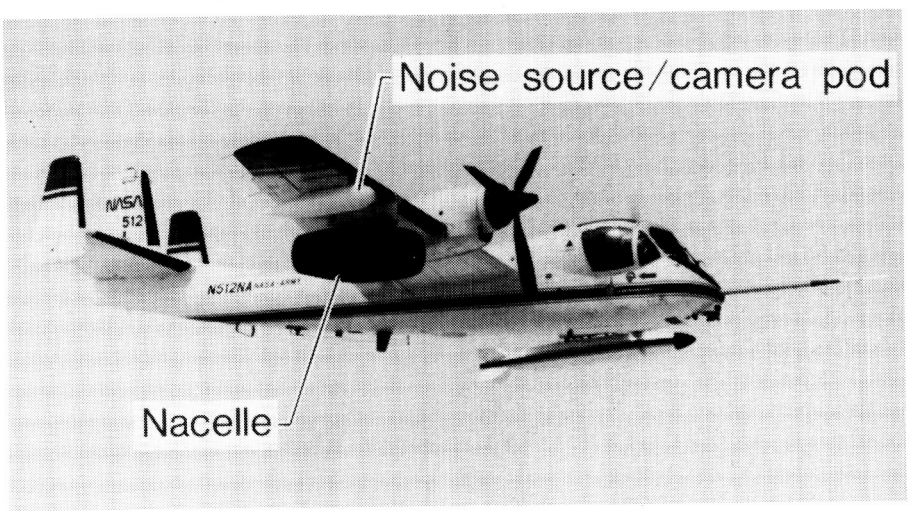

OV-1B aircraft with laminar-flow engine nacelle and noise source pod.

Ride Quality Measurements

General-aviation airplanes have a reputation for poor ride quality due in large part to the extremely rough ride exhibited by this class of airplanes in turbulent weather conditions. To investigate ways of reducing airplane response to turbulence, a Cessna 402B Businessliner (shown in the figure) is being modified to incorporate a ride quality augmentation system. The system control laws are being designed by the University of Kansas using modern control theory, and the modifications of the control surfaces and other airplane systems are being designed by the Cessna Aircraft Company.

A Langley-developed ride quality meter (RQM) has been applied to the unmodified Cessna 402B to provide a data base for establishing the baseline ride quality in both smooth and turbulent flight conditions. The RQM

Cessna 402B Businessliner used in ride quality studies. L-82-10,156

was designed to provide real-time estimates of passenger ride comfort as a function of the vehicle noise and vibration (high-frequency accelerations). The mathematical model used in the RQM is based on extensive ratings given by over 3000 test subjects in a ground-based ride quality apparatus. The readings produced by the meter pinpoint which aircraft acceleration and band of noise are contributing the most to ride discomfort. The data from the tests have shown that in turbulent air the lateral and vertical accelerations are the predominant sources of passenger discomfort. The longitudinal, pitch, and roll accelerations were found to be relatively unimportant as was the acoustic noise. In smooth air (or a near perfectly gust-alleviated airplane), the high noise levels would still produce a high percentage of uncomfortable passengers. The primary source of noise discomfort is in the noise band containing the propeller blade passing frequency.
(E. C. Stewart, 3274)

NASA
National Aeronautics and Space Administration

Report Documentation Page

1. Report No.	2. Government Accession No.	3. Recipient's Catalog No.
NASA TM-100595		

4. Title and Subtitle	5. Report Date
Langley Aerospace Test Highlights—1987	May 1988
	6. Performing Organization Code
7. Author(s)	8. Performing Organization Report No.
9. Performing Organization Name and Address NASA Langley Research Center Hampton, VA 23665-5225	10. Work Unit No. 11. Contract or Grant No.
12. Sponsoring Agency Name and Address National Aeronautics and Space Administration Washington, DC 20546-0001	13. Type of Report and Period Covered Technical Memorandum 14. Sponsoring Agency Code

15. Supplementary Notes

16. Abstract

The role of the Langley Research Center is to perform basic and applied research necessary for the advancement of aeronautics and space flight, to generate new and advanced concepts for the accomplishment of related national goals, and to provide research advice, technological support, and assistance to other NASA installations, other government agencies, and industry. This report highlights some of the significant tests which were performed during calendar year 1987 in Langley test facilities, a number of which are unique in the world. The report illustrates both the broad range of the research and technology activities at the Langley Research Center and the contributions of this work toward maintaining United States leadership in aeronautics and space research. Other highlights of Langley research and technology for 1987 are described in *Research and Technology 1987 Annual Report of the Langley Research Center*. Further information about both reports is available from the Office of the Chief Scientist, Mail Stop 105-A, Langley Research Center, Hampton, Virginia 23665-5225 (804-865-3316).

17. Key Words (Suggested by Authors(s))	18. Distribution Statement
Research and technology Tests Facilities Wind tunnels Models	Unclassified—Unlimited Subject Category 99

19. Security Classif.(of this report)	20. Security Classif.(of this page)	21. No. of Pages	22. Price
Unclassified	Unclassified	112	A06

NASA FORM 1626 OCT 86 NASA-Langley, 1988

For sale by the National Technical Information Service, Springfield, Virginia 22161-2171